# 实用中子衍射晶体学

Practical Neutron Diffraction Crystallography

(II)

# 峰型剖面方法精修和分析结构

黄清镇

HUANG QINGZHEN

中国散裂中子源

China Spallation Neutron Source

# X射线和中子粉末衍射峰的位置，强度和结构因子

## Powder diffraction positions, intensity, and structural factors for XRPD & NPD

**Peaks Position:** $2d_{hkl}\sin\theta_{hkl} = n\lambda$

where $\boldsymbol{l}$ is the incident beam wavelength, $\boldsymbol{d}$ and $\boldsymbol{\theta}$ are the distance between successive *hkl* planes and Bragg angles of reflections, respectively.

**Diffraction Intensity:** $I_{hkl} = C|F_{hkl}|^2$

where $|\boldsymbol{F}_{hkl}|^2$ is the *hkl* reflection amplitude of the diffracted X-ray, or neutron, or magnetic, and **C** is all others.

**X-ray:** $|F_{hkl}|^2 = |\sum f_j \exp(2\pi i\,(hx + ky + lz))|^2 e^{-2W}$

where $\boldsymbol{f}_j$ is the X-ray atomic scattering factor of atom *j* for X-ray.

**Neutron:** $|F_{hkl}|^2 = \sum b_j \exp(2\pi i\,(hx + ky + lz))|^2 e^{-2W}$

where $\boldsymbol{b}_j$ is the neutron scattering length for atom *j*.

**Magnetic:** $|F_{hkl}|^2 = \sum q_j f_{Mj} \exp(2\pi i\,(hx + ky + lz))|^2 e^{-2W}$

where $\boldsymbol{q}_j$ and $\boldsymbol{f}_{Mj}$ are the magnetic interaction vector and the magnetic form factor for atom *j*, respectively.

X-射线衍射与中子衍射具有许多共同点。峰的位置都遵循Bragg方程:

$$2d_{hkl}\sin\theta_{hkl} = n\lambda$$

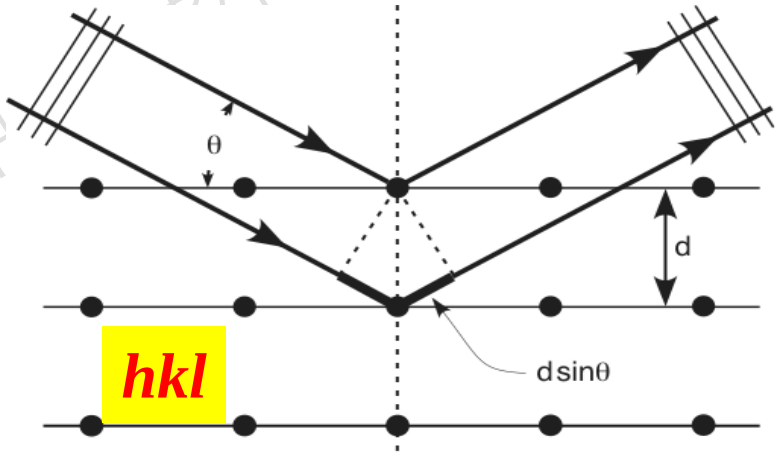


衍射峰的强度:

$$I_{hkl} = C|F_{hkl}|^2$$

式中 C 是与晶体结构无关的参数，$F_{hkl}$ 是结构因子。

（1）在结构因子中，除了由于元素的散射因子差异使得衍射峰强度不同外，其它与结构有关的参数都一样。

（2）在中子衍射中，磁有序的衍射谱图是一套独立于晶体结构的衍射图，因此磁相可作为一个独立的相精化得到磁结构信息。

# XRPD & NPD 是结构分析的有力的工具

$$2d_{hkl}\sin\theta_{hkl} = n\lambda \qquad I_{hkl} = C|F_{hkl}|^2$$

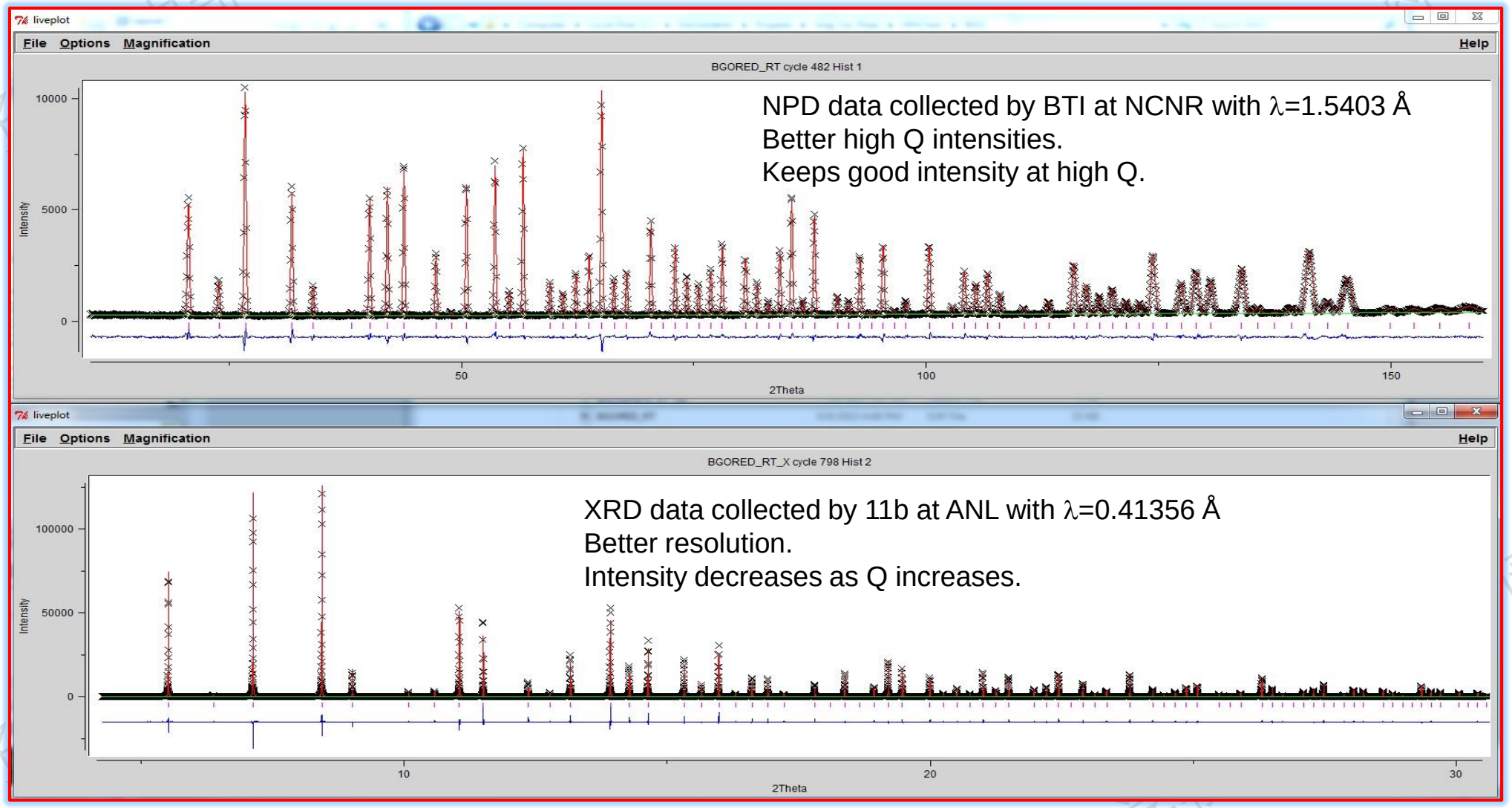


XRD and NPD patterns for $Bi_4Ge_3O_{12}$ compound

*Sample comes from Jintai Zhao's group*

# 衍射峰重叠严重

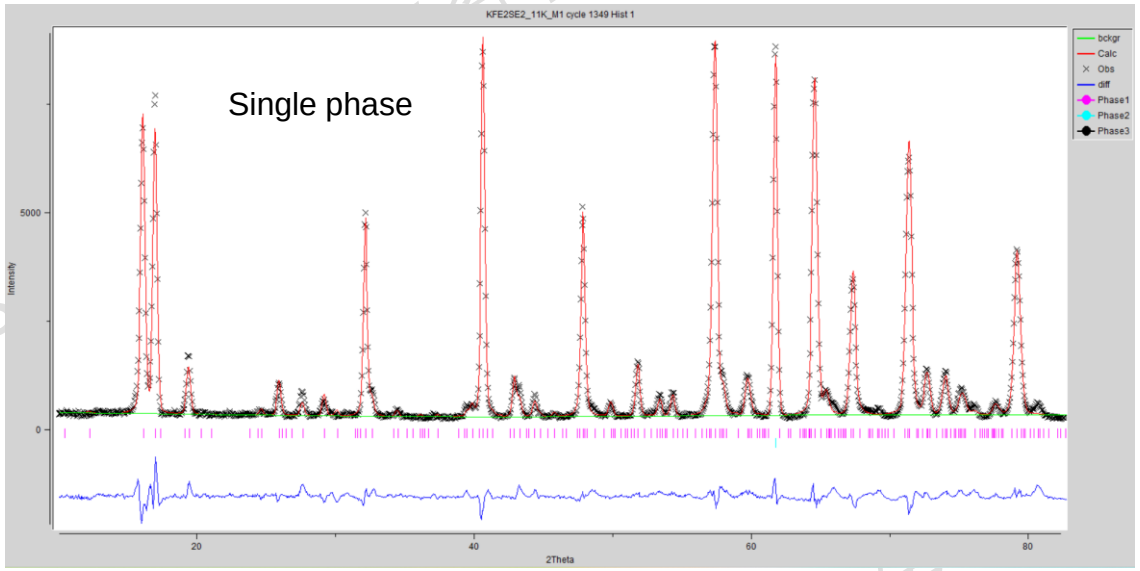


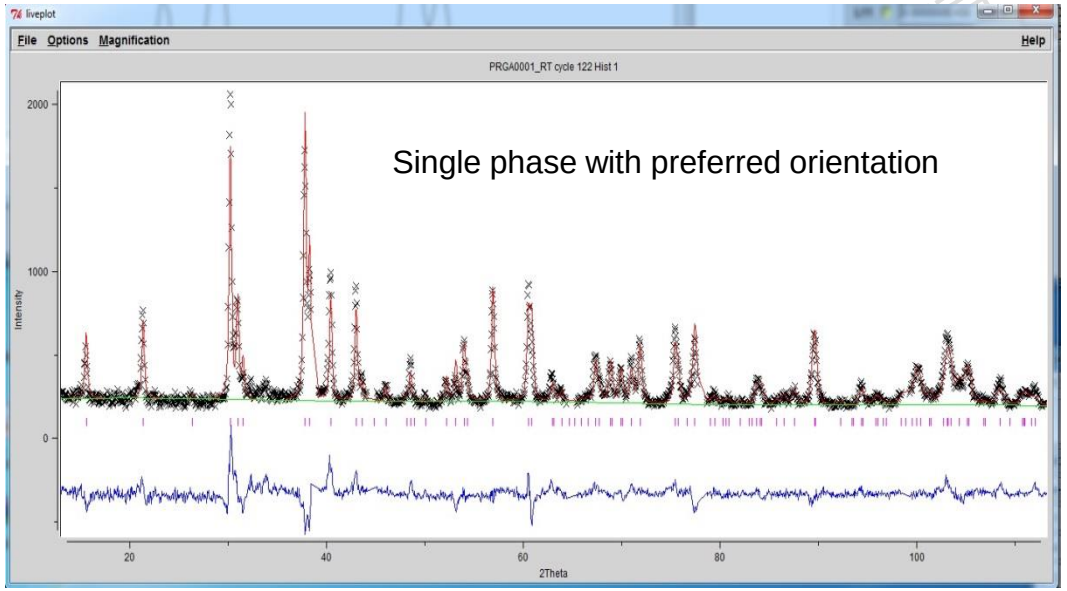


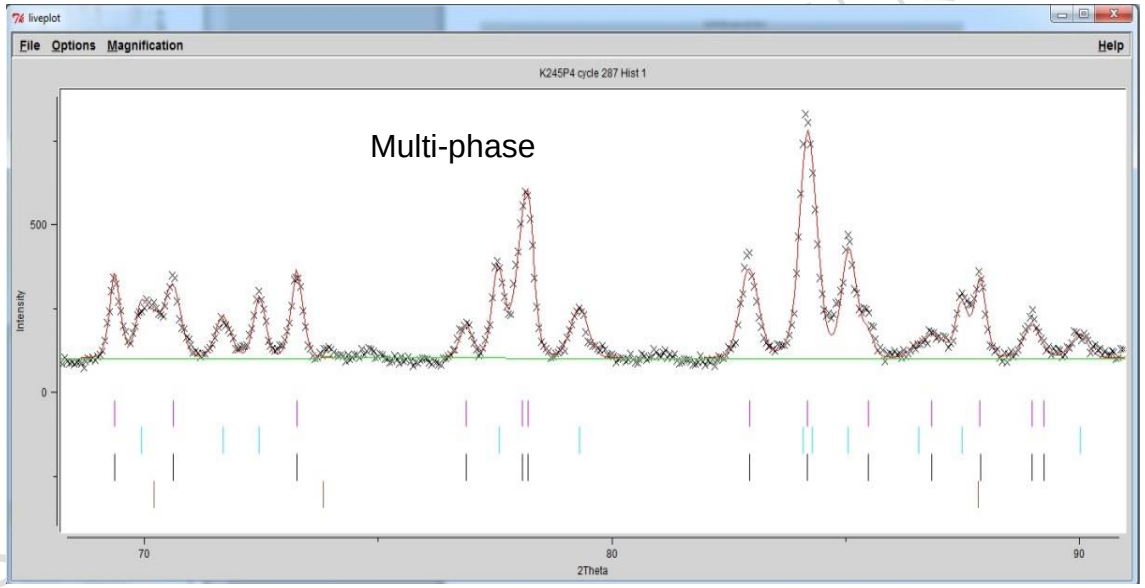


Difficulty to get each reflection intensity due to overlaps

- Large unite cell and low symmetry;
- Sample with multi-phase;
- Poor crystalline and particle shape;
- Defect and strain;
- Instrumental resolution
- Improper experimental condition

…

# Rietveld (峰型剖面)方法分析粉末衍射数据
## Rietveld (Profile) Refinement Method for the Analysis of Powder Diffraction Data

Hugo M. Rietveld and Dorothy Crowfoot Hodgkin
(She is The Nobel Prize winner in chemistry 1964).*

*Hugo M. Rietveld

The Rietveld method.
*Phys. Scr. 89 (2014) 098002 (6pp)*
A Profile Refinement Method for Nuclear and Magnetic Structures.
*J. Appl. Cryst.* **2**, 65-71 (1969)
Sum of the time cited: 8720+
Line profiles of neutron powder-diffraction peaks for structure refinement.
*Acta Cryst. (1967). **22**, 151-152*
Sum of the time cited: 1766

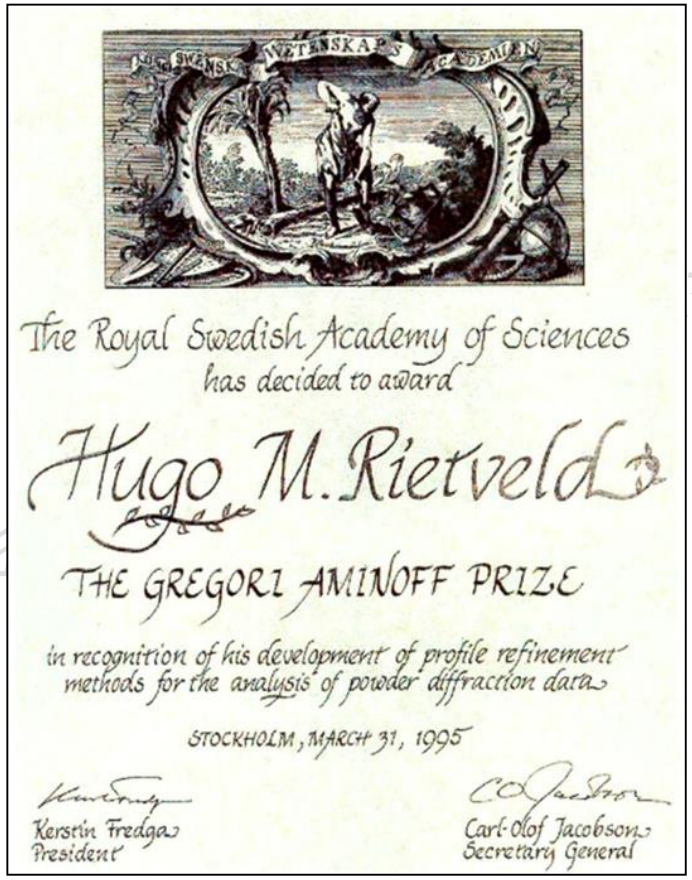


Albinati, A., & Willis, B. T. M. T*he Rietveld method. International Tables for Crystallography. Vol.* **C**, **8.6**, 710-712(2006).
Young, A. (1993) Edited. *The Rietveld Method. International Monographs on Crystallography.* **5**. Oxford University Press Inc., New York(1993).

## 爱明诺夫奖

**格雷戈里·阿米诺夫奖**（英语：**Gregori Aminoff Prize**）是由瑞典皇家科学院于1979年设立的国际奖项，得名于瑞典科学家格雷戈里·阿米诺夫（瑞典语：Gregori Aminoff）(1883-1947)，以奖励世界范围内在晶体学领域做出重要突出贡献的科学家，每年颁发给不超过3人。被认为是晶体学的Nobel奖。

## Chinese winner of Aminoff Preize

Mao Ho-kwang (毛河光)
2005, "for his pioneering research of solid materials at ultrahigh pressures and temperatures"

Shi Yigong (施一弓)
2014, *"for his groundbreaking crystallographic studies of proteins and protein complexes that regulate programmed cell death"*

# 峰型剖面精化方法定量相分析$Mn_{1.1}Fe_{0.9}P_{0.8}Ge_{0.2}$

Profile Refinement for Quantitative Phase Analysis of $Mn_{1.1}Fe_{0.9}P_{0.8}Ge_{0.2}$

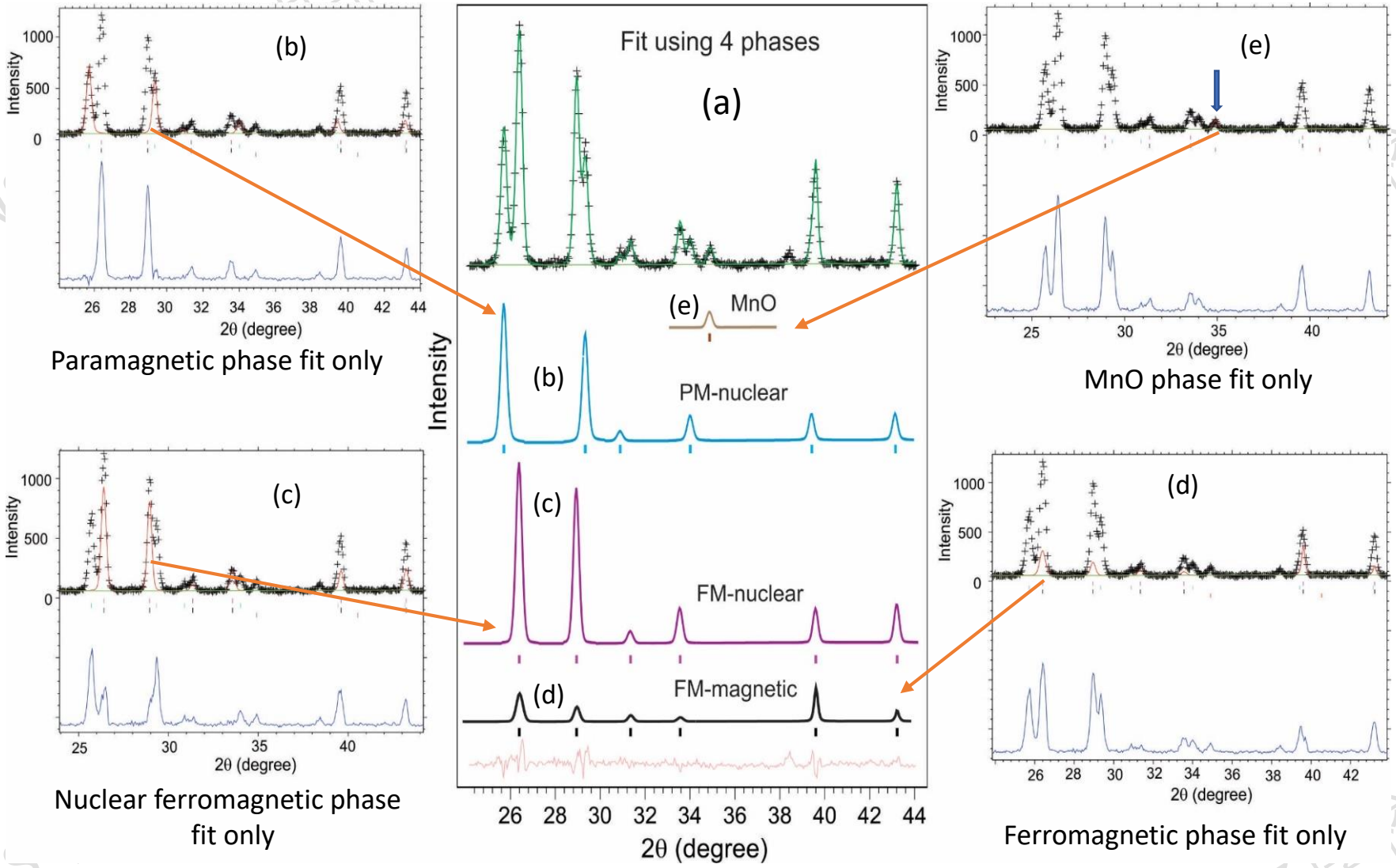


**Rietveld方法是用在已有结构模型的情况对模型进行精化，并不是用来解结构的方法。**

用粉末衍射数据分析晶体结构的最大困难是如何分离部分和完全重叠的各个衍射峰强度，Hugo M. Rietveld提出用峰型剖面分析方法，改连续扫描为步进扫描收集数据，把衍射谱图数据化。有效地解决了这一困难。如图：

（1）图（a）是含有4个物相的中子粉末衍射谱图。

（2）根据这4个物相的已知模型建立4条中子粉末衍射谱图（b, c, e, d）。

（3）调整结构参数（晶胞参数，原子位置及其分布，温度因子，占有率等），选择合适的峰型函数和背底函数，以及各个相的含量，再用最小二乘法逐步进行上述各个参数的修正，直至计算的谱图完全拟合观察的谱图，完成晶体结构和磁结构的精修。

粉末衍射谱图大致包含两大部分，背底和衍射峰。背底主要来自两部分：1）入射光束打在空气，样品盒，环镜，等产生；这部分的不含我们所需要的结构信息，因此应该尽量减少，来自空气的散射可通过在光路上抽真空减少空气颗粒来消除，或充氦气来减少，因为氦气颗粒小。如NIST的BT1中子谱仪在入射光路中冲氦气提高入射中子~8%；2）来自样品的散射。样品的散射则主要有康普顿散射与样品本身的漫散射。漫散射由其样品中无序部分和晶格动力学引起。以后主要讨论与有序结构有关的衍射特征和信息提取。


我们关注的是衍射峰所包含的结构信息。重点在：1）峰位置，因为它帮我们确定晶体结构中重复单元的形状和大小，对称性，以及缺陷所引起的峰位变化，如宏观应变；而峰强则包含结构中的化学成分，元素位置及分布，原子偏离平均位置大小（温度因子）等等。这两部分是利用衍射进行结构分析的主体。而峰形包含谱仪参数以及晶体结构不完整部分的信息和样品晶体颗粒的形状及大小。

# 多相混合的水泥试样

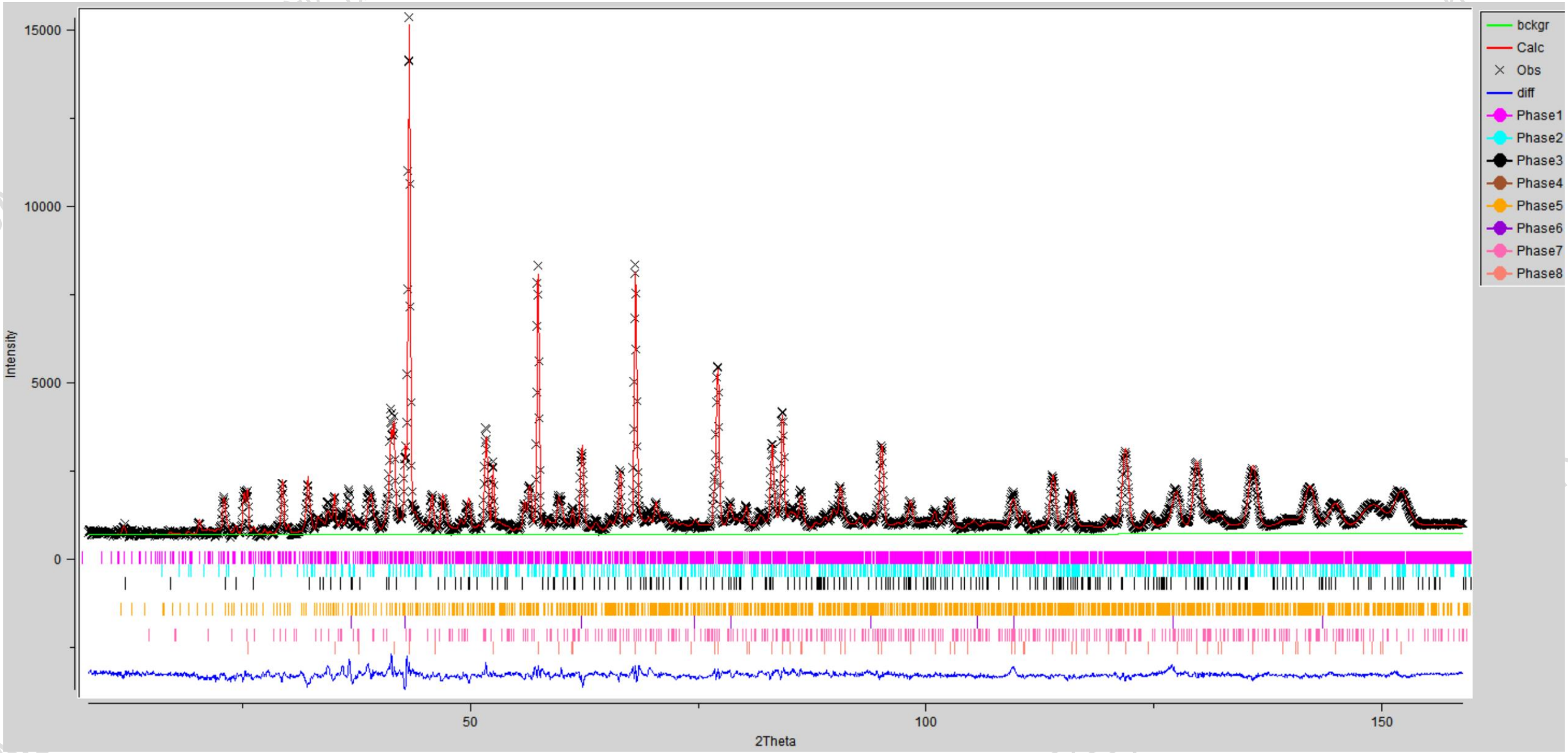
15000
10000
5000
0
Intensity
50
100
150
2Theta
bckgr
Calc
Obs
diff
Phase1
Phase2
Phase3
Phase4
Phase5
Phase6
Phase7
Phase8

# GSAS-EXPGUI: expnam

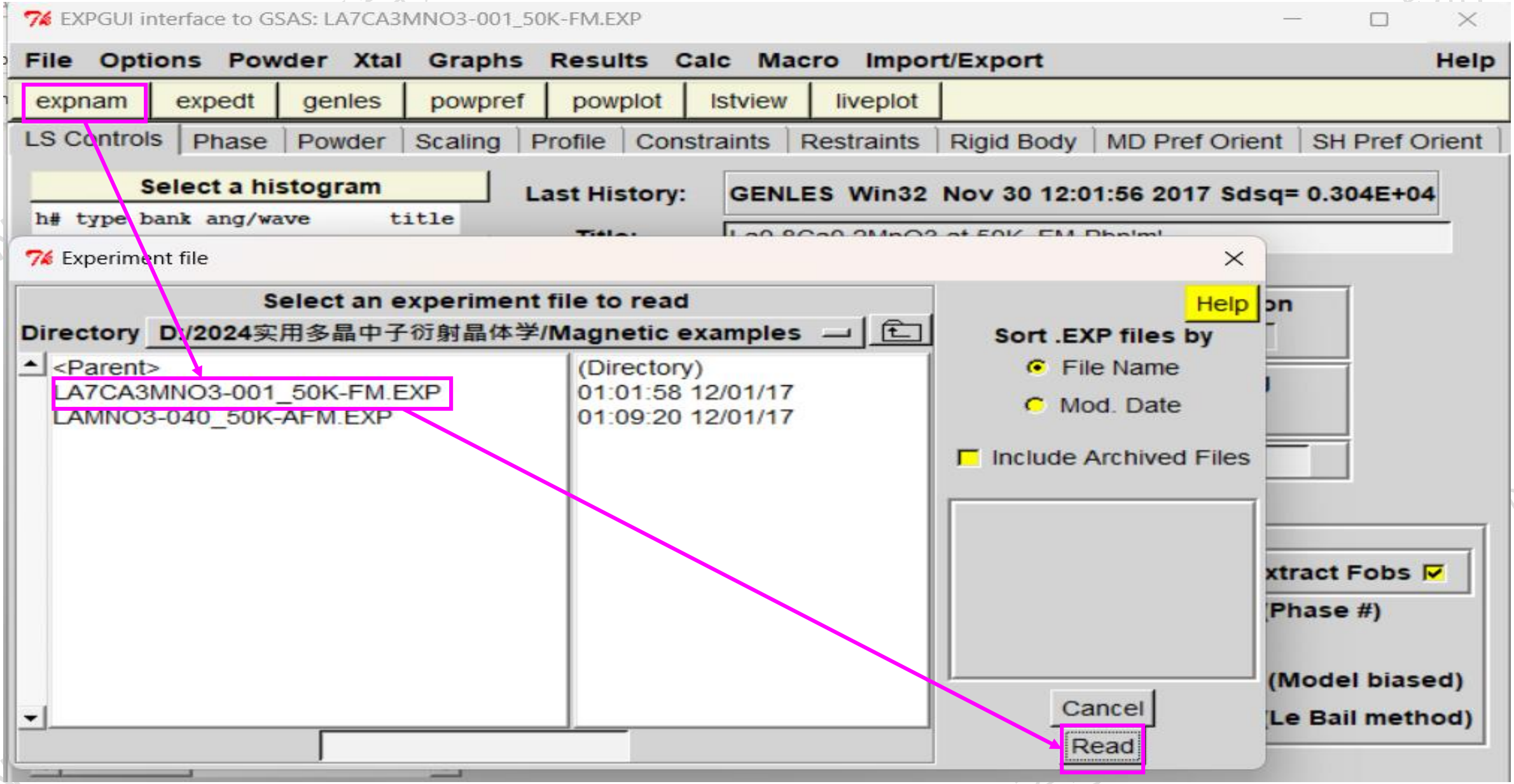

# GSAS-EXPGUI: LS Controls

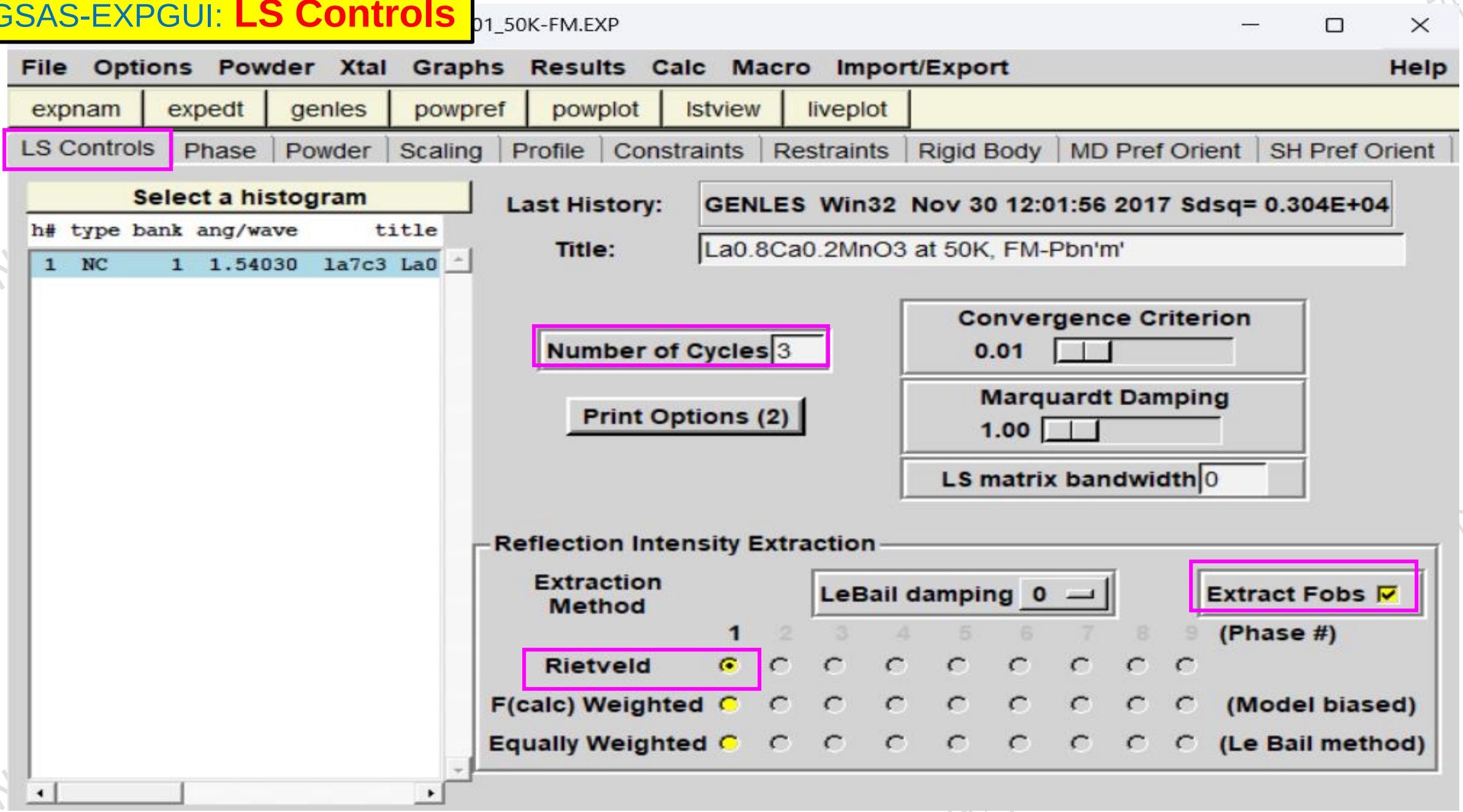

# GSAS-EXPGUI: Scaling

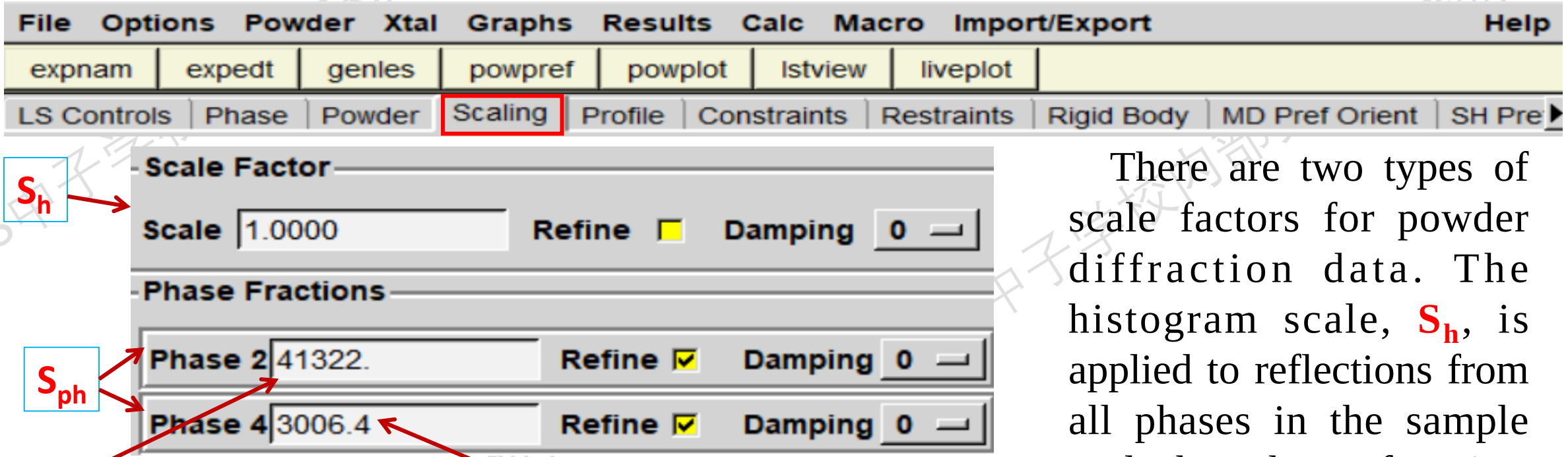


**Phase/element fractions for phase no. 2**

Hist Elem: 1 1 PNC
Fraction : 41322.0
Sigmas : 0.00000
Shift/esd: 0.00
Wt. Frac.: 0.95605
Sigmas : 0.00000

**Phase/element fractions for phase no. 4**

Hist Elem: 1 1 PNC
Fraction : 3006.41
Sigmas : 76.4528
Shift/esd: 0.00
Wt. Frac.: 0.43946E-01
Sigmas : 0.106842E-02

There are two types of scale factors for powder diffraction data. The histogram scale, $S_h$, is applied to reflections from all phases in the sample and the phase fraction scale, $S_{ph}$, is applied only to reflections from the **p-th** phase. These latter scales can be used for quantitative phase analysis for powder mixtures.

# GSAS-EXPGUI: Powder

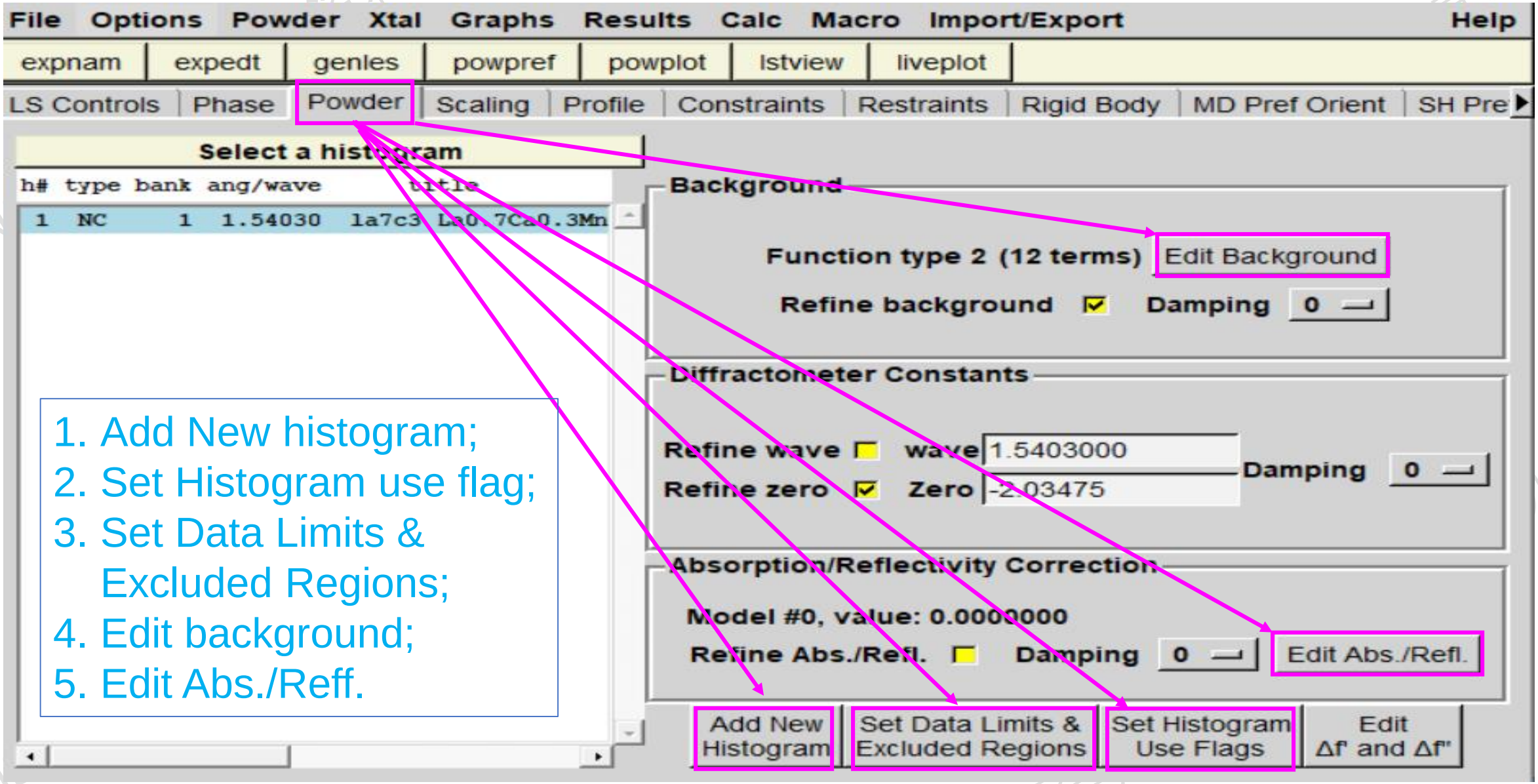


1. Add New histogram;
2. Set Histogram use flag;
3. Set Data Limits & Excluded Regions;
4. Edit background;
5. Edit Abs./Reff.

# GSAS-EXPGUI: Phase

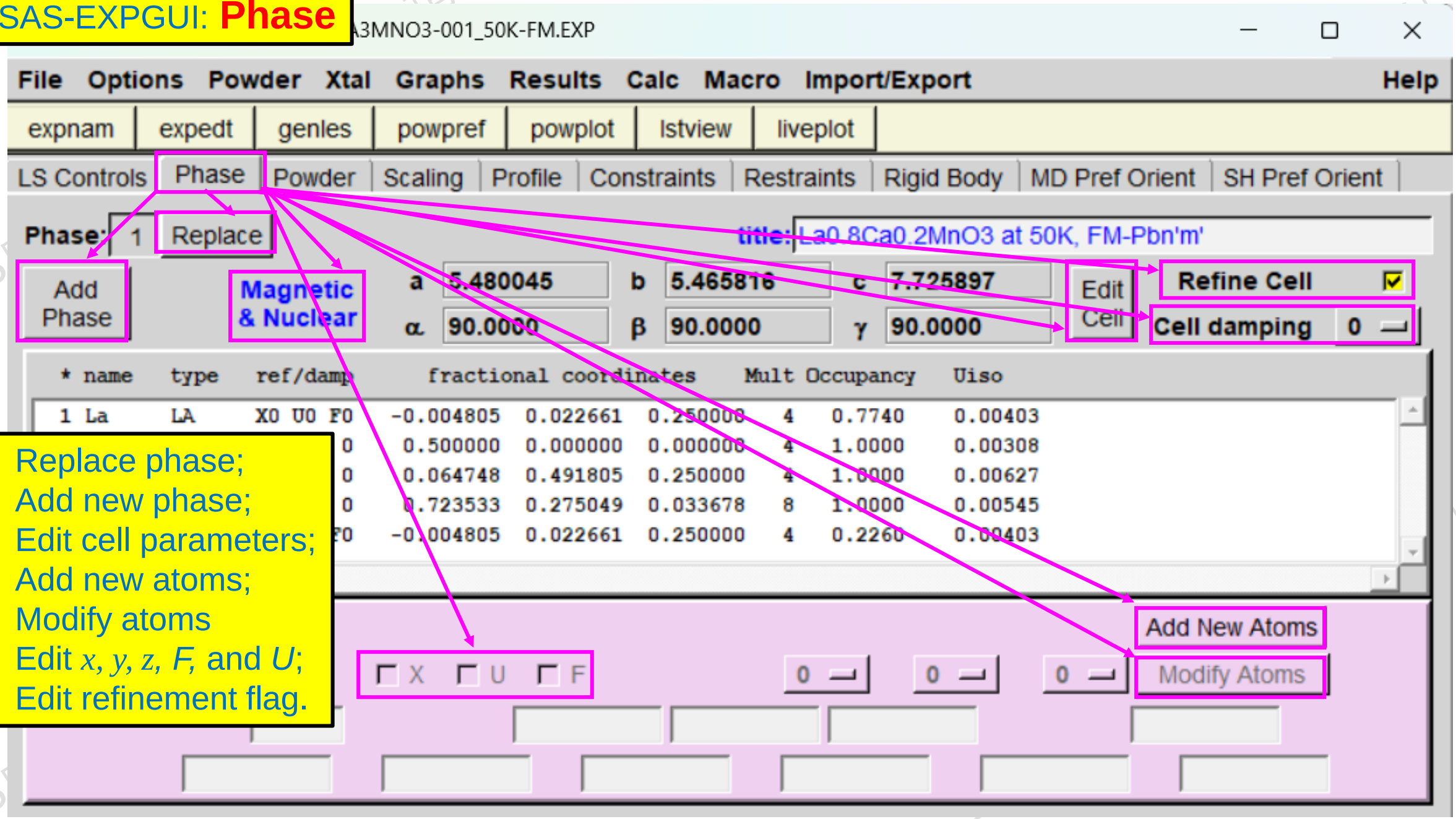


1. Replace phase;
2. Add new phase;
3. Edit cell parameters;
4. Add new atoms;
5. Modify atoms
6. Edit *x*, *y*, *z*, *F*, and *U*;
7. Edit refinement flag.

# GSAS-EXPGUI: Phase-Replace

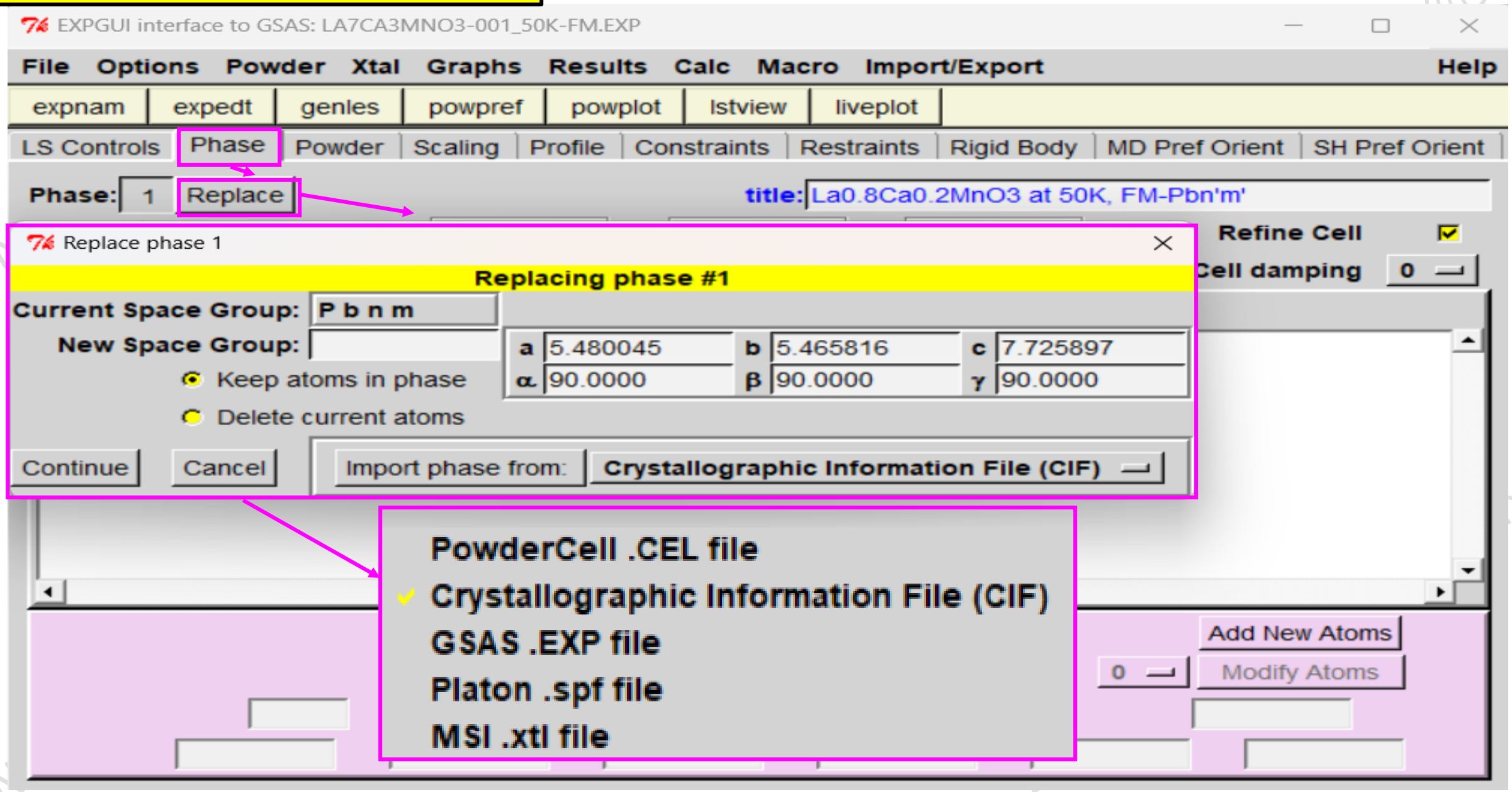

# GSAS-EXPGUI: Phase-Add phase

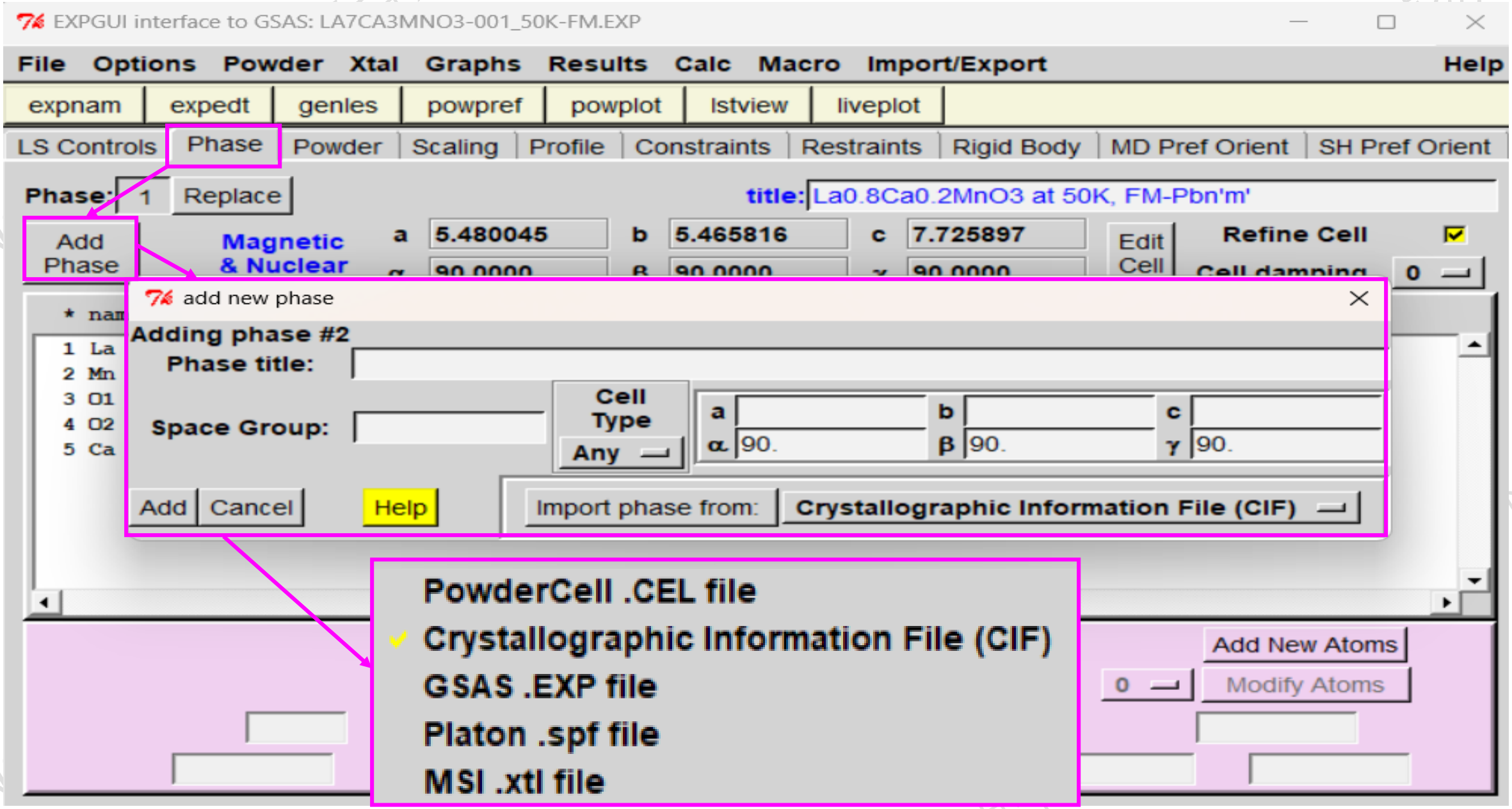

# GSAS-EXPGUI: Powder-Add New Histogram

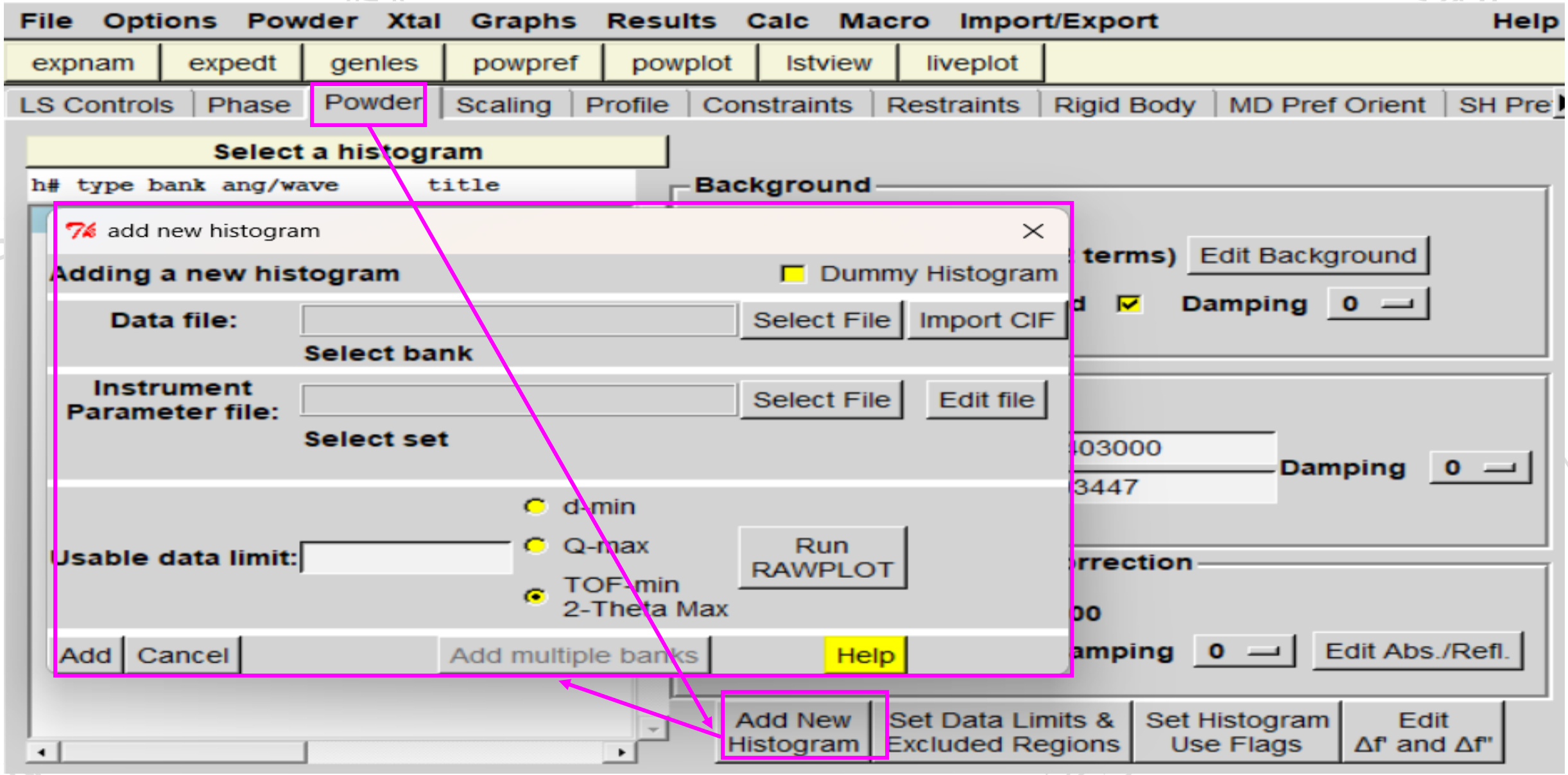

# GSAS-EXPGUI: Powder-Set Data Limits and Excluded Regions

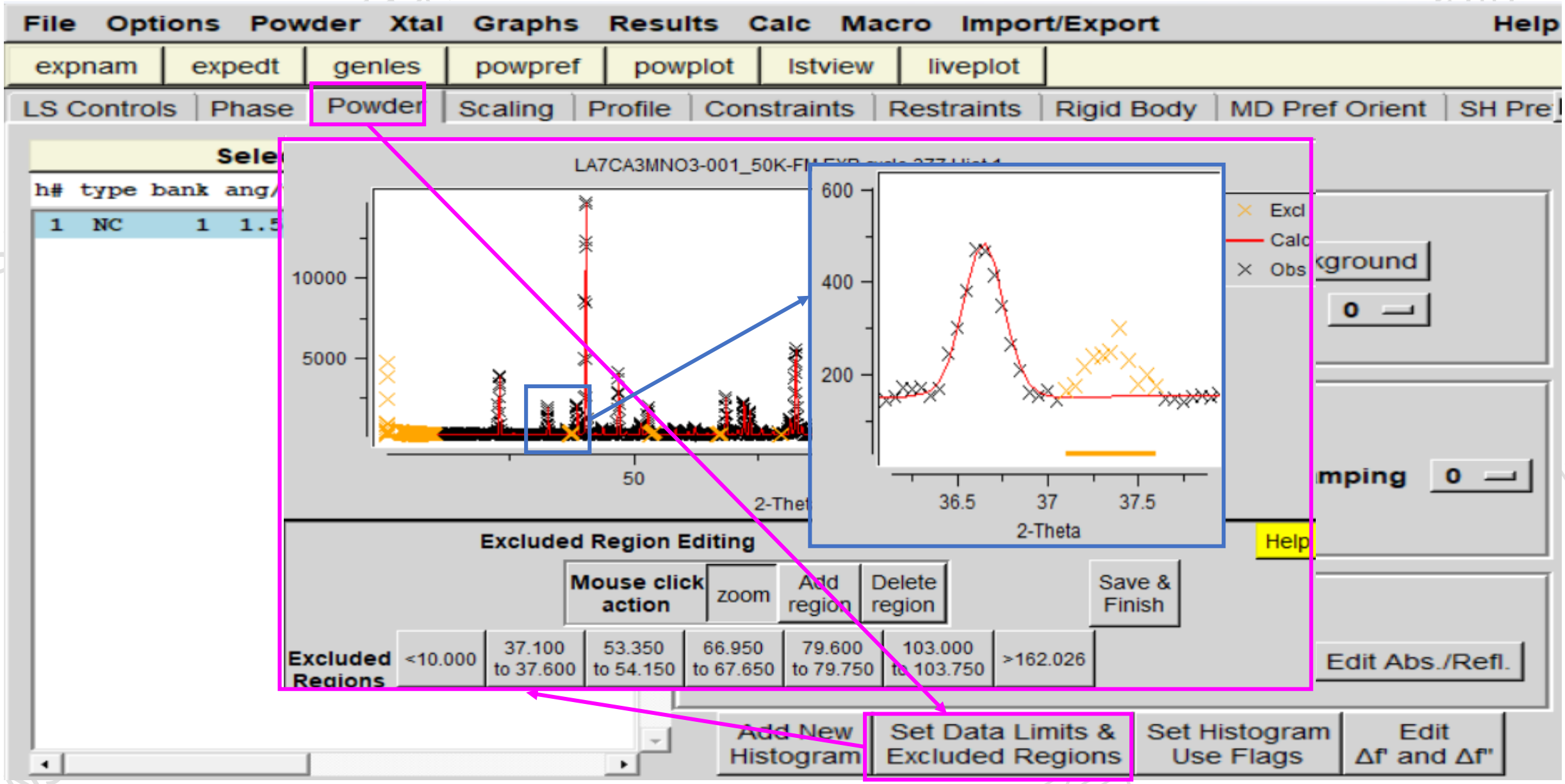

# GSAS-EXPGUI: Edit Background

## Set background function and number of coefficients

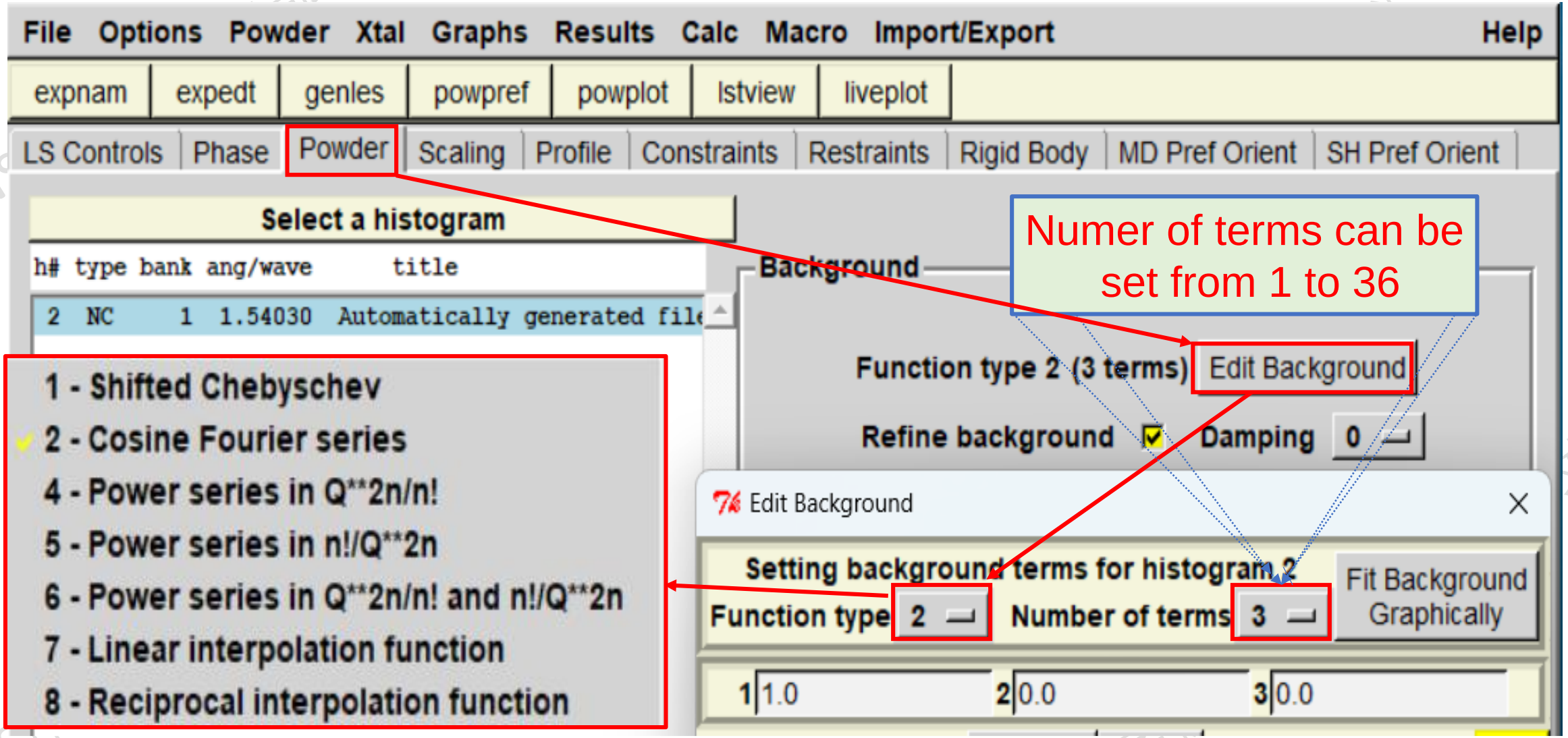

GSAS-EXPGUI: **Profile**

# CW profile function type 1

## Gaussian function

CW-Profile

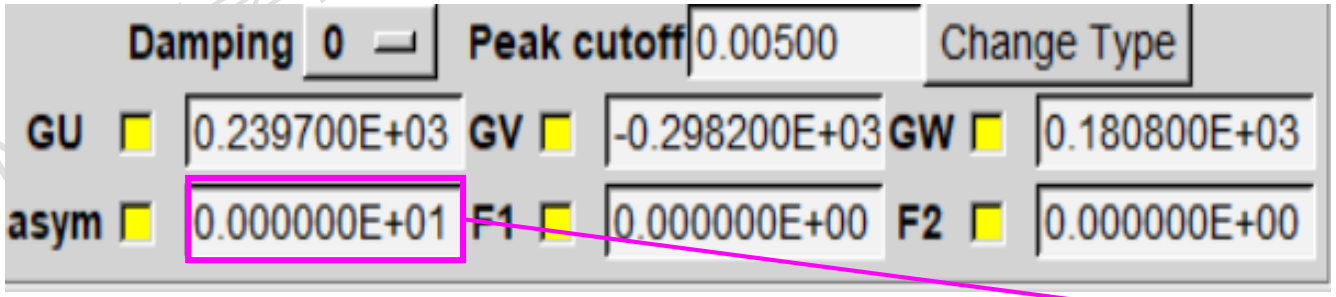


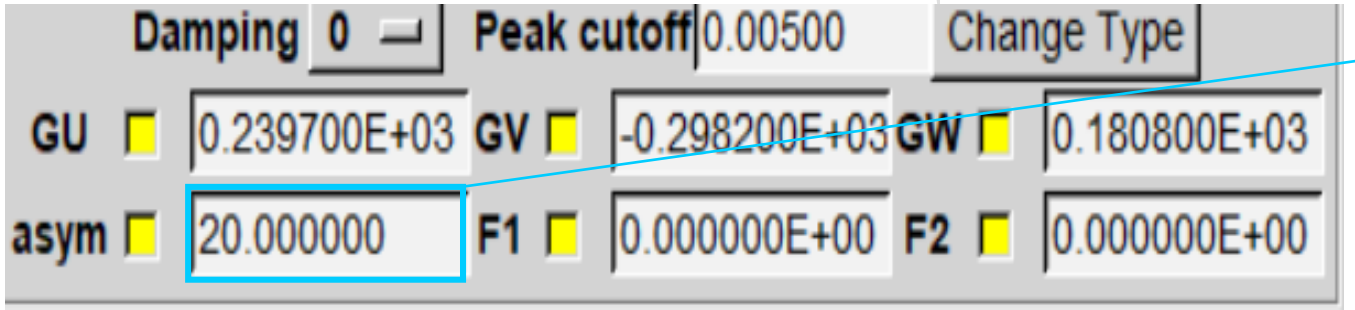


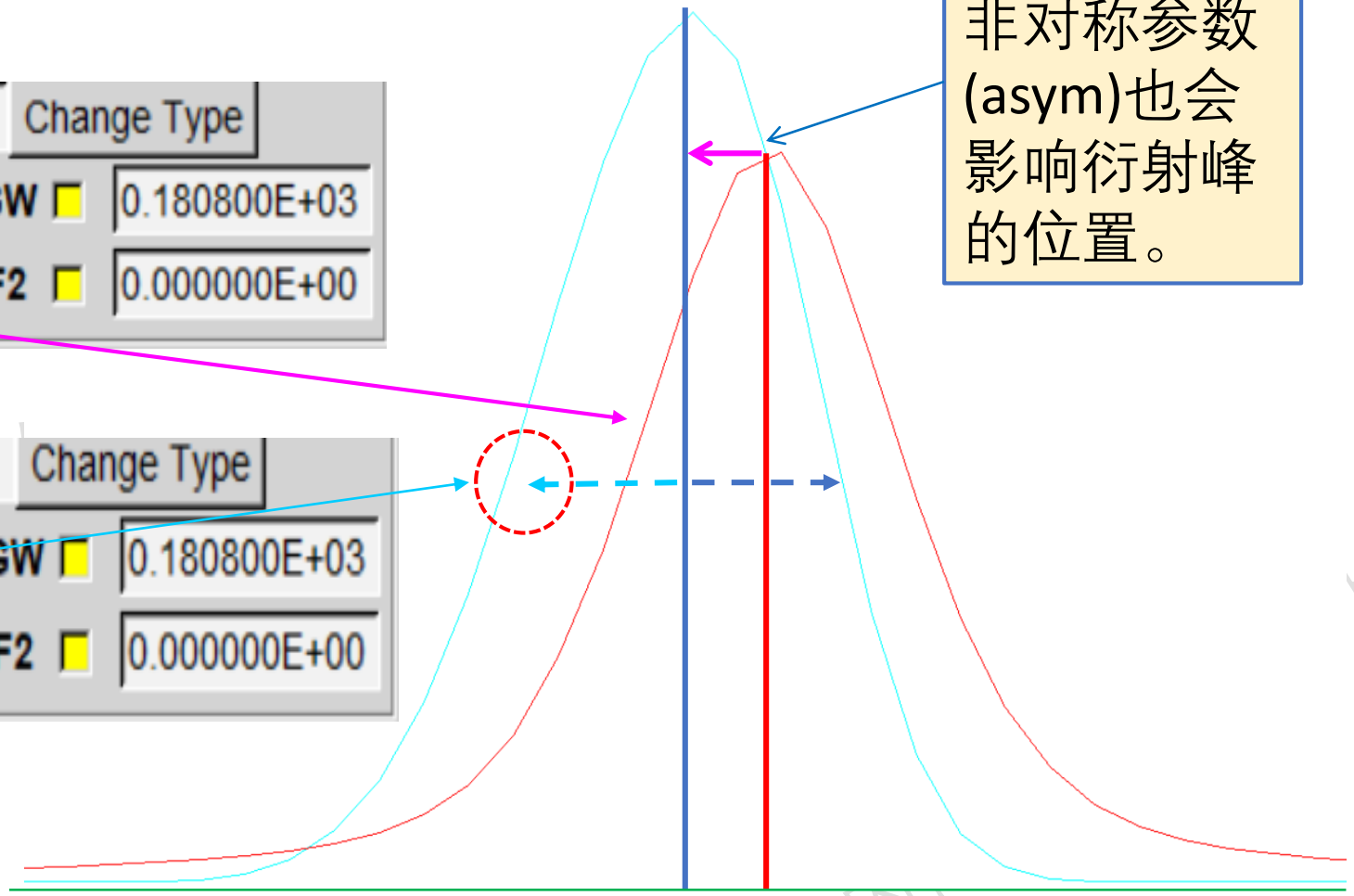


Rietveld and others (H.M. Rietveld, J. Appl. Cryst., **2**, 65-71, 1969; Cooper & Sayer, J. Appl. Cryst., **8**, 615-618, 1975; & Thomas, J. Appl. Cryst., **10**, 12-13, 1977).

GSAS-EXPGUI: **Profile**

# CW profile function type 2

## Multi-term Simpson's rule integration

CW-Profile

| Damping 0 | | Peak cutoff 0.00500 | | Change Type | |
|---|---|---|---|---|---|
| GU | 239.700000 | GV | -298.200000 | GW | 180.800000 |
| LX | 0.000000 | LY | 0.000000 | trns | 0.000000 |
| asym | 0.000000 | shft | 0.000000 | GP | 0.000000 |
| stec | 0.000000 | ptec | 0.000000 | sfec | 0.000000 |
| L11 | 0.000000 | L22 | 0.000000 | L33 | 0.000000 |
| L12 | 0.000000 | L13 | 0.000000 | L23 | 0.000000 |

| Damping 0 | | Peak cutoff 0.00500 | | Change Type | |
|---|---|---|---|---|---|
| GU | 239.700000 | GV | -298.200000 | GW | 180.800000 |
| LX | 40.000000 | LY | 0.000000 | trns | 0.000000 |
| asym | 0.000000 | shft | 0.000000 | GP | 0.000000 |
| stec | 0.000000 | ptec | 0.000000 | sfec | 0.000000 |
| L11 | 0.000000 | L22 | 0.000000 | L33 | 0.000000 |
| L12 | 0.000000 | L13 | 0.000000 | L23 | 0.000000 |

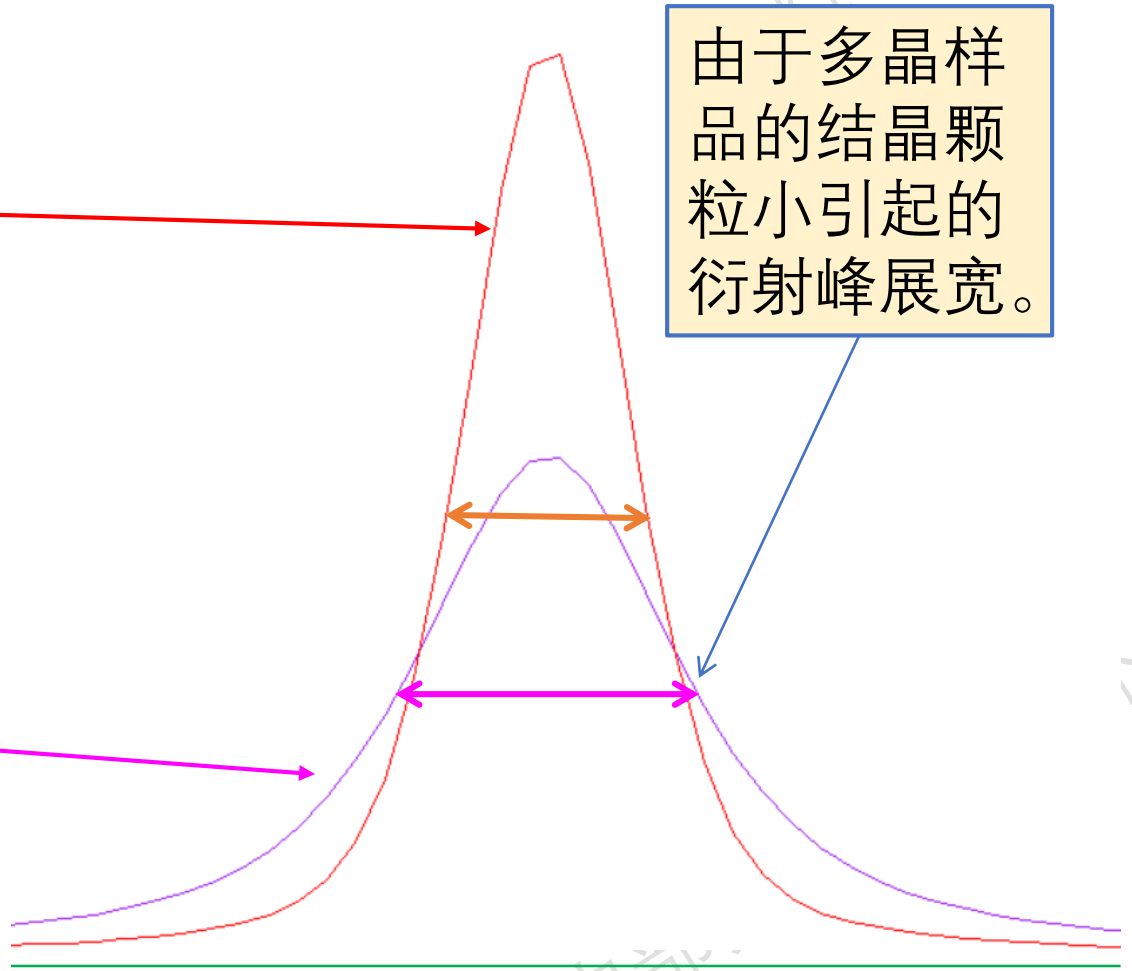


C.J. Howard (J. Appl. Cryst.,**15**, 615-620, 1982) of the pseudo-Voigt, F(ΔT), described by Thompson, et al. and used above in the second and third functions for TOF data.

# CW profile function type 3



The third CW profile function is a similar variation on the pseudo-Voigt function used in the second function. However, it uses a much more successful description of the reflection asymmetry due to axial described by Finger, Cox & Jephcoat, J. Appl. Cryst., **27**,892-900 (1994) as an implementation of the peak shape function described by Van Laar & Yelon, J. Appl. Cryst., **17**, 47-54 (1984).

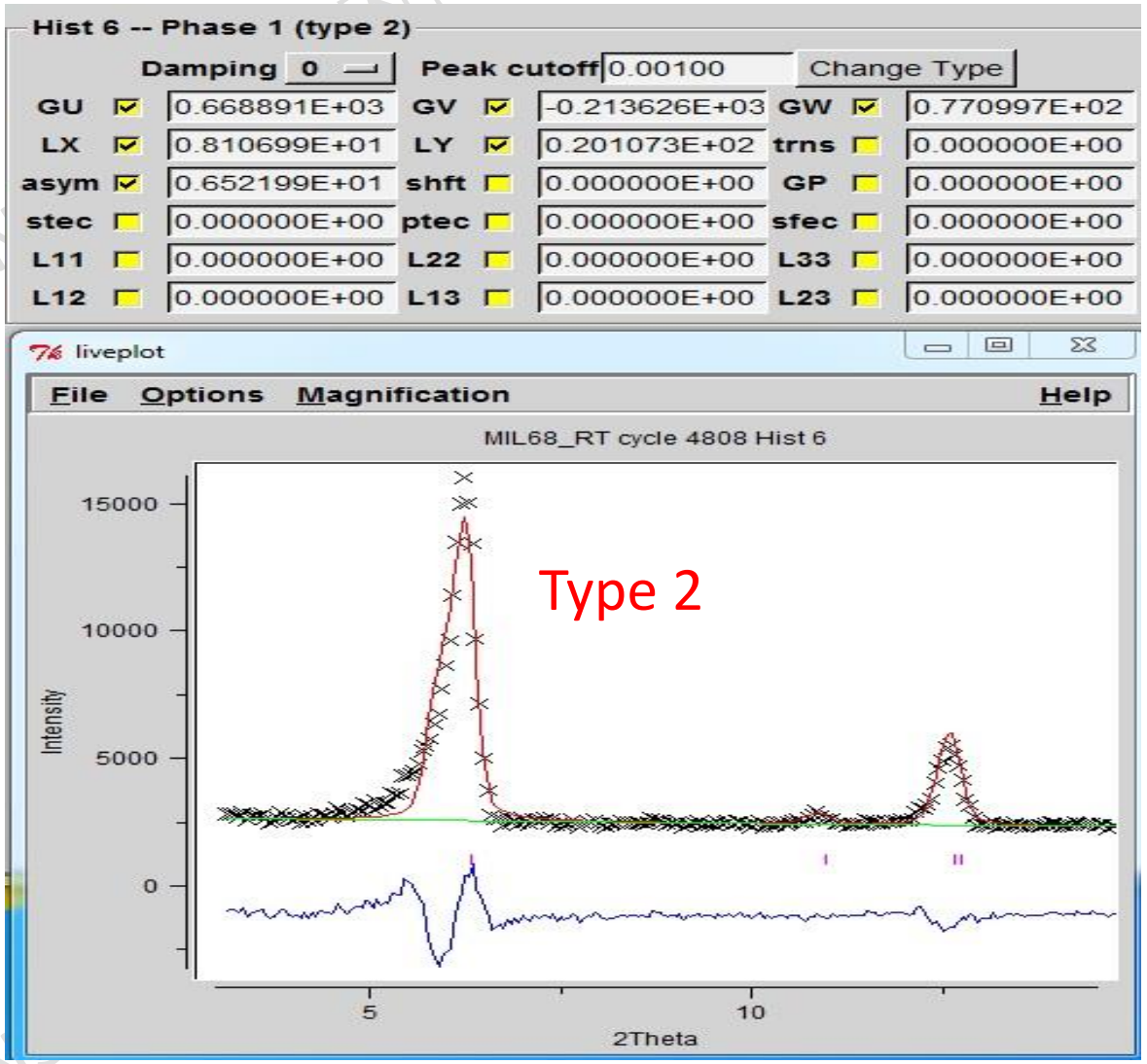


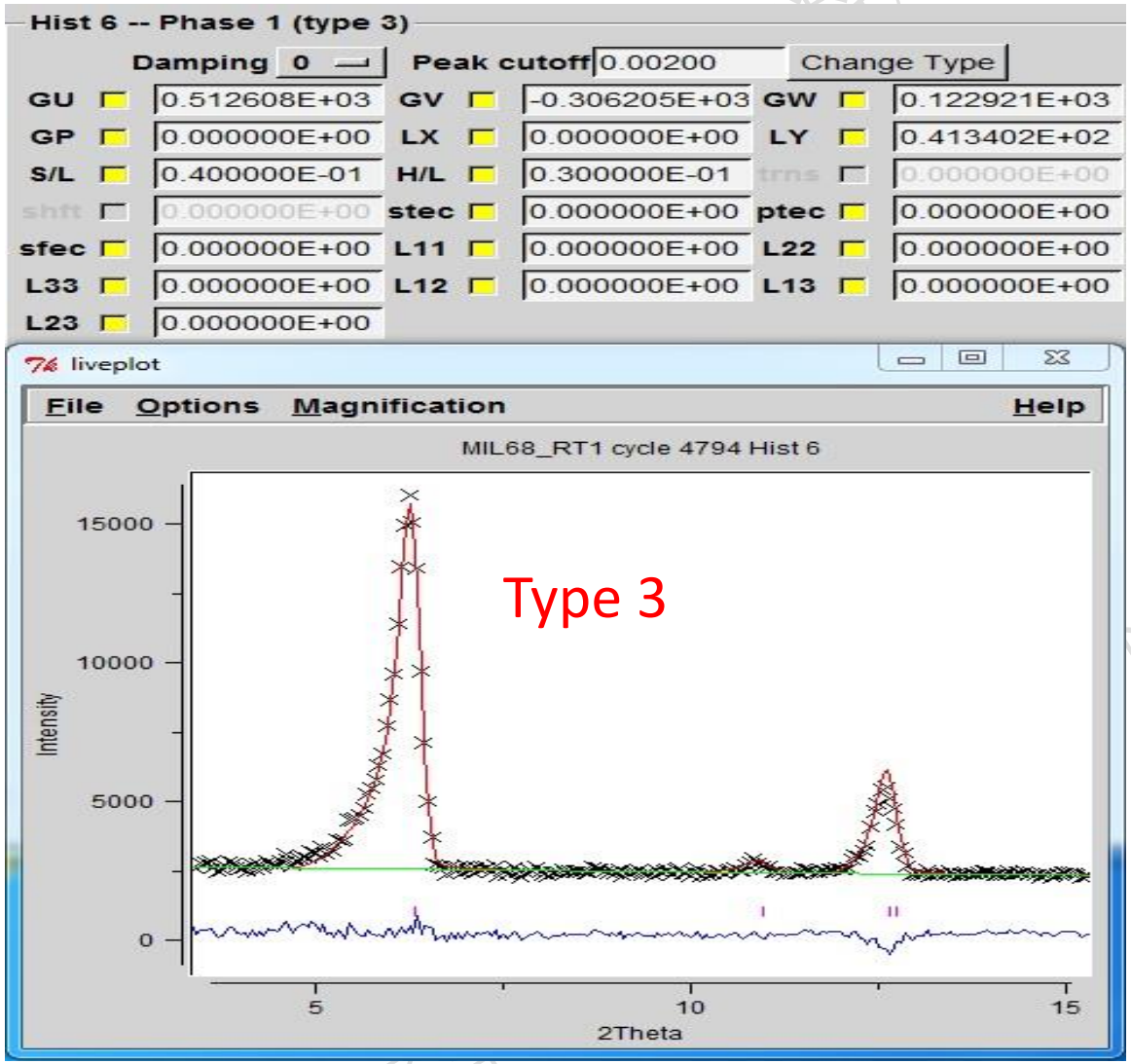

GSAS-EXPGUI: **Profile**

# CW profile function type 4

## Multi-term Simpson's rule integration

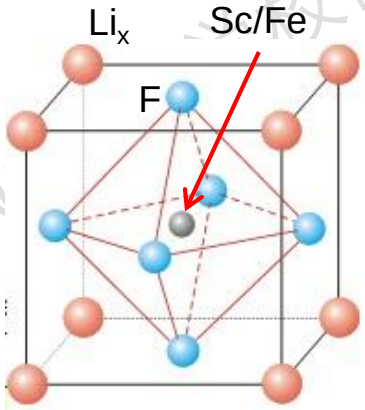


Ionic radius

$Li^{+1}$: 0.60
$Sc^{+3}$: 0.81
$Fe^{+3}$: 0.64
$Fe^{+2}$: 0.76
$F^{-1}$: 1.36

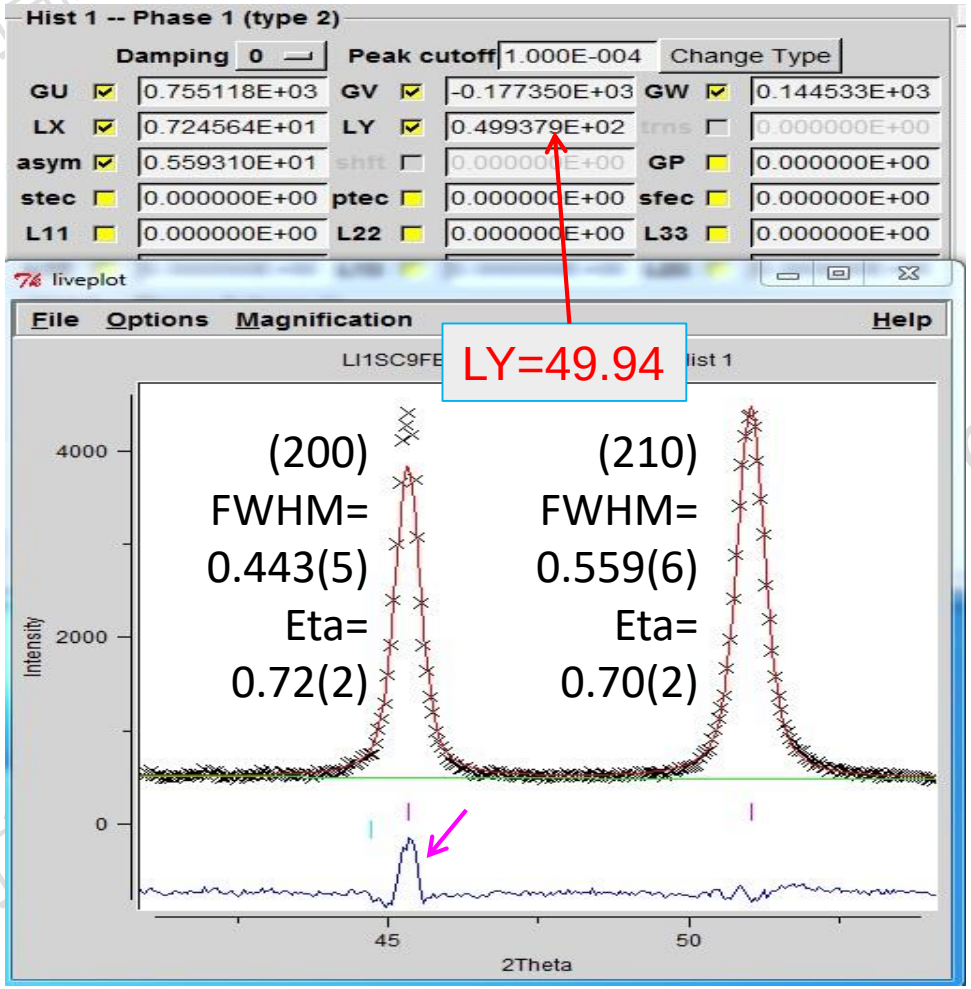


Fit by profile #2, isotropic strain broadening

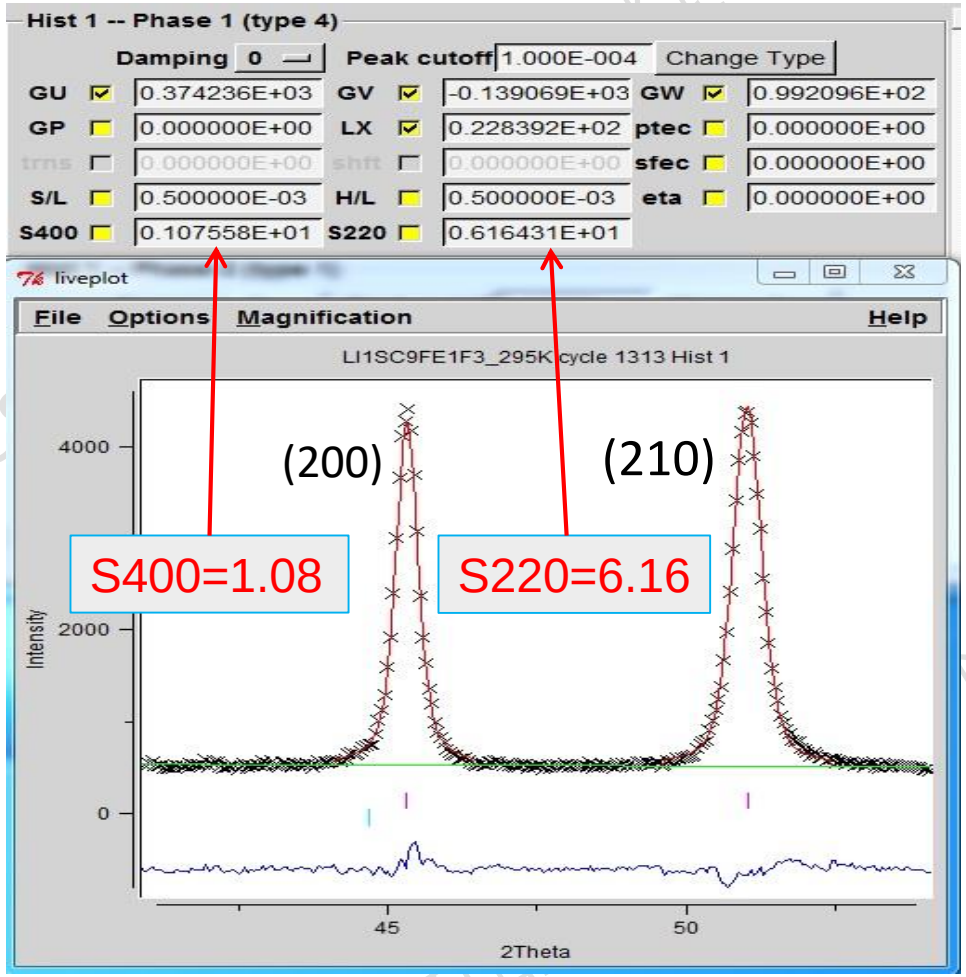


Fit by profile #4, anisotropic strain broadening

# CW profile function type 5

The fifth CW profile function is a modification of the third function to include generalized macroscopic strain. In place of the six $\gamma_{ij}$ coefficients used in that function to describe an empirical anisotropic microstrain broadening there are a maximum of six $\delta_{ij}$ coefficients to describe an offset of each reflection position. This profile function thus becomes useful for refinements with multiple data sets taken at a, for example, range of temperatures where the $\delta_{ij}$ can describe the effect of thermal expansion on the lattice parameters. In this case set the $\delta_{ij}$=0 for one histogram and allow them to vary for the others.

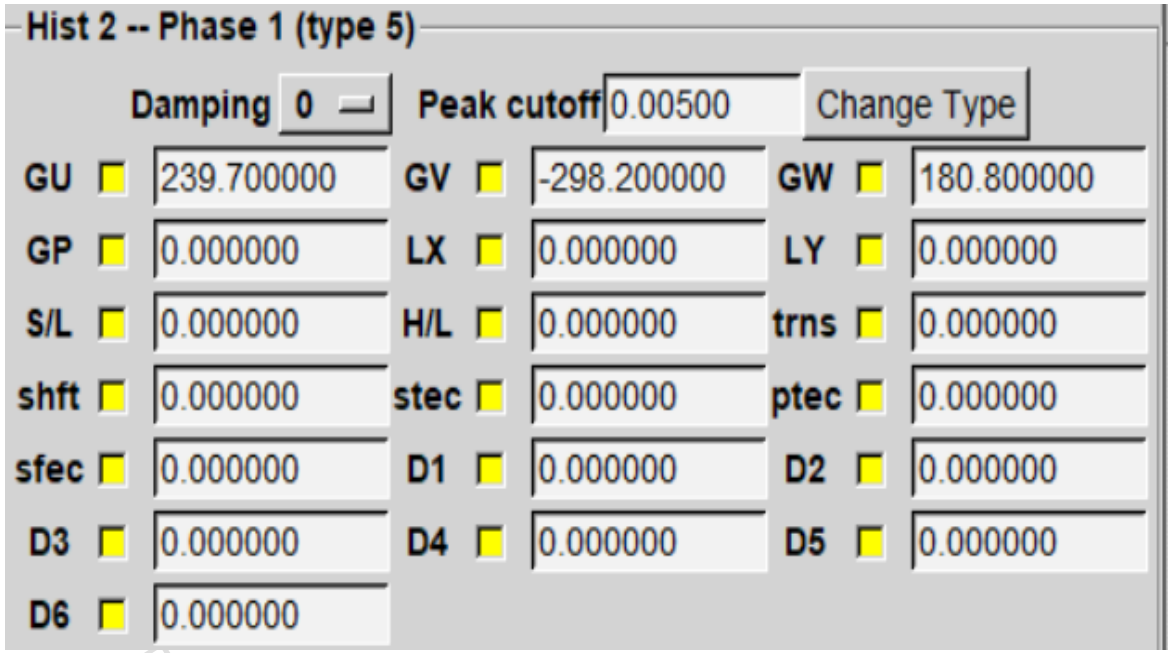


type 5

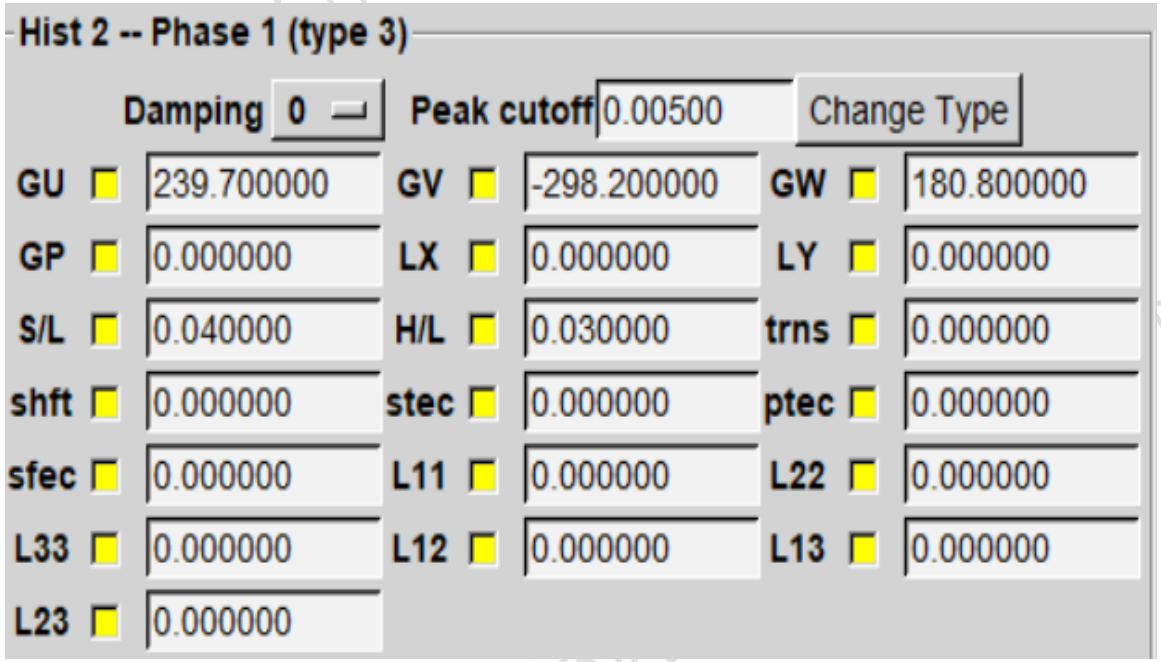


type 3

# GSAS-EXPGUI: Profile

## Set peak cutoff

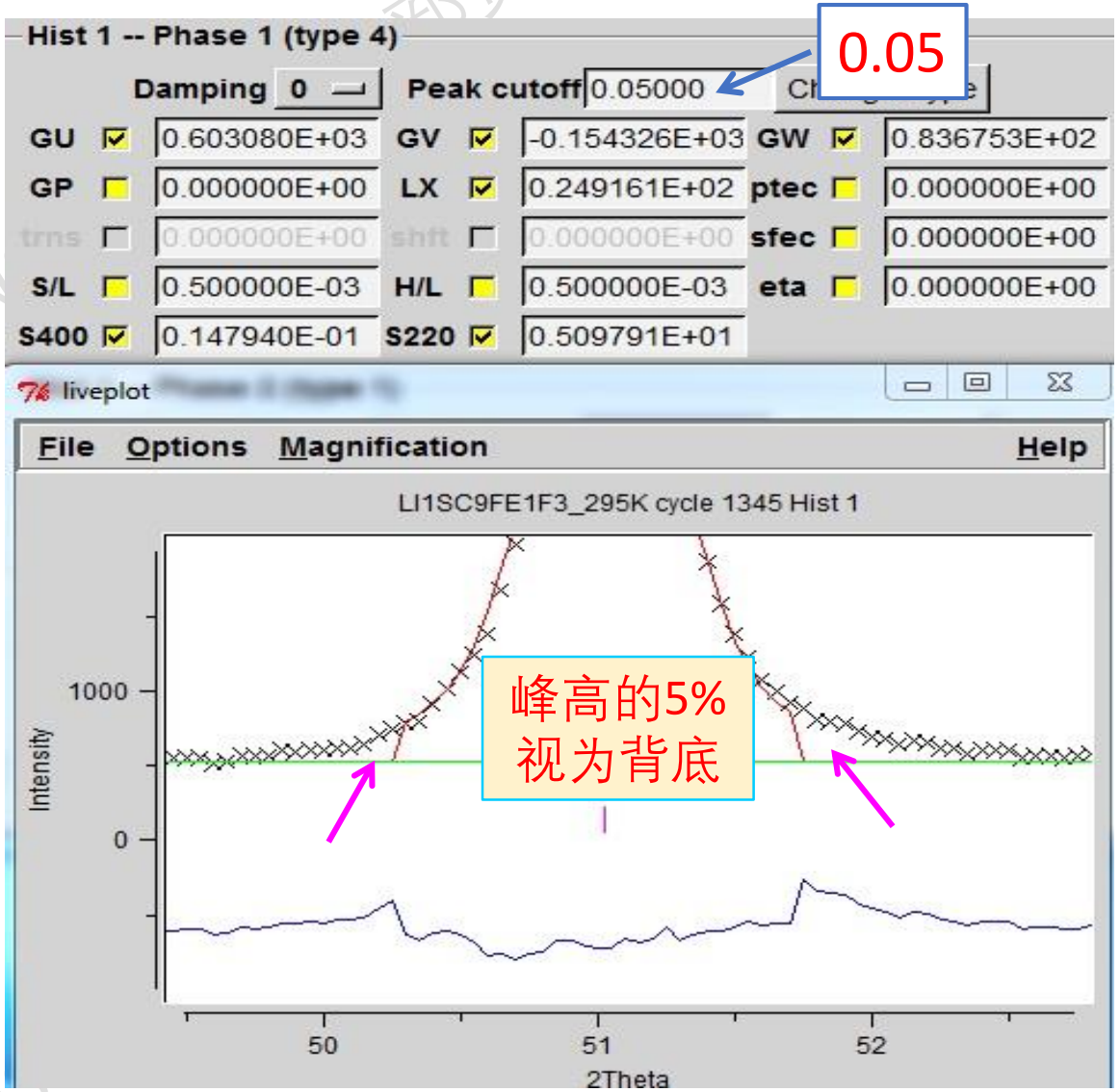


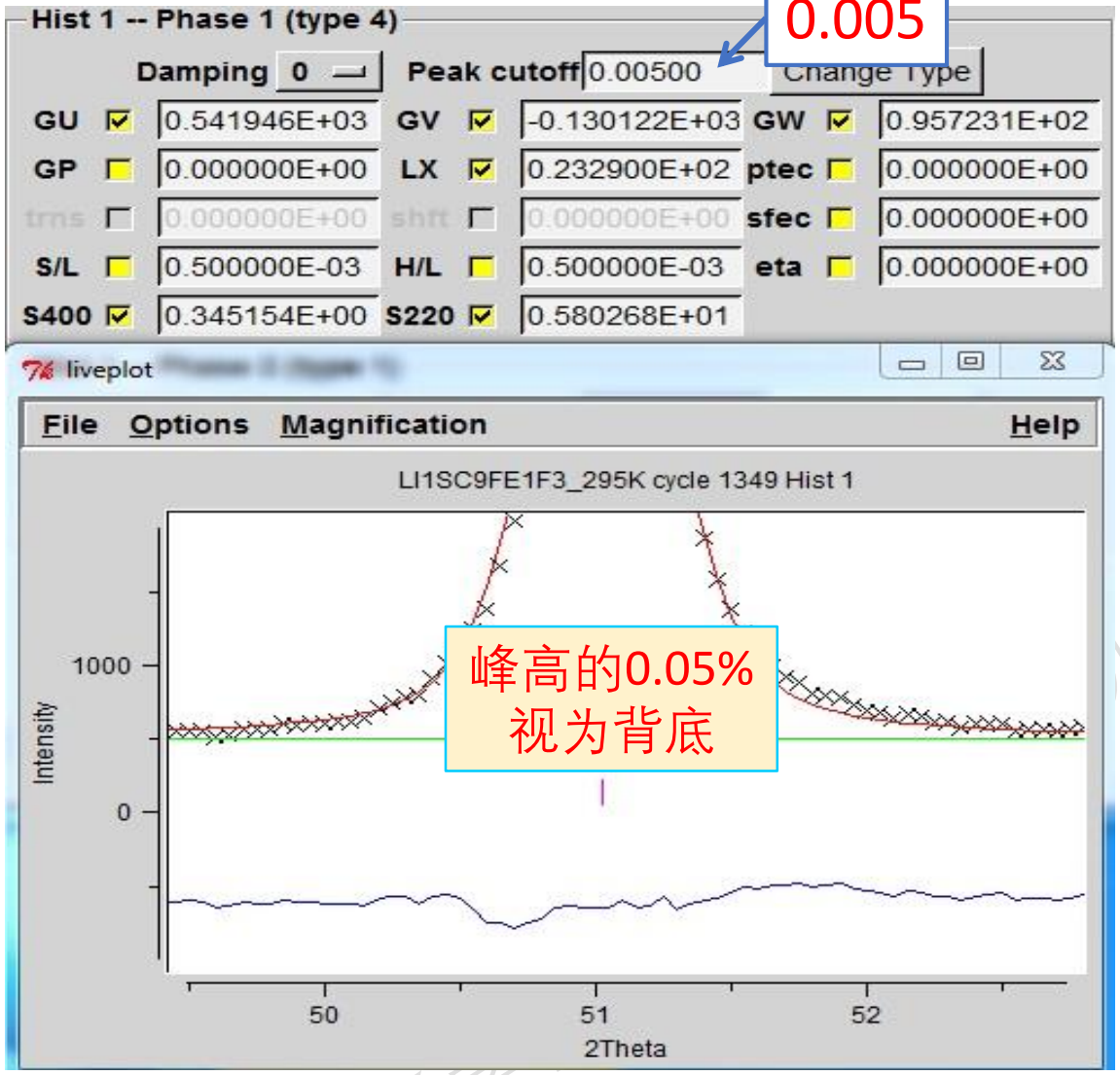

# GSAS-EXPGUI: Powder-Edit Edit Abs./Reff-Absorption

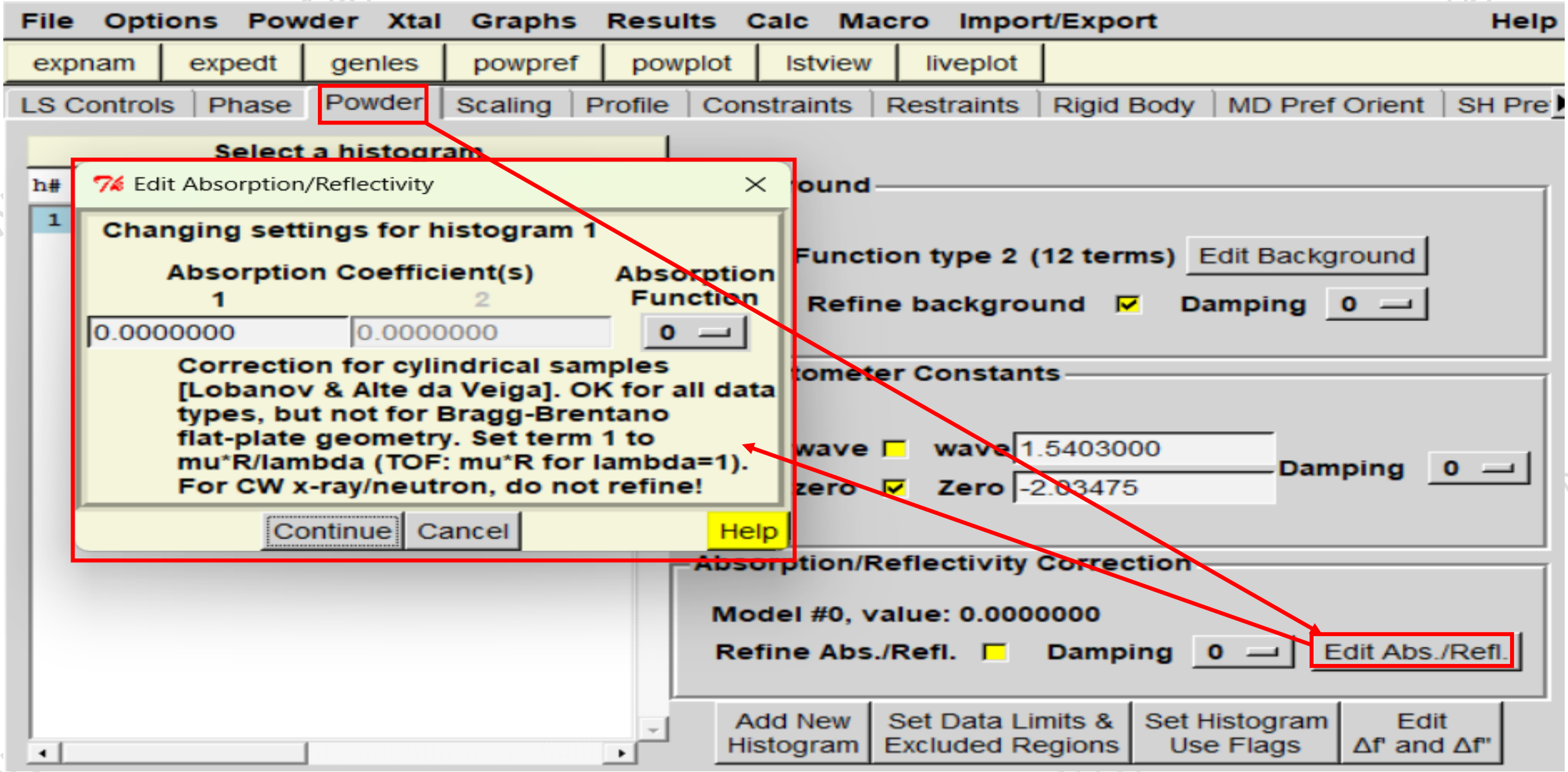

# GSAS-EXPGUI: Powder-Edit Edit Abs./Reff-Absorption

## 样品的吸收校正不足

样品含有大量的元素Tb和Co，室温中子数据在中国散裂中子源高分辨中子通用粉末衍射仪(GPPD)上收集。

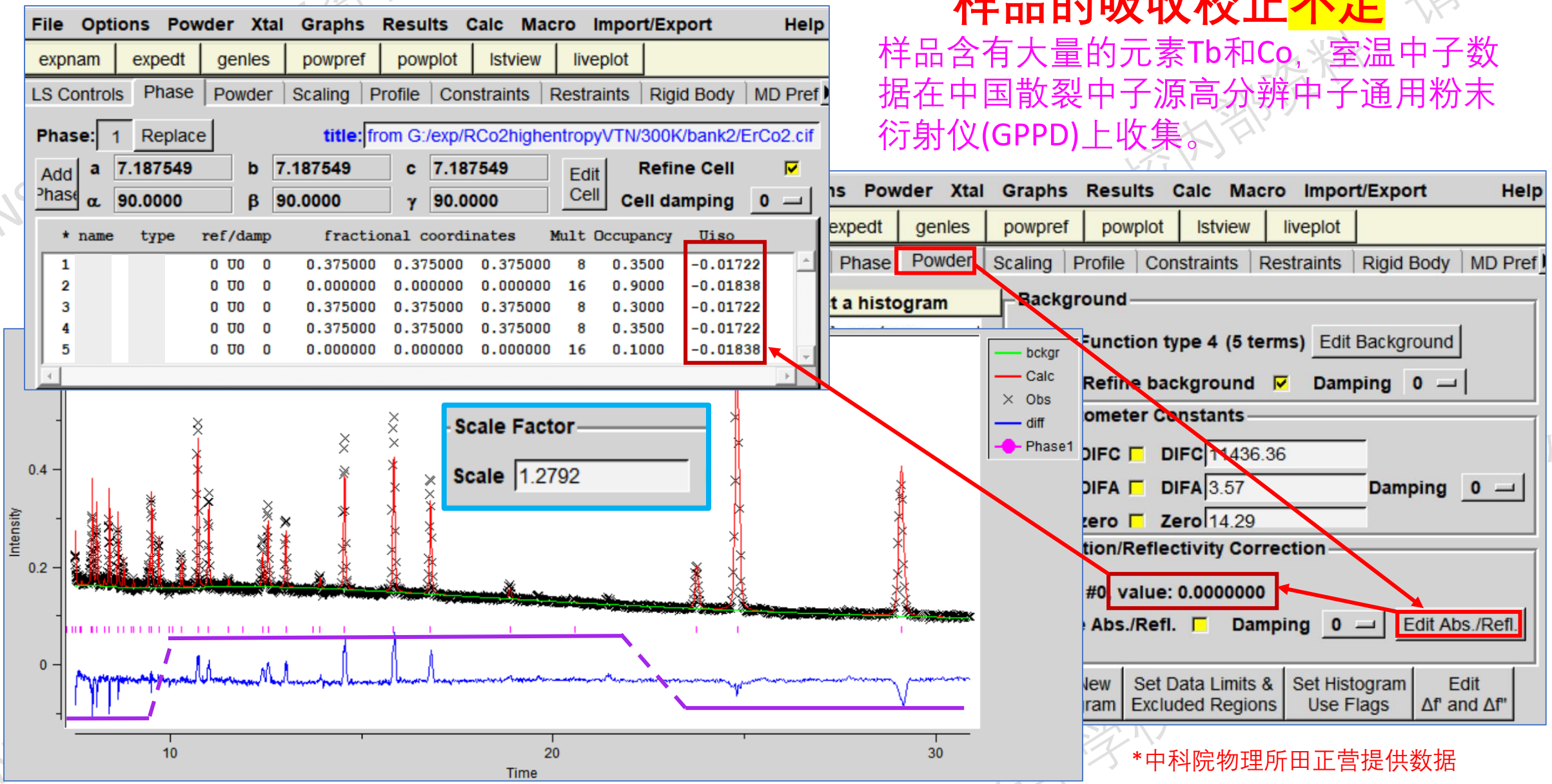


*中科院物理所田正营提供数据

# GSAS-EXPGUI: Powder-Edit Edit Abs./Reff-Absorption

## 样品的吸收校正恰当

| * name | type | ref/damp | | fractional coordinates | | | Mult | Occupancy | Uiso |
|---|---|---|---|---|---|---|---|---|---|
| | | 0 | U0 0 | 0.375000 | 0.375000 | 0.375000 | 8 | 0.3500 | 0.00332 |
| | | 0 | U0 0 | 0.000000 | 0.000000 | 0.000000 | 16 | 0.9000 | 0.00321 |
| | | 0 | U0 0 | 0.375000 | 0.375000 | 0.375000 | 8 | 0.3000 | 0.00332 |
| | | 0 | U0 0 | 0.375000 | 0.375000 | 0.375000 | 8 | 0.3500 | 0.00332 |
| | | 0 | U0 0 | 0.000000 | 0.000000 | 0.000000 | 16 | 0.1000 | 0.00321 |

**Absorption/Reflectivity Correction**

Model #1, value: 0.5500000

Refine Abs./Refl. ☐ Damping 0 Edit Abs./Refl.

**Scale Factor**

Scale 8.0053

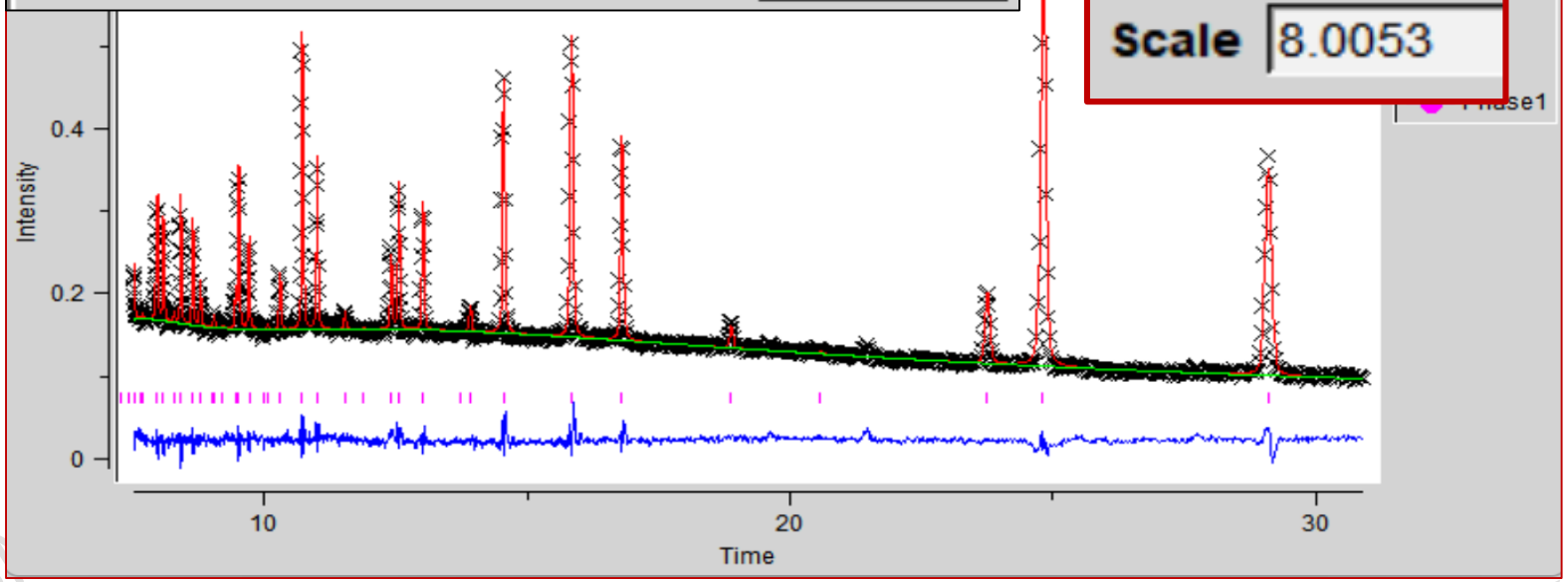


CW-N

**Absorption Coefficient(s)** 1: 0.00000 2: 0.0000000 — **Absorption Function** 0

Correction for cylindrical samples [Lobanov & Alte da Veiga]. OK for all data types, but not for Bragg-Brentano flat-plate geometry. Set term 1 to mu*R/lambda (TOF: mu*R for lambda=1). For CW x-ray/neutron, do not refine!

TOF-N

**Absorption Coefficient(s)** 1: 0.00000 2: 0.0000000 — **Absorption Function** 1

Wavelength-dependent correction for container penetration. Use with TOF & Energy Disp x-ray only.

**Absorption Coefficient(s)** 1: 0.00000 2: 0.0000000 — **Absorption Function** 2

Surface roughness correction [Pitschke, Hermann & Muttern]. Use with flat-plate reflection geometry (usually Bragg-Brentano) only.

**Absorption Coefficient(s)** 1: 0.00000 2: 0.0000000 — **Absorption Function** 3

Surface roughness correction, [Suortti]. Use with flat-plate reflection geometry (usually Bragg-Brentano) only.

**Absorption Coefficient(s)** 1: 0.00000 2: 0.0000000 — **Absorption Function** 4

Flat plate samples in transmission mode. OK for all data types, but not Bragg-Brentano geometry. Term 2 is angle w/r to beam (usually 0). For CW, do not refine.

# GSAS-EXPGUI: Edit Background-Absorption

## 样品的吸收校正过头

| * | name | type | ref/damp | fractional coordinates | | | Mult | Occupancy | Uiso |
|---|---|---|---|---|---|---|---|---|---|
| 1 | | | 0 U0 0 | 0.375000 | 0.375000 | 0.375000 | 8 | 0.3500 | 0.01413 |
| 2 | | | 0 U0 0 | 0.000000 | 0.000000 | 0.000000 | 16 | 0.9000 | 0.01371 |
| 3 | | | 0 U0 0 | 0.375000 | 0.375000 | 0.375000 | 8 | 0.3000 | 0.01413 |
| 4 | | | 0 U0 0 | 0.375000 | 0.375000 | 0.375000 | 8 | 0.3500 | 0.01413 |
| 5 | | | 0 U0 0 | 0.000000 | 0.000000 | 0.000000 | 16 | 0.1000 | 0.01371 |

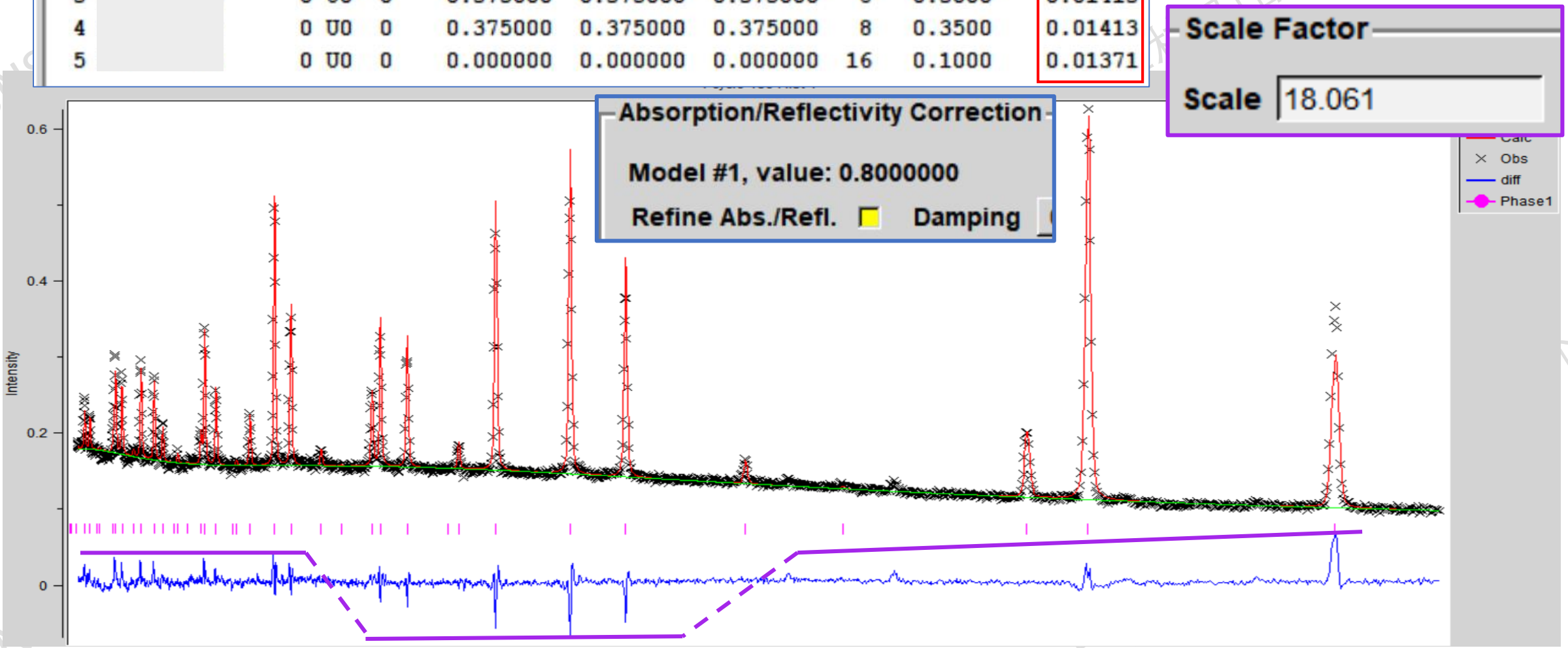

# GSAS-EXPGUI: Constraints

File Options Powder Xtal Graphs Results Calc Macro Import/Export Help

expnam | expedt | genles | powpref | powplot | lstview | liveplot

LS Controls | Phase | Powder | Scaling | Profile | Constraints | Restraints | Rigid Body | MD Pref Orient | SH Pref Orient

| # | | Phase | Atom(s) | Variable | Multiplier | Atom(s) | Variable | Multiplier | Delete |
|---|---|---|---|---|---|---|---|---|---|
| 1 | edit | 1 | 1,5 | X | x 1.0000 | | | | ☐ |
| 2 | edit | 1 | 1,5 | Y | x 1.0000 | | | | ☐ |
| 3 | edit | 1 | 1,5 | UISO | x 1.0000 | | | | ☐ |
| 4 | edit | 1 | 5 | FRAC | x -1.0000 | 1 | FRAC | x 1.0000 | ☐ |

| * | name | type | ref/damp | | | fractional coordinates | | | Mult | Occupancy | Uiso |
|---|---|---|---|---|---|---|---|---|---|---|---|
| 1 | La | LA | X0 | U0 | F0 | -0.004805 | 0.022661 | 0.250000 | 4 | 0.7740 | 0.00403 |
| 2 | Mn | MN+3 | X0 | U0 | 0 | 0.500000 | 0.000000 | 0.000000 | 4 | 1.0000 | 0.00308 |
| 3 | O1 | O | X0 | U0 | 0 | 0.064747 | 0.491805 | 0.250000 | 4 | 1.0000 | 0.00627 |
| 4 | O2 | O | X0 | U0 | 0 | 0.723533 | 0.275049 | 0.033679 | 8 | 1.0000 | 0.00545 |
| 5 | Ca | CA | X0 | U0 | F0 | -0.004805 | 0.022661 | 0.250000 | 4 | 0.2260 | 0.00403 |

# Carbon Content and Temperature Dependence of the $T_c$ and Structure Parameters in the Non-oxide Perovskite Superconductor $MgC_xNi_3$

He T., Huang Q. Z., *et al.*, *Nature*. **411**, 2001, 54-56.

Qingzhen Huang
*China Spallation Neutron Source*

# $T_c$ vs C content for $MgC_xNi_3$

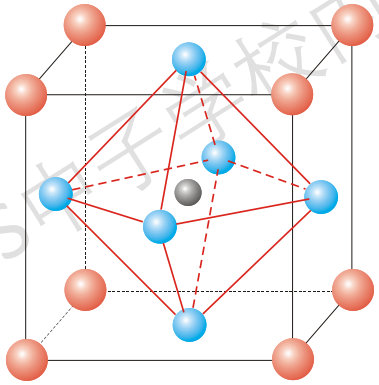


**Structure of Perovskite $ABX_3$**

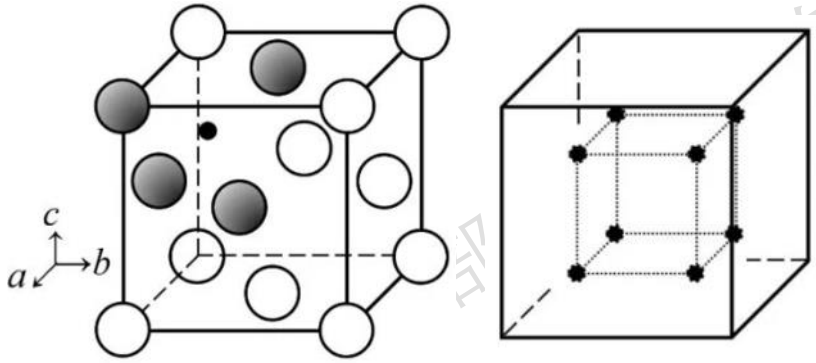


面心立方的四面体间隙及空间排布

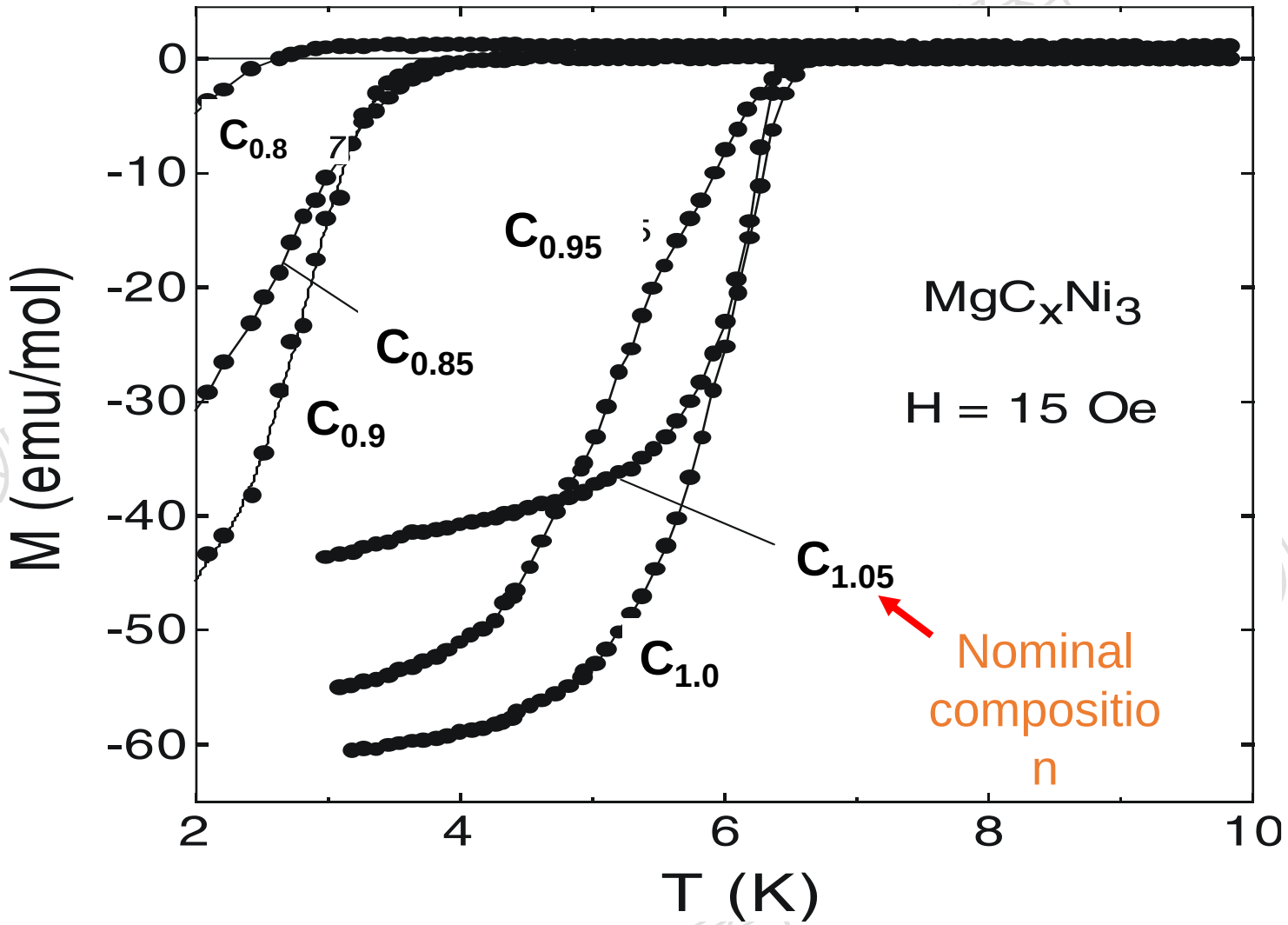

# Neutron diffraction pattern of $MgC_xNi_3$

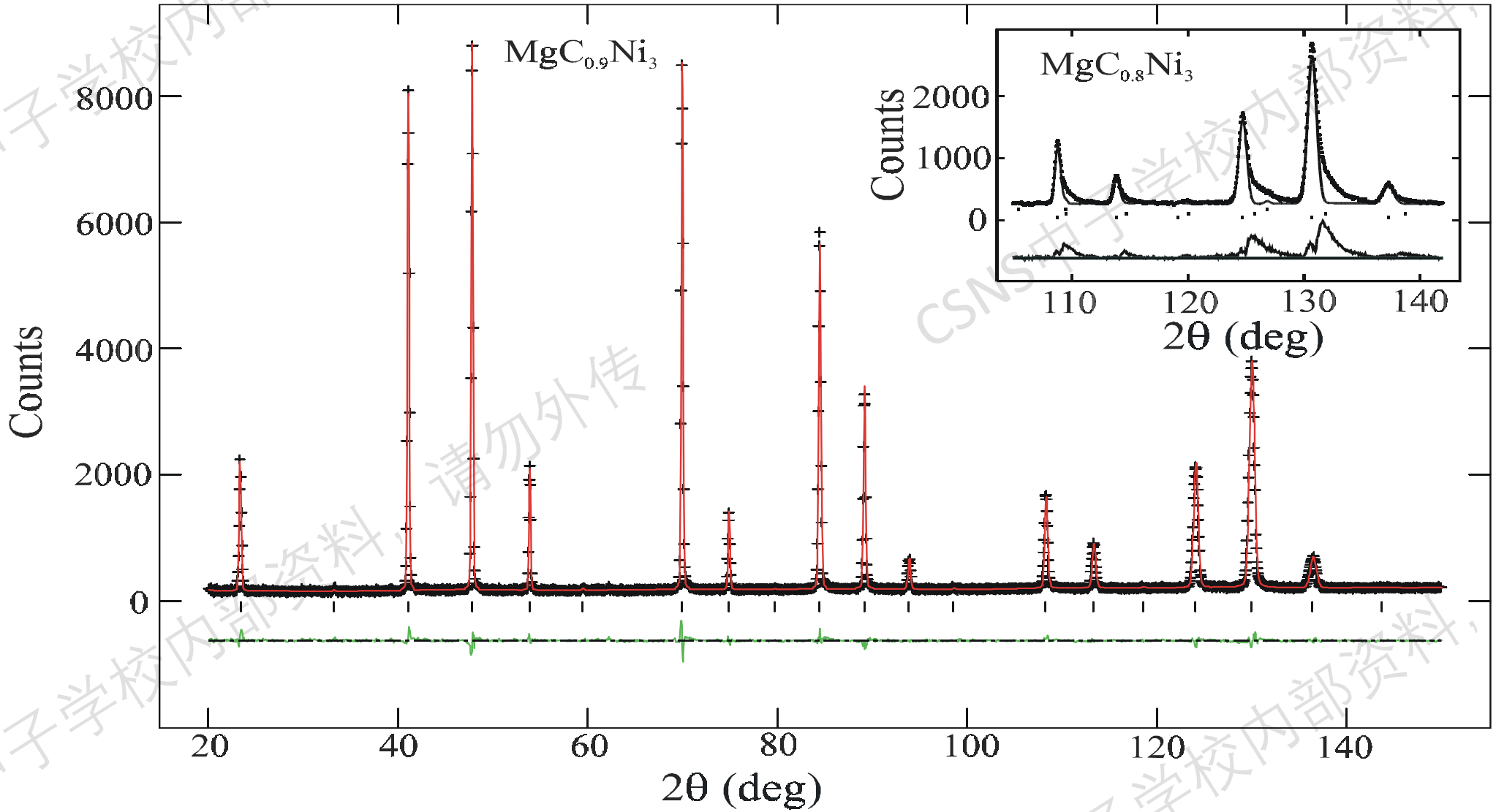

# Constant neutron scattering length gives stronger intensities in higher angle range.

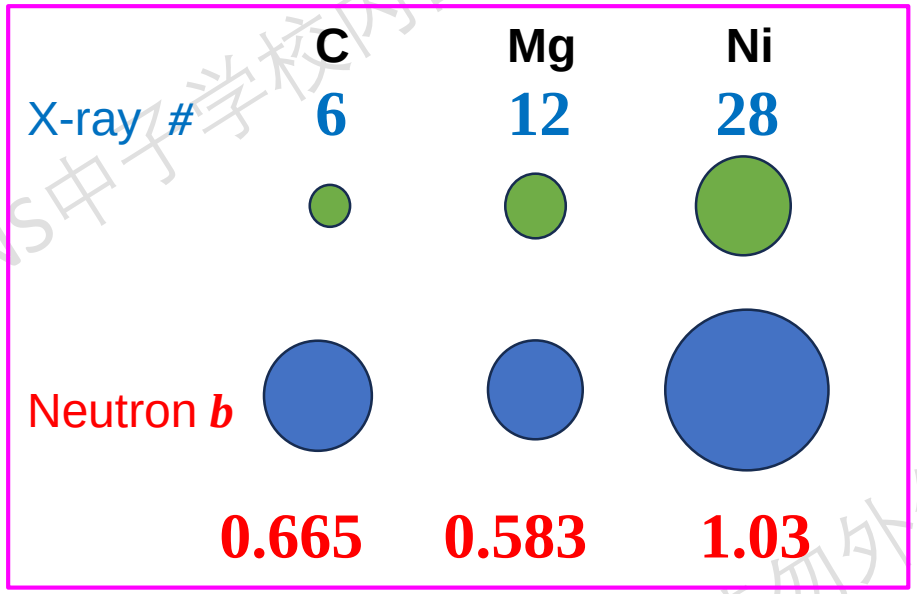


*Ne*(Mg):*Ne*(C):*Ne*(Ni) 0.429:0.214:1

*b*(Mg):*b*(C):*b*(Ni) 0.522:0.646:1

**X-ray**: $|F_{hkl}|^2 = |\sum f_j \exp(2\pi i (hx + ky + lz))|^2 e^{-2W}$

**Neutron**: $|F_{hkl}|^2 = \sum b_j \exp(2\pi i (hx + ky + lz))|^2 e^{-2W}$

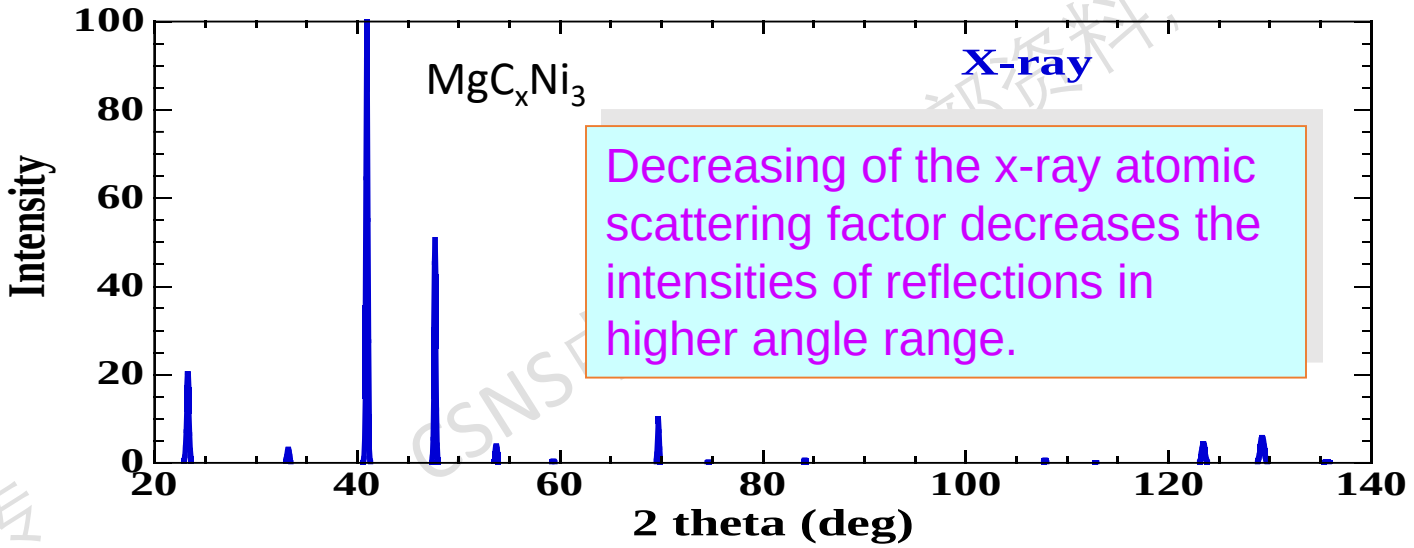


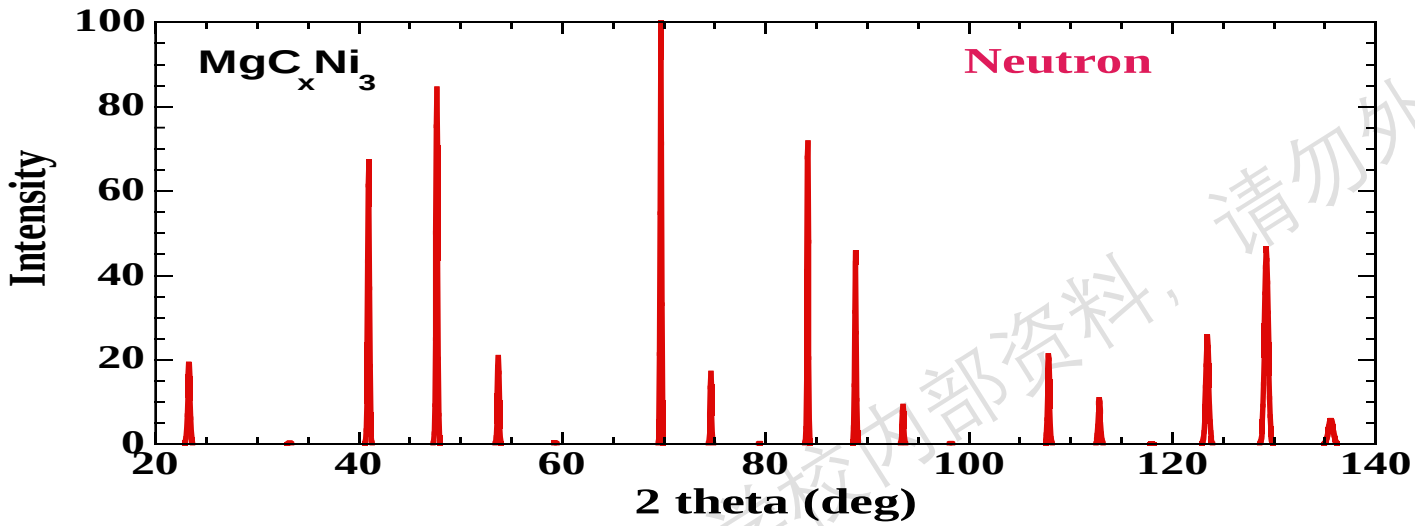

# Differences in Intensities

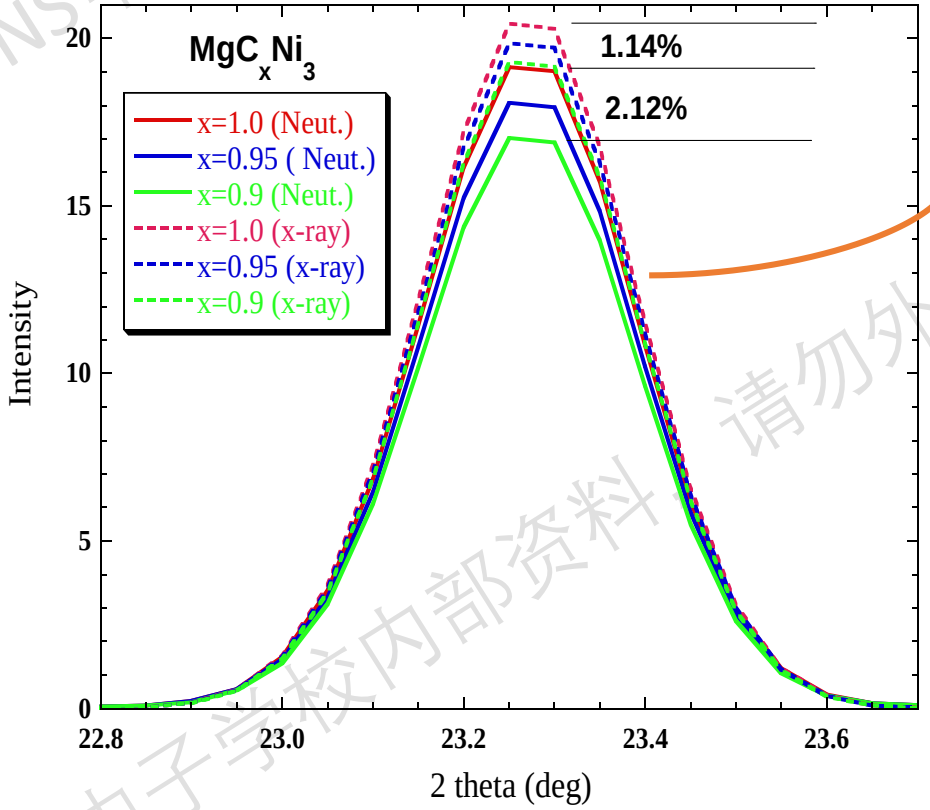


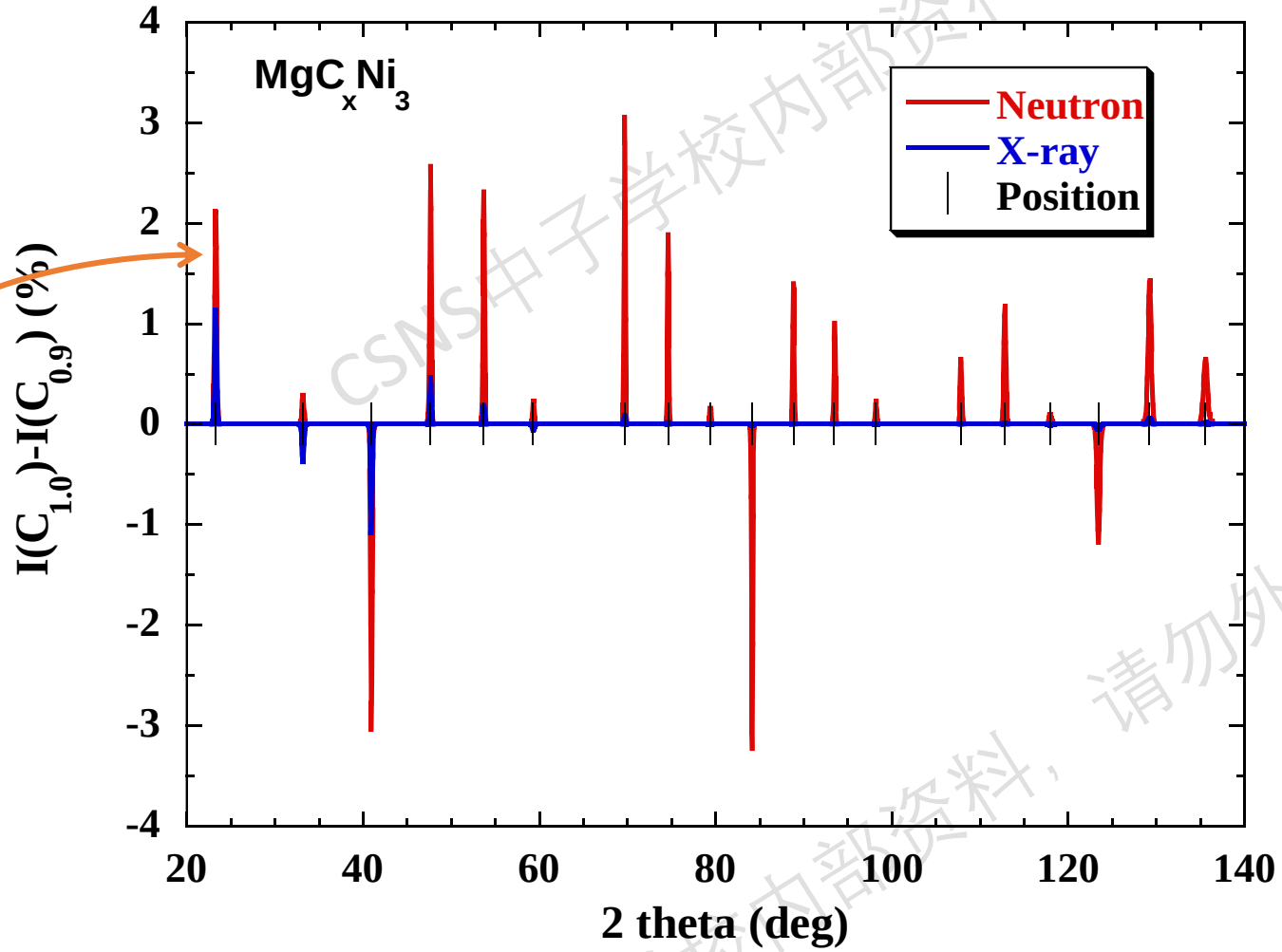

# $MgC_{0.978}Ni_3$, $T_c$=7.30 K

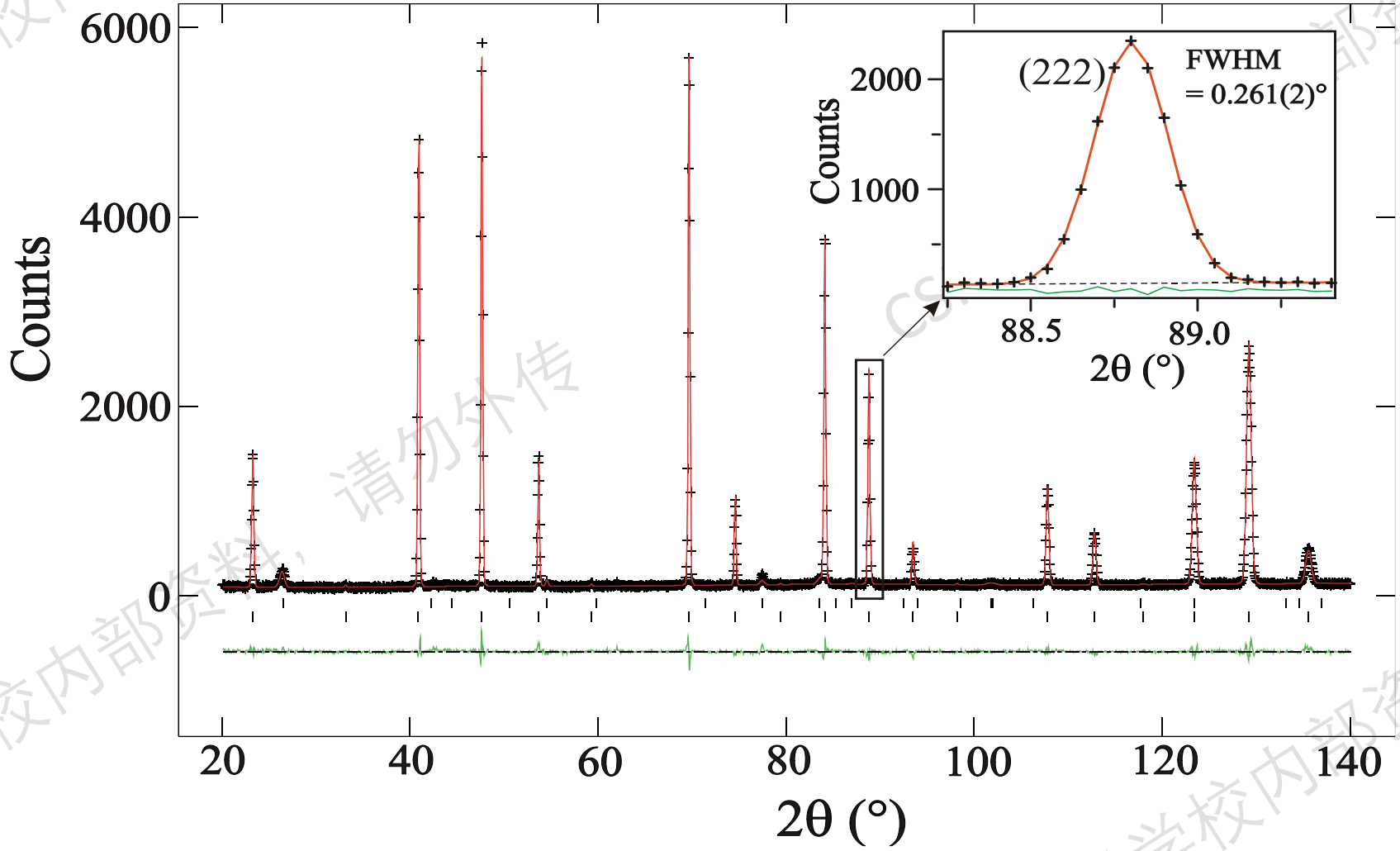

# Table. Structure Information of the $MgC_xNi_3$ Sample

| | | | Phase Fraction (%) | | | a (Å) | | | | |
|---|---|---|---|---|---|---|---|---|---|---|
| $x_{nominal}$ | $T_c$ (K) | $x_{neutron}$ | I | II | III | I | II | $\chi^2$ | $R_p$(%) | $R_{wp}$(%) |
| 1.25 | 7.30 | 0.978(8) | 98.0 | 0.0 | 2.0 | 3.81221(5) | - | 1.191 | 4.49 | 5.95 |
| 1.05 | 6.59 | 0.968(4) | 97.3 | 0.0 | 2.7 | 3.81207(2) | - | 1.166 | 3.32 | 3.84 |
| 1.0 | 6.49 | 0.970(5) | 96.8 | 0.0 | 3.2 | 3.81060(2) | - | 1.174 | 3.79 | 4.76 |
| 0.95 | 6.30 | 0.965(5) | 98.5 | 0.0 | 1.5 | 3.80990(2) | - | 1.413 | 4.15 | 5.36 |
| 0.9 | 3.38 | 0.906(5) | 100 | 0 | 0.0 | 3.80014(2) | - | 1.612 | 4.28 | 5.53 |
| 0.85 | 3.51 | 0.907(6) | 64.0 | 34.6 | 1.4 | 3.80147(5) | 3.78844(23) | 1.311 | 4.13 | 5.31 |
| 0.8 | <1.8 | 0.887(7) | 58.5 | 38.0 | 3.5 | 3.79515(5) | 3.77802(25) | 1.690 | 3.85 | 4.89 |

# $T_c$ vs C content

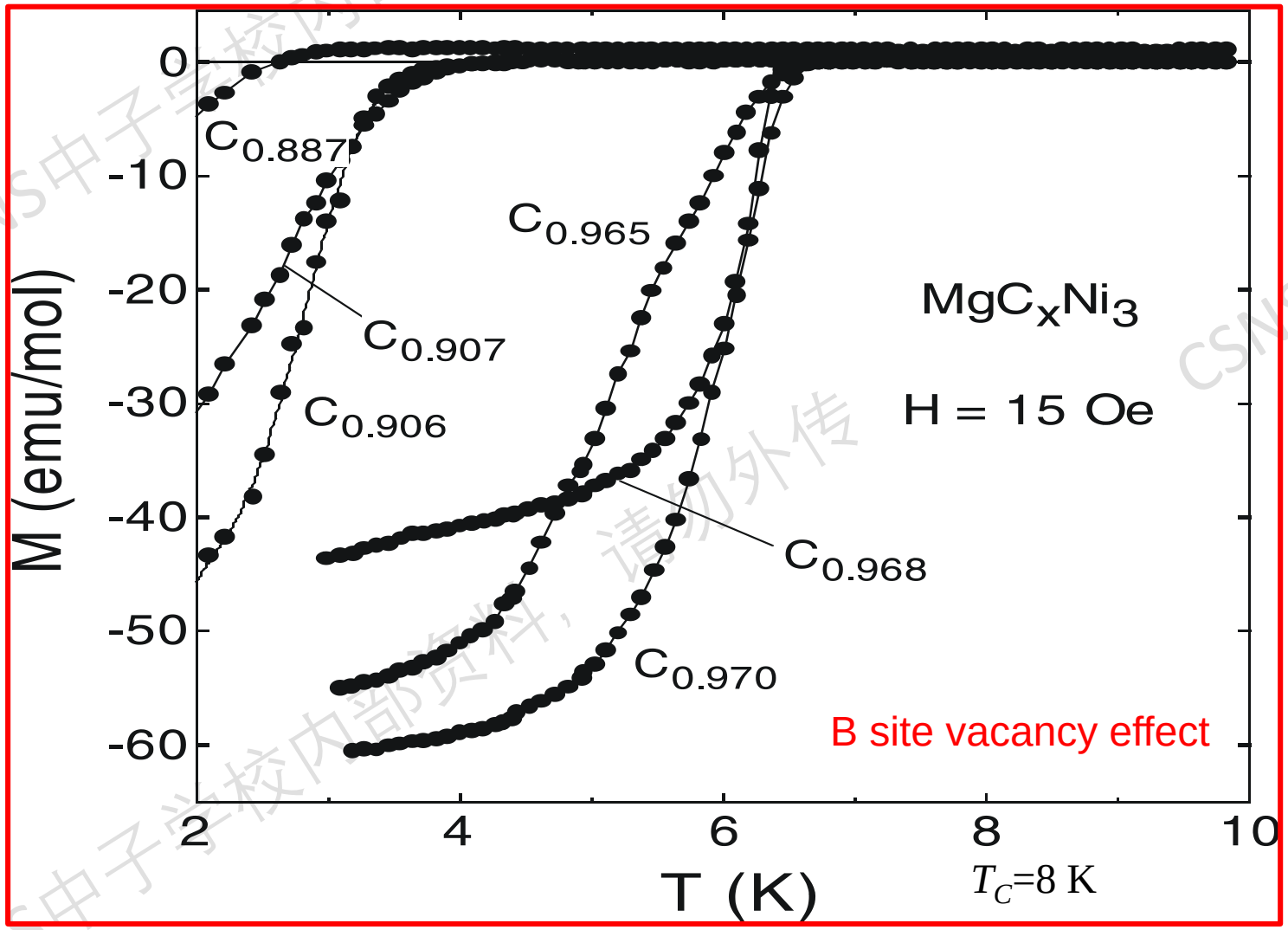


| $x_{nominal}$ | $T_c$ (K) | $x_{neutron}$ |
|---|---|---|
| 1.25 | 7.30 | 0.978(8) |
| 1.05 | 6.59 | 0.968(4) |
| 1.0 | 6.49 | 0.970(5) |
| 0.95 | 6.30 | 0.965(5) |
| 0.9 | 3.38 | 0.906(5) |
| 0.85 | 3.51 | 0.907(6) |
| 0.8 | <1.8 | 0.887(7) |

# Plot of $T_c$ as a Function of Carbon Content x in $MgC_xNi_3$

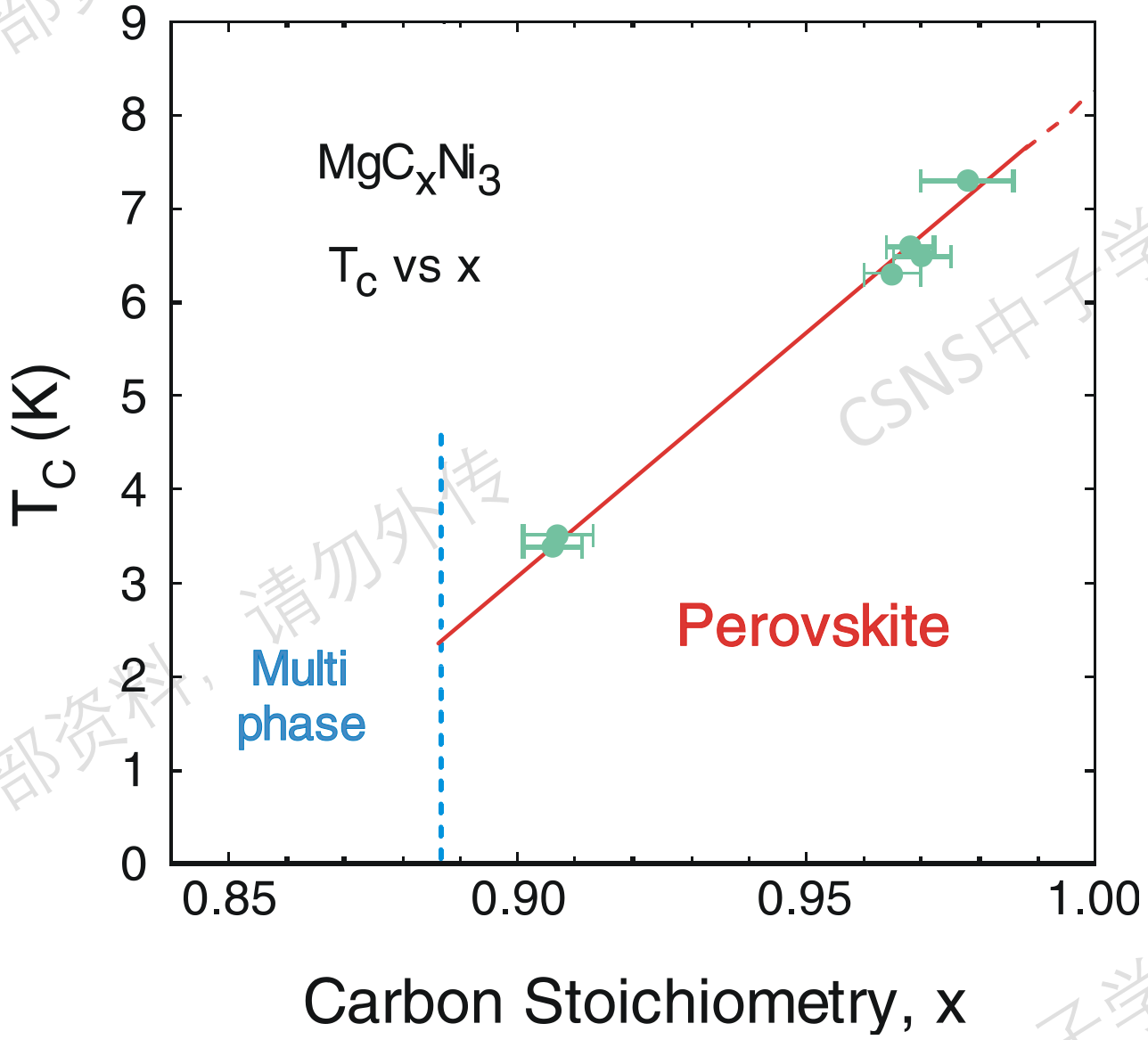

# No Detectable Structural Transition Observed Between 2 and 300 K for $MgC_xNi_3$

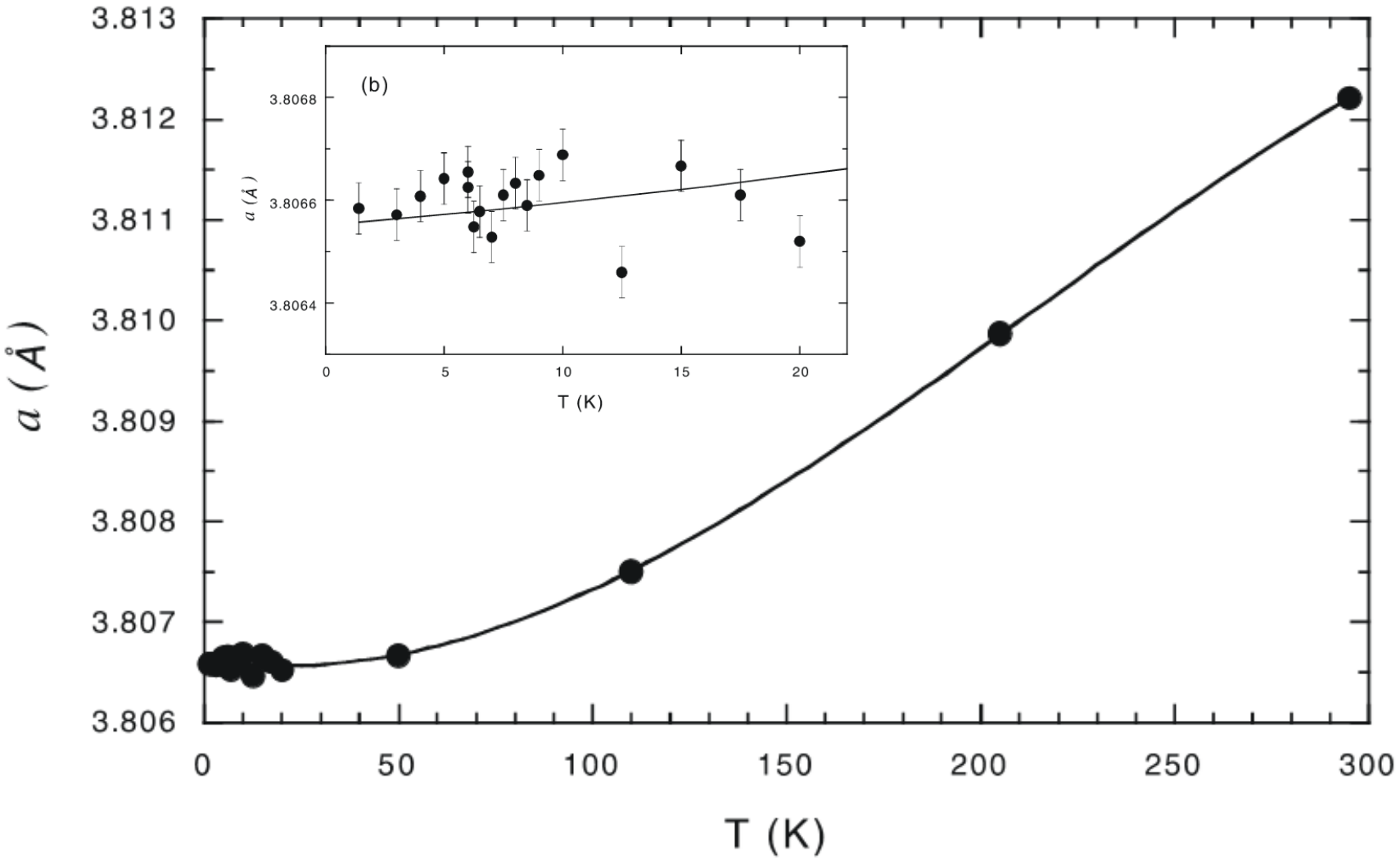

# $MgC_xNi_3$中C的占有率引起的温度因子变化

## Variation of the Temperature Factors as a Function of Carbon Content x for $MgC_xNi_3$

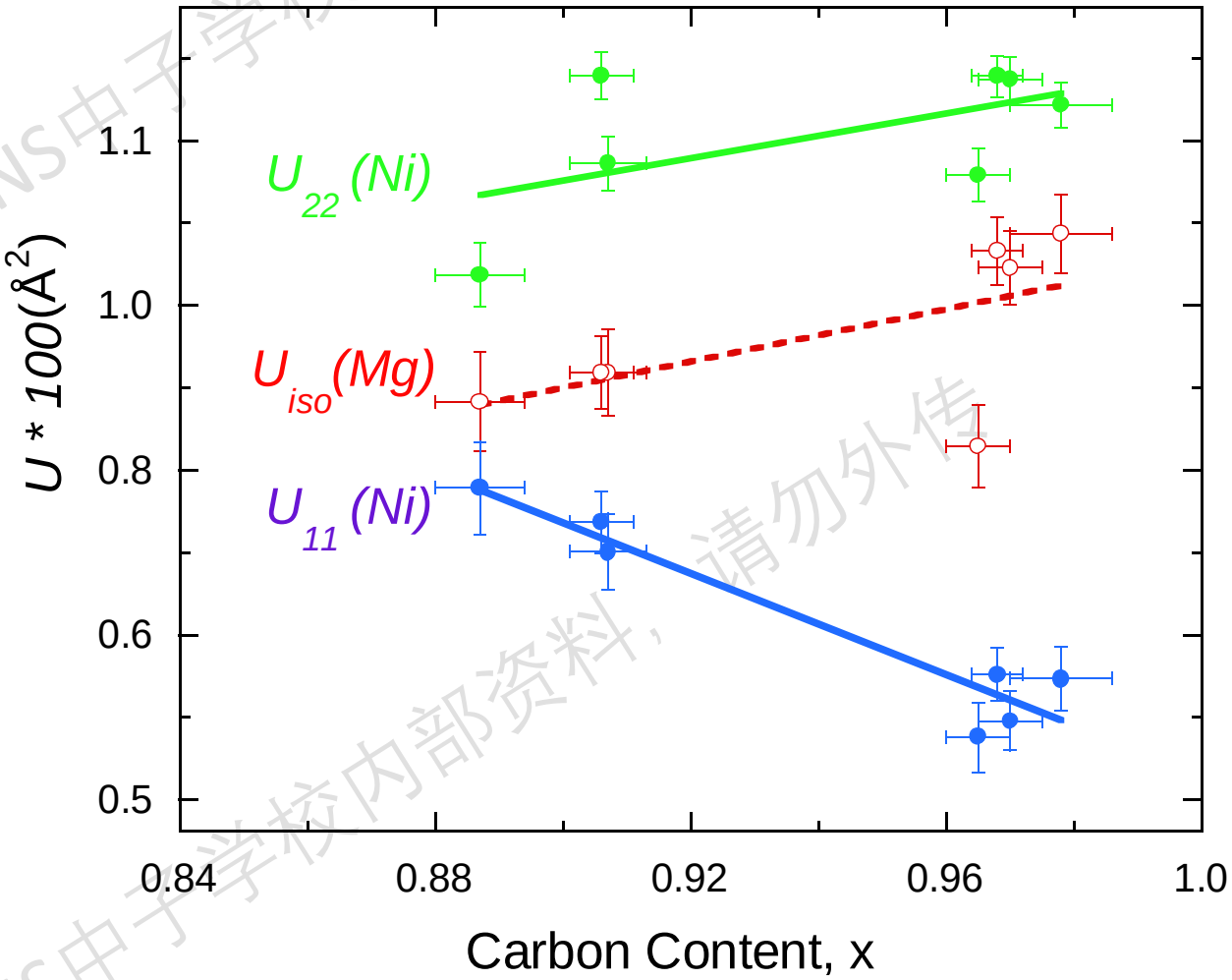


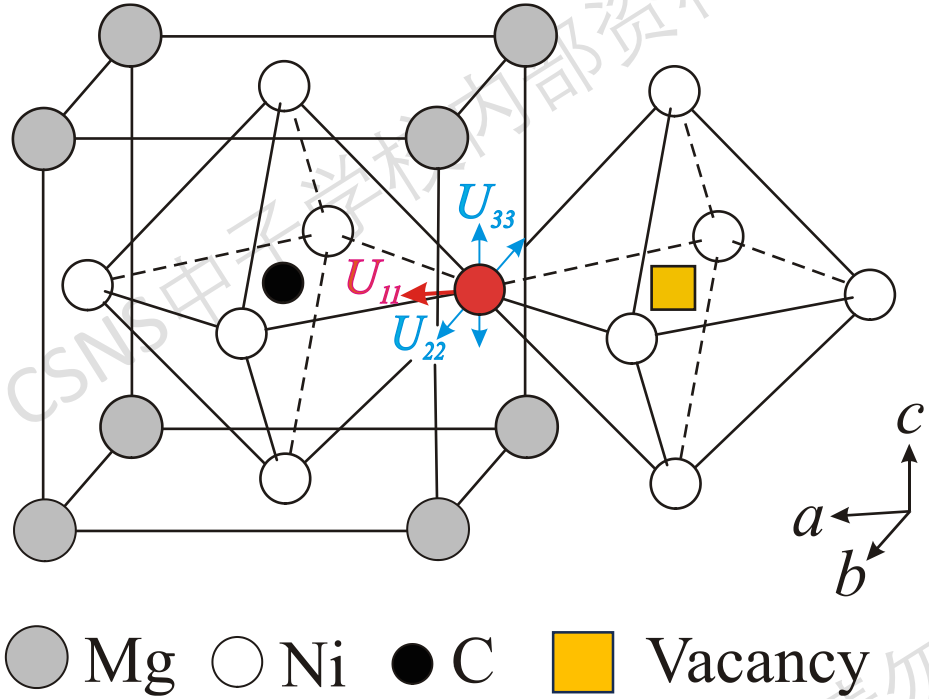


在室温，右图中所示的温度因子$U_{11}$(Ni)随着C的占有率减少而增大，说明当产生C缺位时，近邻Ni向邻近的C原子位移，如上图。

# Neutron intensity showing the short-range graphite peak

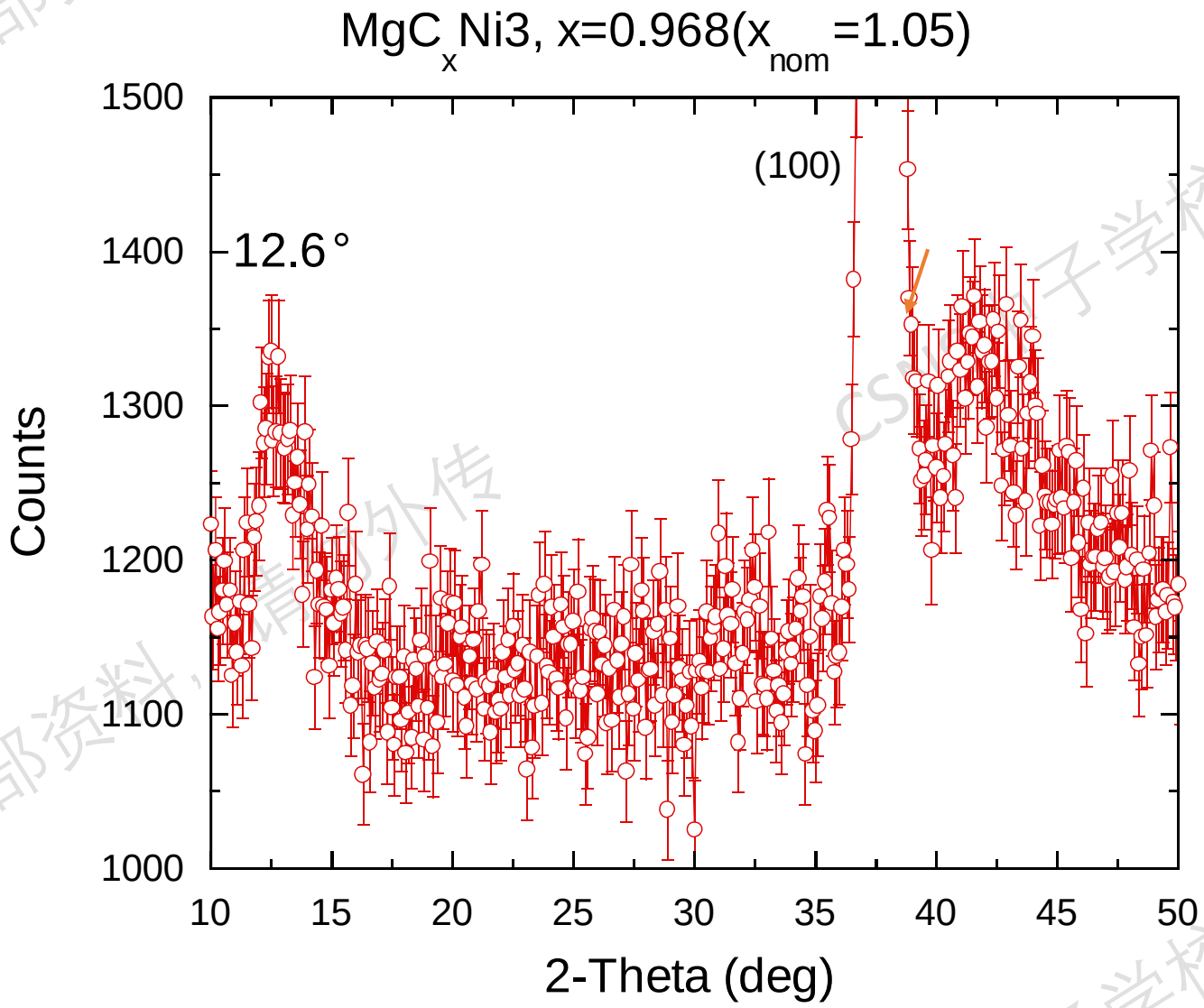

# Summary

* Perovskite phase stability range $0.88 < x < 1.0$ for $MgC_xNi_3$.

* $T_c$ monotonically decreases with decreasing $x$.

* Carbon vacancy affects the position of the Ni atoms.

* No detectable structural transition and magnetic order.

# 结构精化中反常的温度因子与结构的相关性

## Correlation between abnormal temperature factors and structure in structure refinement

$$|F_{hkl}|^2 = |\sum b_j \exp(2\pi i (hx + ky + lz))|^2 e^{-2W}$$

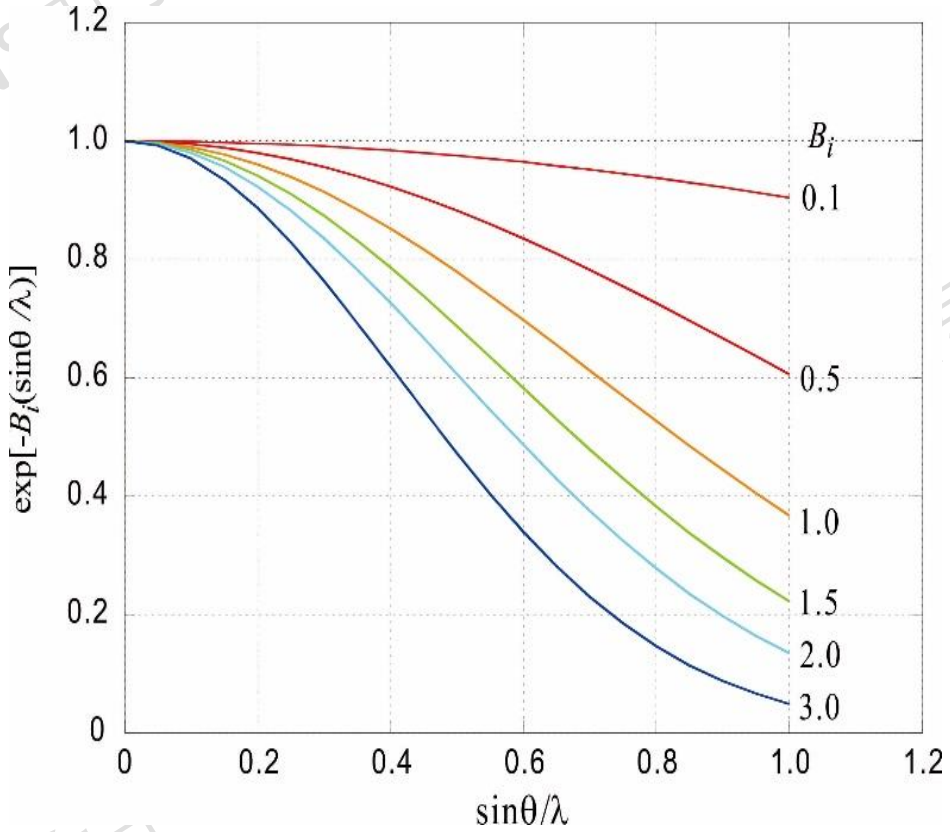


**(a)** $B_i$ 与 $f_i(b_i, q_i)$ 成正比：因此当结构中某个结晶学位置上有空位，或被散射因子小的元素占有， 即是该位置的散射本领偏小，这时 $B_i$ 减小，可以考虑占有率或占位问题；

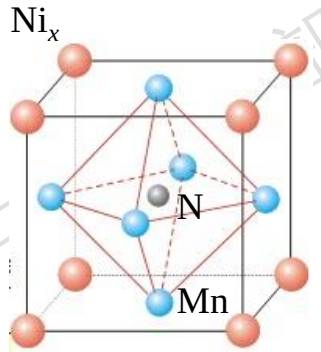


| $x_{Ni}$ | $B_{ISO}$(Å$^2$) |
|---|---|
| 0.6 | -0.43 |
| 1.0 | 0.99 |
| 1.4 | 1.82 |

**(b)** 与原子位置的位移相关：原子位置偏离，或静态位移，或劈裂；

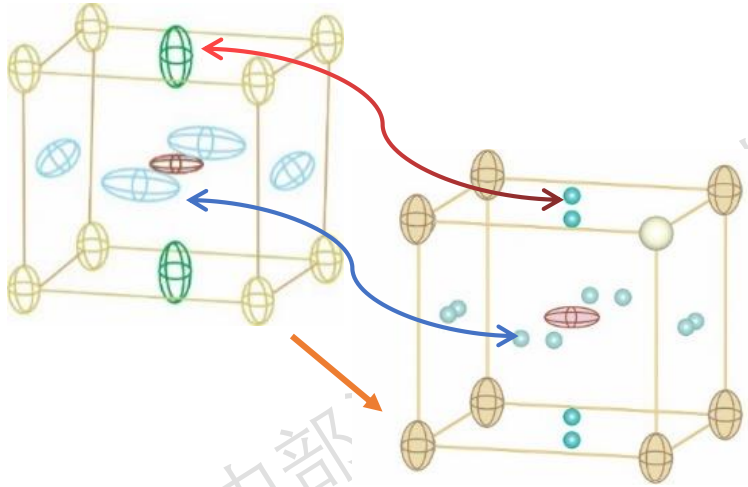

**(c)** 与原子动态位移有关：配位多面体，低键联， 轻元素，各向异性环境等等;

**(d)** 与物性有关：声子振动等。

# 大各向异性温度因子与原子位置的静态位移和占有率

Strong Anisotropic Temperature Factor Associated with Atomic Shift and Occupancy

探询$Ba_2CuO_{4-x}$比$La_{1.85}Sr_{0.15}CuO_4$的超导温度高出33K的原因，了解其晶体结构异同能够提供有力的信息。

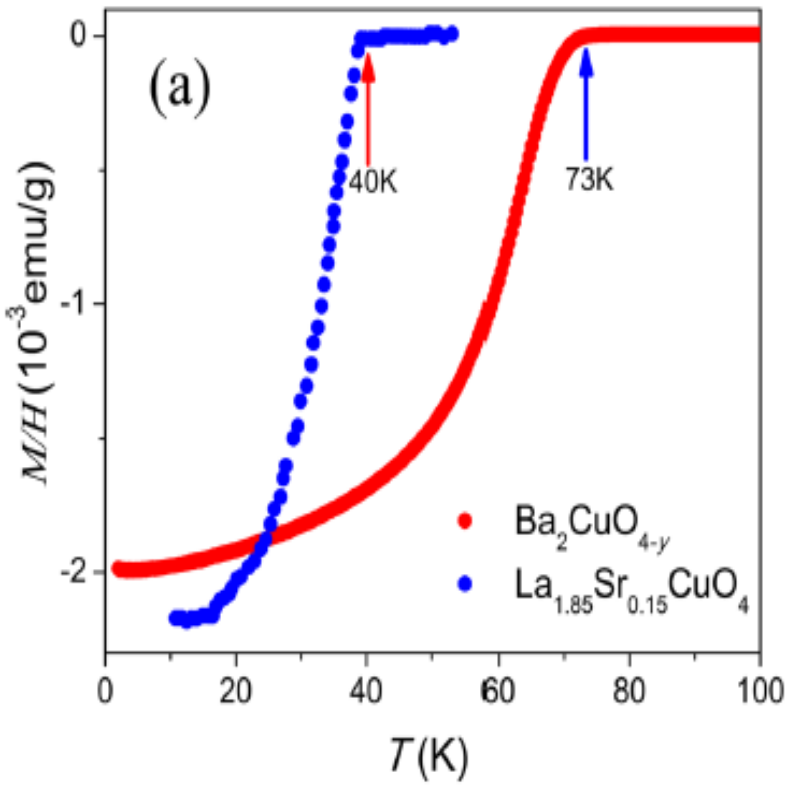


Temperature dependence of field-cooling (FC) dc magnetic susceptibility of Ba214 and optimum doped $La_{1.85}Sr_{0.15}CuO_4$.

Table 1. Refined structure parameters using three different models for $Ba_2CuO_{4-x}$ at 6 K. Space group *I*4/*mmm* (#139), atomic position: Ba: 4*e* (0 0 *z*); Cu: 2*a* (0 0 0); O(1): 4*e* (0 0 *z*); O(2): 4*c* (0, ½, 0); O'(2): 8*j* (*x*, ½, 0); O(11): 4*e* (0 0 *z*); and O(12): 4*e* (0 0 *z*).

Model I. Isotropic temperature and full occupation.

$a = b$ = 3.9931(2) (Å), $c$ = 12.921(1) (Å)

| Atom | *z* | *n* | $100 \times U_{iso}$ (Å$^2$) |
|---|---|---|---|
| Ba | 0.3570(5) | 1 | -1.1(2) |
| Cu | 0 | 1 | -0.5(2) |
| O(1) | 0.1453(4) | 1 | 0.9(2) |
| O(2) | 0 | 1 | 9.9(4) |

$R_{WP}$ = 5.03%, $R_P$ = 3.97%, $\chi^2$ = 2.200

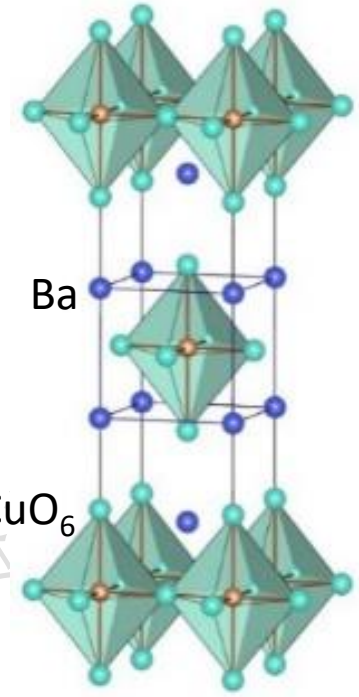


**O(2)的温度因子大暗示其占有率或/和偏离现有的位置**

W. M. Li, *et al*. Journal of Superconductivity and Novel Magnetism (2020) 33:81–85 ; W. M. Li, *et al*. PNAS, 116, 12156, (2019).

Table. Refined structure parameters using three different models for $Ba_2CuO_{4-x}$ at 6 K. Space group *I*4/*mmm* (#139), atomic position: Ba: 4*e* (0 0 *z*); Cu: 2*a* (0 0 0); O(1): 4*e* (0 0 *z*); O(2): 4*c* (0, ½, 0); O'(2): 8*j* (*x*, ½, 0); O(11): 4*e* (0 0 *z*); and O(12): 4*e* (0 0 *z*).

Model II. Isotropic temperature.

*a* = *b* = 3.9931(2) (Å), *c* = 12.921(1) (Å)

| Atom | *z* | *n* | 100 × $U_{iso}$ (Å$^2$) |
|---|---|---|---|
| Ba | 0.3580(4) | 1 | 0.3(1) |
| Cu | | 1 | 0.7(2) |
| O(1) | 0.1436(4) | 1 | 2.3(2) |
| O(2) | | 0.58(2) | 3.6(4) |

$R_{WP}$ = 4.37%, $R_P$ = 3.47%, $\chi^2$ = 1.665

Model III. Anisotropic temperature.

*a* = *b* = 3.9932(2) (Å), *c* = 12.919(1) (Å)

| Atom | *z* | *n* | $U_{11}$ (Å$^2$) | $U_{22}$ (Å$^2$) | $U_{33}$ (Å$^2$) |
|---|---|---|---|---|---|
| Ba | 0.3576(4) | 1 | 0.2(2) | =$U_{11}$ | 0.9(4) |
| Cu | 0 | 1 | 1.8(3) | =$U_{11}$ | 0 |
| O(1) | 0.1446(4) | 1 | 1.6(2) | =$U_{11}$ | **4.7(5)** |
| O(2) | 0 | 0.58(2) | **13(1)** | 2.2(7) | 0 |

$R_{WP}$ = 4.19%, $R_P$ = 3.29%, $\chi^2$ = 1.532

Model II 的结构中O(2)有42%的空位，但O(1)和O(2)的各向同性温度因子偏大，这可能是由于空位引起原子位置的静态位移。

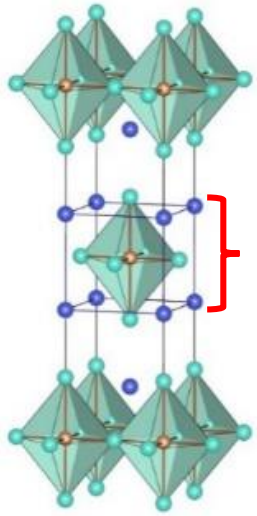

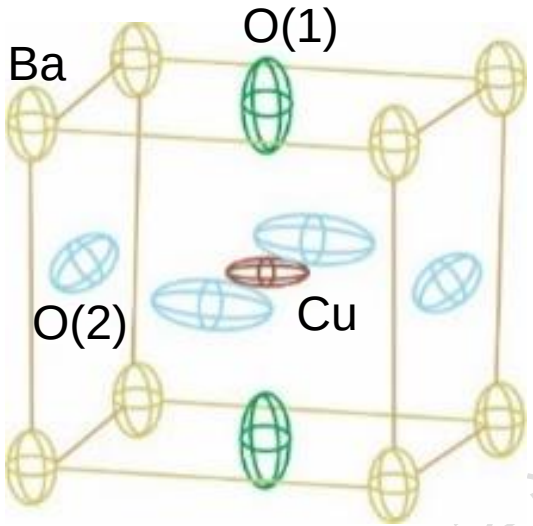


Model III 各个原子位置的各向异性温度因子的精修结果，*R*因子有了明显减小。其中BaO层的Ba原子和O(1)的$U_{33}$明显偏大，而$CuO_2$层中的Cu原子和O(2)的$U_{11}$也明显偏大。

Table. Refined structure parameters using three different models for $Ba_2CuO_{4-x}$ at 6 K. Space group *I*4/*mmm* (#139), atomic position: Ba: 4*e* (0 0 *z*); Cu: 2*a* (0 0 0); O(1): 4*e* (0 0 *z*); O(2): 4*c* (0, ½, 0); O'(2): 8*j* (*x*, ½, 0); O(11): 4*e* (0 0 *z*); and O(12): 4*e* (0 0 *z*).

Model IV. Oxygen atoms splitting. $R_{WP}$ = 4.16%, $R_P$ = 3.26%, $\chi^2$ = 1.511

*a* = *b* = 3.9932(2) (Å), *c* = 12.919(1) (Å).

| Atom | *x* | *z* | *n* | $U_{iso}$ (Å$^2$) | $U_{11}$ (Å$^2$) | $U_{22}$ (Å$^2$) | $U_{33}$ (Å$^2$) ×100 |
|---|---|---|---|---|---|---|---|
| Ba | 0 | 0.3577(4) | 1 | | 0.0 | =$U_{11}$ | 0.9(3) |
| Cu | 0 | 0 | 1 | | 1.8(3) | =$U_{11}$ | 0 |
| O(11) | 0 | 0.132(1) | 0.5 | 1.5(2) | | | |
| O(12) | 0 | 0.157(1) | 0.5 | 1.5(2) | | | |
| O'(2) | 0.077(4) | 0 | 0.297(8) | 0.8(5) | | | |

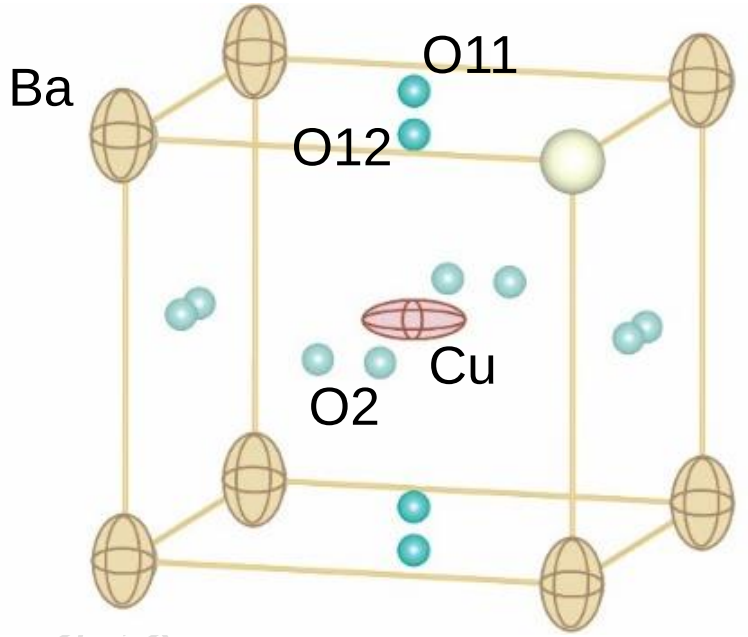


Model IV 的结构中O(1)以及Cu和O(2)各沿着向$U_{33}$和及$U_{11}$的方向劈裂成两个位置，如上图所示。

# 温度因子反映原子位置的静态位移和占有率

Ba-O1: 2.751(6)　　Cu-O1: 1.868(5) × 2;
2.8238(2) × 4　Cu-O2: 1.9967(1) × 2.4
Ba-O2: 2.715(4) × 2.4

$V(Cu^{2+}\text{-}O11)=0.920 \times 2=1.84$
$V(Cu^{2+}\text{-}O12)=0.387 \times 2=0.774$
$V(Cu^{1+}\text{-}O11)=0.728 \times 2=1.456$
$V(Cu^{1+}\text{-}O12)=0.307 \times 2=0.307$

$V(Cu^{2+}\text{-}O2)= 0.398 \times 2.4=0.955$
$V(Cu^{1+}\text{-}O12)=0.315 \times 2.4=0.756$

$V(Cu^{2+})=2.217$
$V(Cu^{1+})=1.711$

晶体结构研究发现Ba214与其它214等在结构上最大的不同是氧八面体沿着c方向被压缩，使得在面上的Cu-O键长比顶端的Cu-O键长更长。

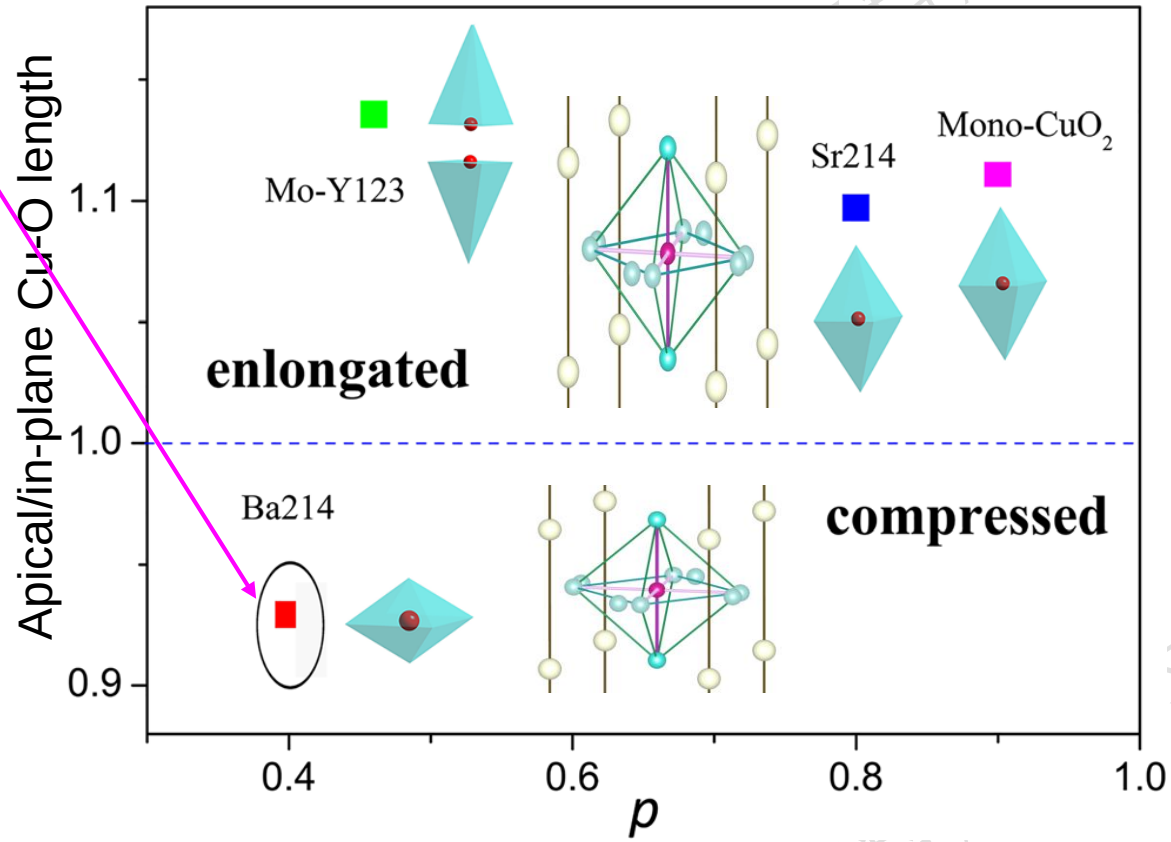


The ratio between the bond lengths of in-plane Cu–O and copper apical oxygen of heavily over doped cuprates $Cu_{0.75}Mo_{0.25}Sr_2YCu_2O_{7.54}$ (Mo-Y123), monolayer $CuO_2$ (Mono-$CuO_2$), and $Sr_2CuO_{4-\delta}$ (Sr214), compared with Ba214.

# Crystal structure and possible Cu-$O_x$ polyhedron in $Ba_2CuO_{3.2}$

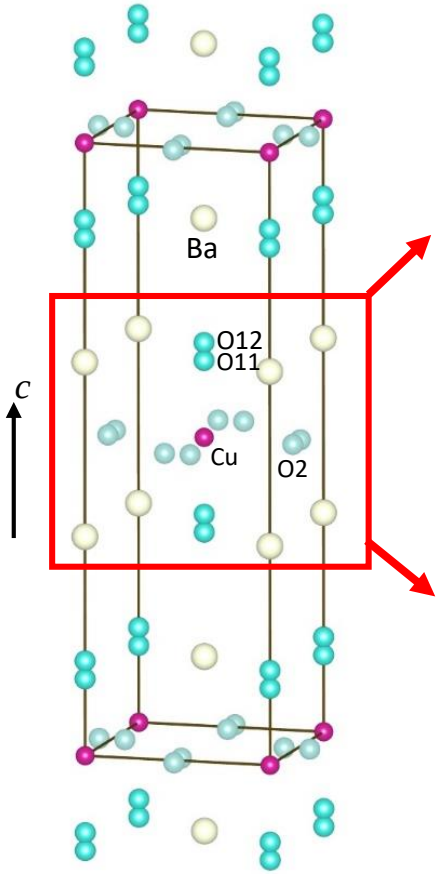


Disordered structure

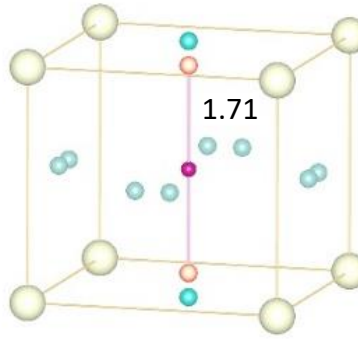


$V_{BVC}$=1.84-0.774
$V_{BVC-A}$=1.2

a) Dumbbell

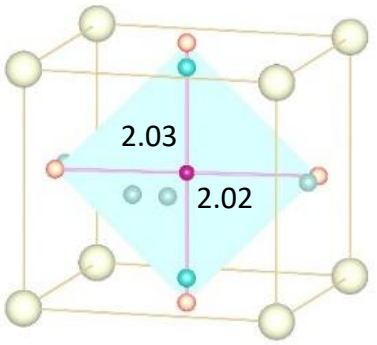


$V_{BVC}$=2.636-1.57, $V_{ch}$=2+
$V_{BVC-A}$=2.048

b) Square plane

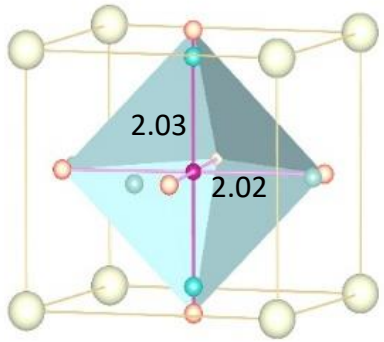


$V_{BVC}$=3.432-2.366, $V_{ch}$ =4+
$V_{BVC-A}$=2.896

c) Octahedron

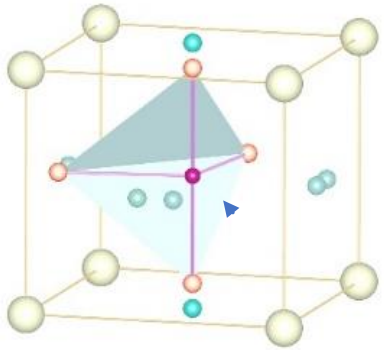

$V_{BVC}$=2.636-1.57, $V_{ch}$ =2+
$V_{BVC-A}$=2.048

d) Tetrahedron

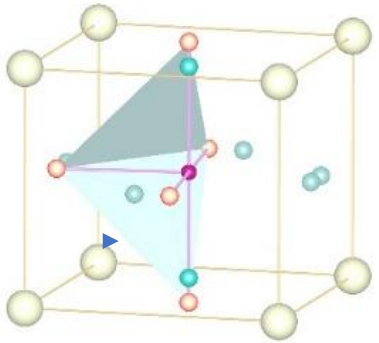

$V_{Cu}$=3.034-1.968, $V_{ch}$ =3+
$V_{BVC-A}$=2.472

e) Pyramid

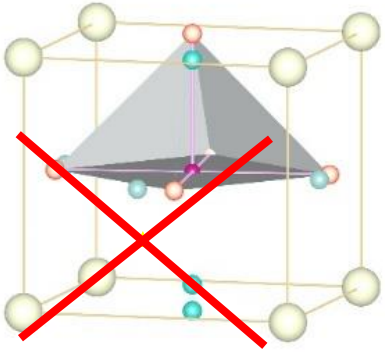

f) Pyramid

Possible polyhedron

# 根据实验测得的键长，用表中的数据计算离子的价态

$V_i = \sum_j v_{ij}$, $v_{ij} = \exp[(R_{ij} - d_{ij})/b]$, e=2.71828, b=0.37, $d_{ij}$ is bond distance

Recommended bond-valence parameters for oxides, fluorides and chlorides

| Cation | O | F | Cl |
|---|---|---|---|
| $Ac^{III}$ | 2·24 | *2·13* | *2·63* |
| $Ag^{I}$ | 1·805 | 1·80 | 2·09 |
| $Al^{III}$ | 1·651 | 1·545 | 2·03 |
| $Am^{III}$ | 2·11 | *2·00* | *2·48* |
| $As^{III}$ | 1·789 | 1·70 | 2·16 |
| $As^{V}$ | 1·767 | 1·62 | *2·14* |
| $Au^{III}$ | 1·833 | 1·81 | 2·17 |
| $B^{III}$ | 1·371 | 1·31 | 1·74 |
| $Ba^{II}$ | 2·29 | 2·19 | 2·69 |
| $Be^{II}$ | 1·381 | 1·28 | *1·76* |
| $Bi^{III}$ | 2·09 | 1·99 | 2·48 |
| $Bi^{V}$ | 2·06 | 1·97 | *2·44* |
| $Bk^{III}$ | 2·08 | *1·96* | *2·46* |
| $Br^{VII}$ | 1·81 | *1·72* | *2·19* |
| $C^{IV}$ | 1·39 | 1·32 | 1·76 |
| $Ca^{II}$ | 1·967 | 1·842 | 2·37 |
| $Cd^{II}$ | 1·904 | 1·811 | 2·23 |
| $Ce^{III}$ | 2·151 | 2·036 | 2·52 |
| $Ce^{IV}$ | 2·028 | 1·995 | *2·41* |
| $Cf^{III}$ | 2·07 | 1·95 | 2·45 |
| $Cl^{VII}$ | 1·632 | *1·55* | *2·00* |
| $Cm^{III}$ | 2·23 | *2·12* | *2·62* |
| $Co^{II}$ | 1·692 | 1·64 | 2·01 |
| $Co^{III}$ | 1·70 | *1·62* | 2·05 |
| $Cr^{II}$ | *1·73* | 1·67 | 2·09 |
| $Cr^{III}$ | 1·724 | 1·64 | 2·08 |
| $Cr^{VI}$ | 1·794 | 1·74 | 2·12 |
| $Cs^{I}$ | 2·42 | 2·33 | 2·79 |
| $Cu^{I}$ | 1·593 | *1·6* | 1·85 |
| $Cu^{II}$ | 1·679 | 1·60 | 2·00 |

| Cation | O | F | Cl |
|---|---|---|---|
| $Mn^{IV}$ | 1·753 | 1·71 | *2·13* |
| $Mn^{VII}$ | 1·79 | 1·72 | *2·17* |
| $Mo^{VI}$ | 1·907 | *1·81* | 2·28 |
| $N^{III}$ | 1·361 | 1·37 | 1·75 |
| $N^{V}$ | 1·432 | *1·36* | *1·80* |
| $Na^{I}$ | 1·80 | 1·677 | 2·15 |
| $Nb^{V}$ | 1·911 | 1·87 | 2·27 |
| $Nd^{III}$ | 2·117 | 2·008 | 2·492 |
| $Ni^{II}$ | 1·654 | 1·599 | 2·02 |
| $Os^{IV}$ | 1·811 | *1·72* | *2·19* |
| $P^{V}$ | 1·604 | 1·521 | 1·99 |
| $Pb^{II}$ | 2·112 | 2·03 | 2·53 |
| $Pb^{IV}$ | 2·042 | *1·94* | 2·43 |
| $Pd^{II}$ | 1·792 | 1·74 | 2·05 |
| $Pr^{III}$ | 2·135 | 2·022 | 2·50 |
| $Pt^{II}$ | 1·768 | *1·68* | 2·05 |
| $Pt^{IV}$ | 1·879 | 1·759 | 2·17 |
| $Pu^{III}$ | 2·11 | 2·00 | 2·48 |
| $Rb^{I}$ | 2·26 | 2·16 | 2·65 |
| $Re^{VII}$ | 1·97 | 1·86 | 2·23 |
| $Rh^{III}$ | 1·791 | 1·71 | *2·17* |
| $Ru^{IV}$ | 1·834 | 1·74 | 2·21 |
| $S^{IV}$ | 1·644 | 1·60 | *2·02* |
| $S^{VI}$ | 1·624 | 1·56 | 2·03 |
| $Sb^{III}$ | 1·973 | 1·90 | 2·35 |
| $Sb^{V}$ | 1·942 | 1·80 | 2·30 |
| $Sc^{III}$ | 1·849 | 1·76 | *2·23* |
| $Se^{IV}$ | 1·811 | 1·73 | 2·22 |
| $Se^{VI}$ | 1·788 | 1·69 | *2·16* |
| $Si^{IV}$ | 1·624 | 1·58 | 2·03 |

| Cation | O | F | Cl |
|---|---|---|---|
| $Dy^{III}$ | 2·036 | 1·922 | 2·41 |
| $Er^{III}$ | 2·010 | 1·906 | 2·39 |
| $Eu^{II}$ | 2·147 | 2·04 | 2·53 |
| $Eu^{III}$ | 2·076 | 1·961 | 2·455 |
| $Fe^{II}$ | 1·734 | 1·65 | 2·06 |
| $Fe^{III}$ | 1·759 | 1·67 | 2·09 |
| $Ga^{III}$ | 1·730 | 1·62 | 2·07 |
| $Gd^{III}$ | 2·065 | 1·95 | 2·445 |
| $Ge^{IV}$ | 1·748 | 1·66 | 2·14 |
| $H^{I}$ | 0·95 | 0·92 | 1·28 |
| $Hf^{IV}$ | 1·923 | 1·85 | *2·30* |
| $Hg^{I}$ | 1·90 | *1·81* | *2·28* |
| $Hg^{II}$ | 1·93 | 1·90 | 2·25 |
| $Ho^{III}$ | 2·023 | 1·908 | 2·401 |
| $I^{V}$ | 2·00 | *1·90* | *2·38* |
| $I^{VII}$ | 1·93 | 1·83 | *2·31* |
| $In^{III}$ | 1·902 | 1·79 | *2·28* |
| $Ir^{V}$ | 1·916 | 1·82 | 2·30 |
| $K^{I}$ | 2·13 | 1·99 | 2·52 |
| $La^{III}$ | 2·172 | 2·057 | 2·545 |
| $Li^{I}$ | 1·466 | 1·360 | 1·91 |
| $Lu^{III}$ | 1·971 | 1·876 | 2·361 |
| $Mg^{II}$ | 1·693 | 1·581 | 2·08 |
| $Mn^{II}$ | 1·790 | 1·698 | 2·13 |
| $Mn^{III}$ | 1·760 | 1·66 | *2·14* |

| Cation | O | F | Cl |
|---|---|---|---|
| $Sm^{III}$ | 2·088 | 1·977 | 2·466 |
| $Sn^{II}$ | 1·984 | 1·925 | *2·36* |
| $Sn^{IV}$ | 1·905 | 1·84 | 2·28 |
| $Sr^{II}$ | 2·118 | 2·019 | 2·51 |
| $Ta^{V}$ | 1·920 | 1·88 | 2·30 |
| $Tb^{III}$ | 2·049 | 1·936 | 2·427 |
| $Te^{IV}$ | 1·977 | 1·87 | 2·37 |
| $Te^{VI}$ | 1·917 | 1·82 | *2·30* |
| $Th^{IV}$ | 2·167 | 2·07 | *2·55* |
| $Ti^{III}$ | 1·791 | 1·723 | *2·17* |
| $Ti^{IV}$ | 1·815 | 1·76 | *2·19* |
| $Tl^{I}$ | 2·172 | 2·15 | *2·56* |
| $Tl^{III}$ | 2·003 | 1·88 | 2·32 |
| $Tm^{III}$ | 2·000 | 1·842 | 2·38 |
| $U^{IV}$ | 2·112 | 2·034 | 2·48 |
| $U^{VI}$ | 2·075 | 1·966 | 2·46 |
| $V^{III}$ | 1·743 | 1·702 | *2·19* |
| $V^{IV}$ | 1·784 | 1·70 | *2·16* |
| $V^{V}$ | 1·803 | 1·71 | 2·16 |
| $W^{VI}$ | 1·921 | 1·83 | 2·27 |
| $Y^{III}$ | 2·014 | 1·904 | 2·40 |
| $Yb^{III}$ | 1·985 | 1·875 | 2·371 |
| $Zn^{II}$ | 1·704 | 1·62 | 2·01 |
| $Zr^{IV}$ | 1·937 | 1·854 | 2·33 |

$Cu^{III}$-O, $R$=1.724; $Co^{IV}$-O, $R$=1.75; $Fe^{IV}$-O, $R$=1.78;
$Ni^{III}$-O, $R$=1.68; $Ni^{IV}$-O, $R$=1.72

N.E.Brese and M.O'Keefe. Bond-Valence Parameters for Solids. Acta Cryst., B47, 192-197(1991)

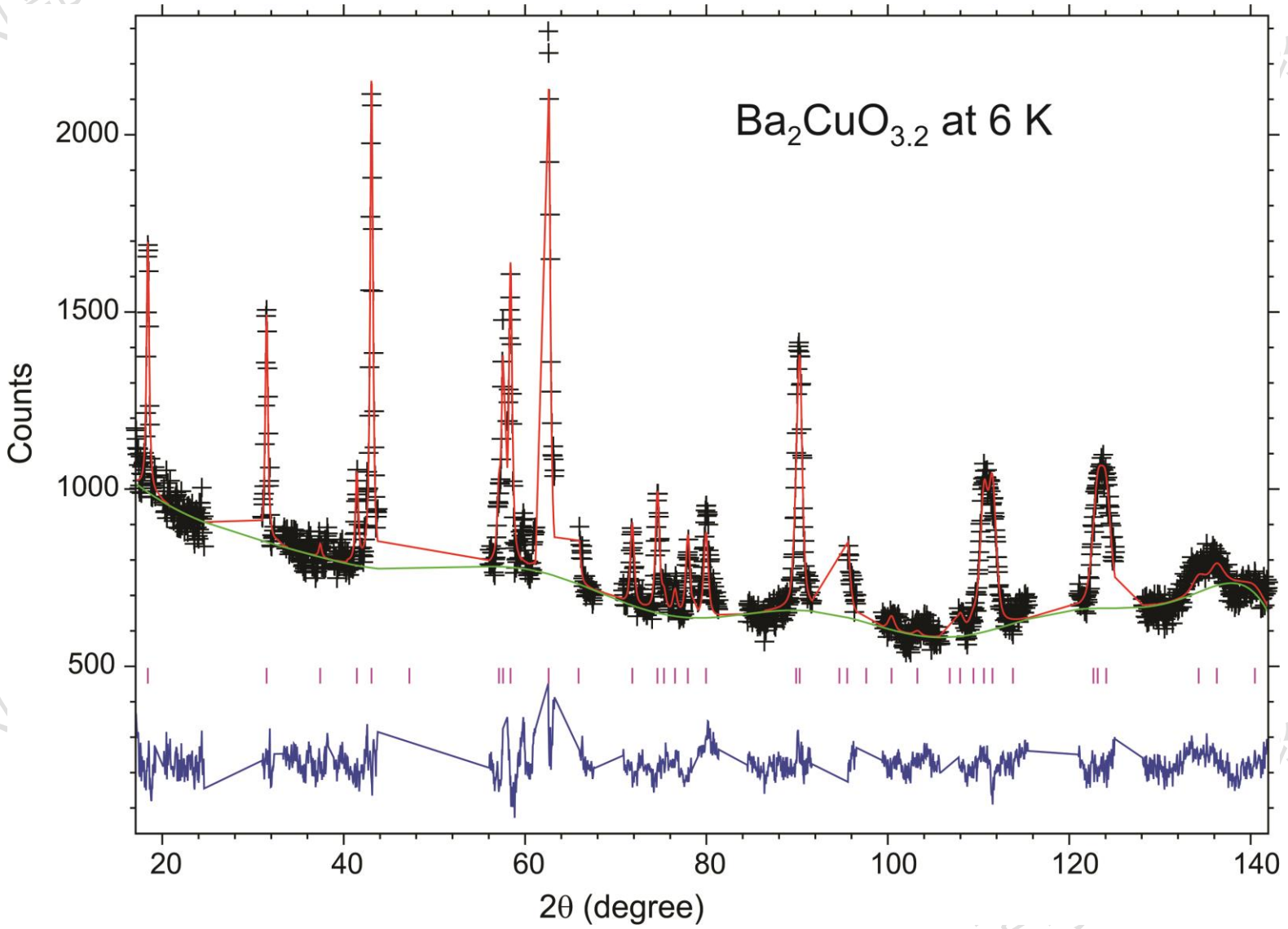

# Oxygen dependence of the crystal structure of $HgBa_2CuO_{4+\delta}$ and its relation to superconductivity



Q. HUANG, J. W. LYNN, Q. XIONG, AND C. W. CHU，Oxygen dependence of the crystal structure of HgBazCuO4+z and its relation to superconductivity. PRB, VOL. 52, NUMBER 1 1, JULY 1995-I

$HgBa_2CuO_{4+\delta}$

# 层状汞系铜基高温超导体 $HgBa_2Ca_{n-1}Cu_nO_{(2n+2)+x}$结构分析

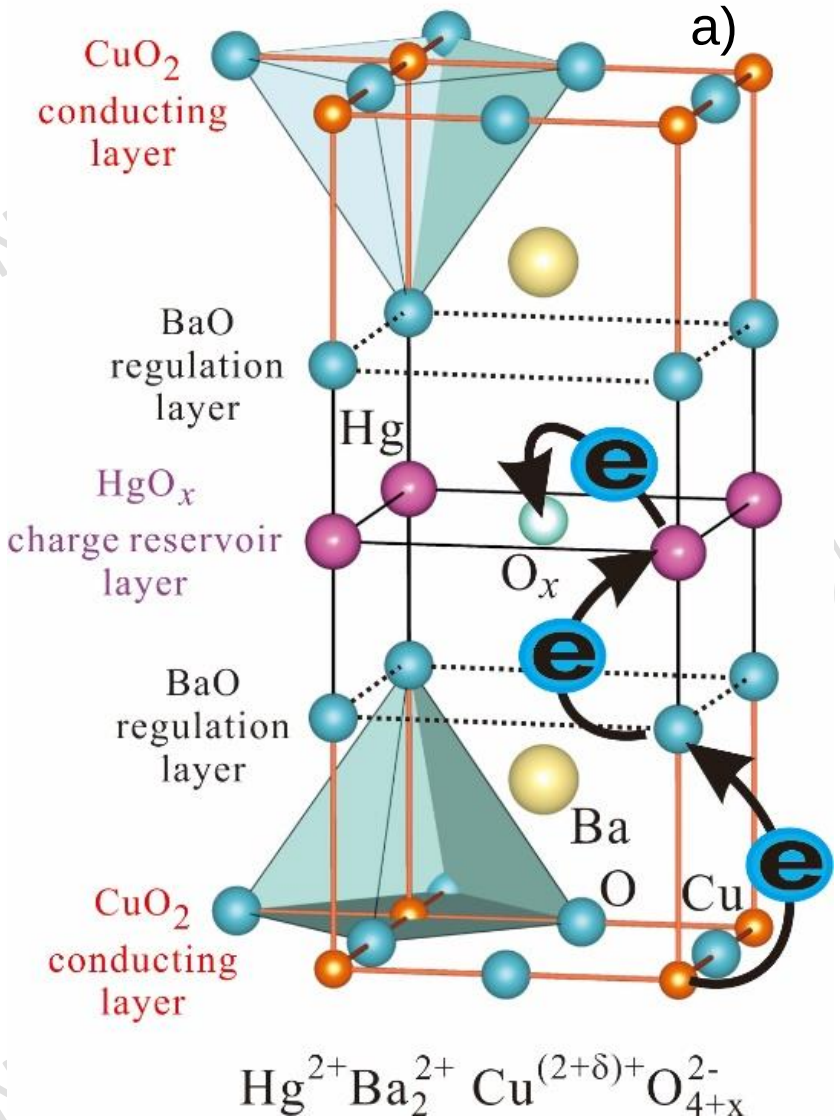


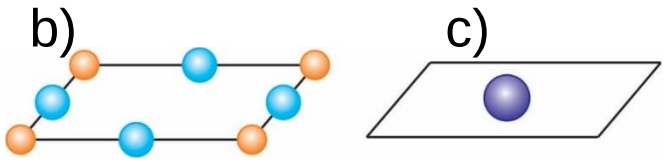


以图**a**的$HgBa_2CuO_{4+x}$的结构为基础，在***c***轴方向叠加图**b**和**c**的平面构成图d的三维层状结构层状汞系铜基高温超导系列化合物$HgBa_2Ca_{n-1}Cu_nO_{(2n+2)+x}$是。最高超导温度达到133 K. 如图所示的电荷转移示意。当$HgO_x$层的X=0时，化合物不超导。因此，准确测定$HgO_x$层中的O的占有率是研究化合物结构与性能的关系的关键。电荷转移可以用半经验方法计算Cu的价态得以估计。同时可以根据层间距估计化合物晶胞***c***轴的长度。

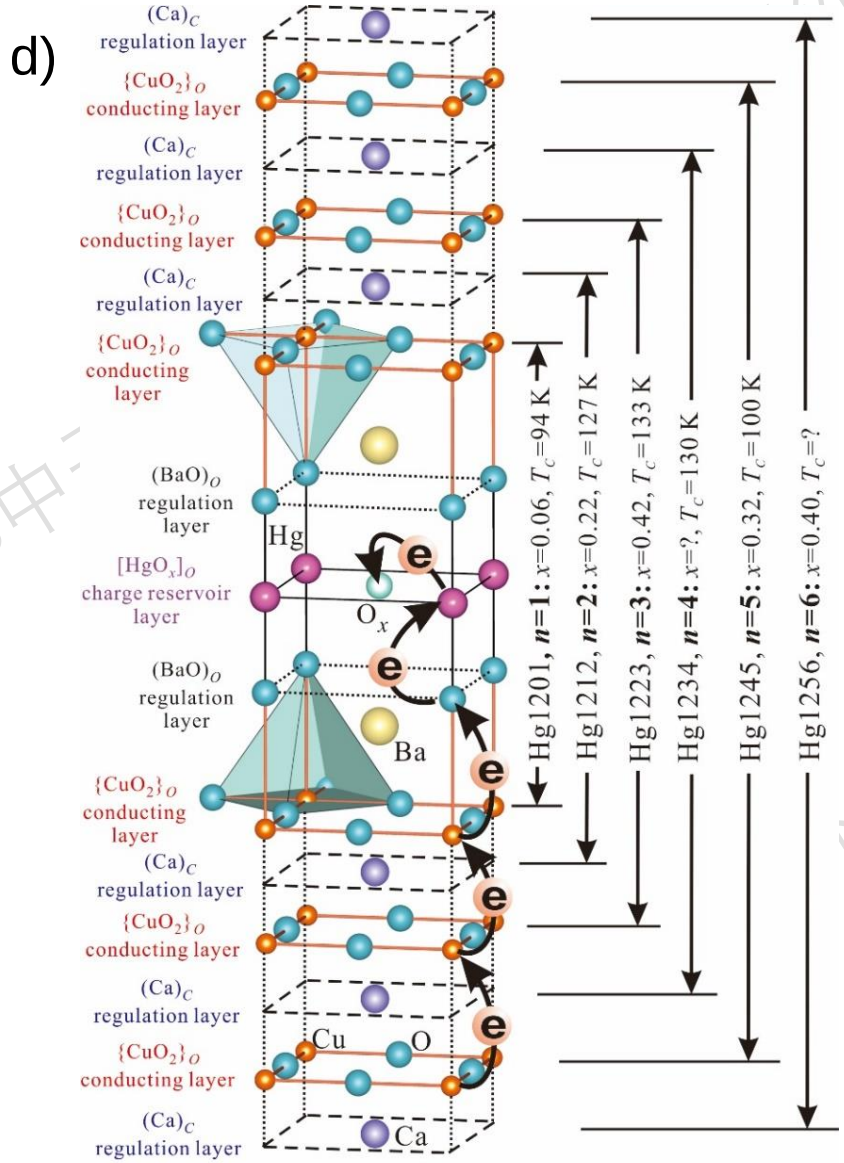


***P4/mmm***

$HgBa_2Ca_{n-1}Cu_nO_{(2n+2)+x}$

# Oxygen dependence of the crystal structure of $HgBa_2CuO_{4+\delta}$ and its relation to superconductivity

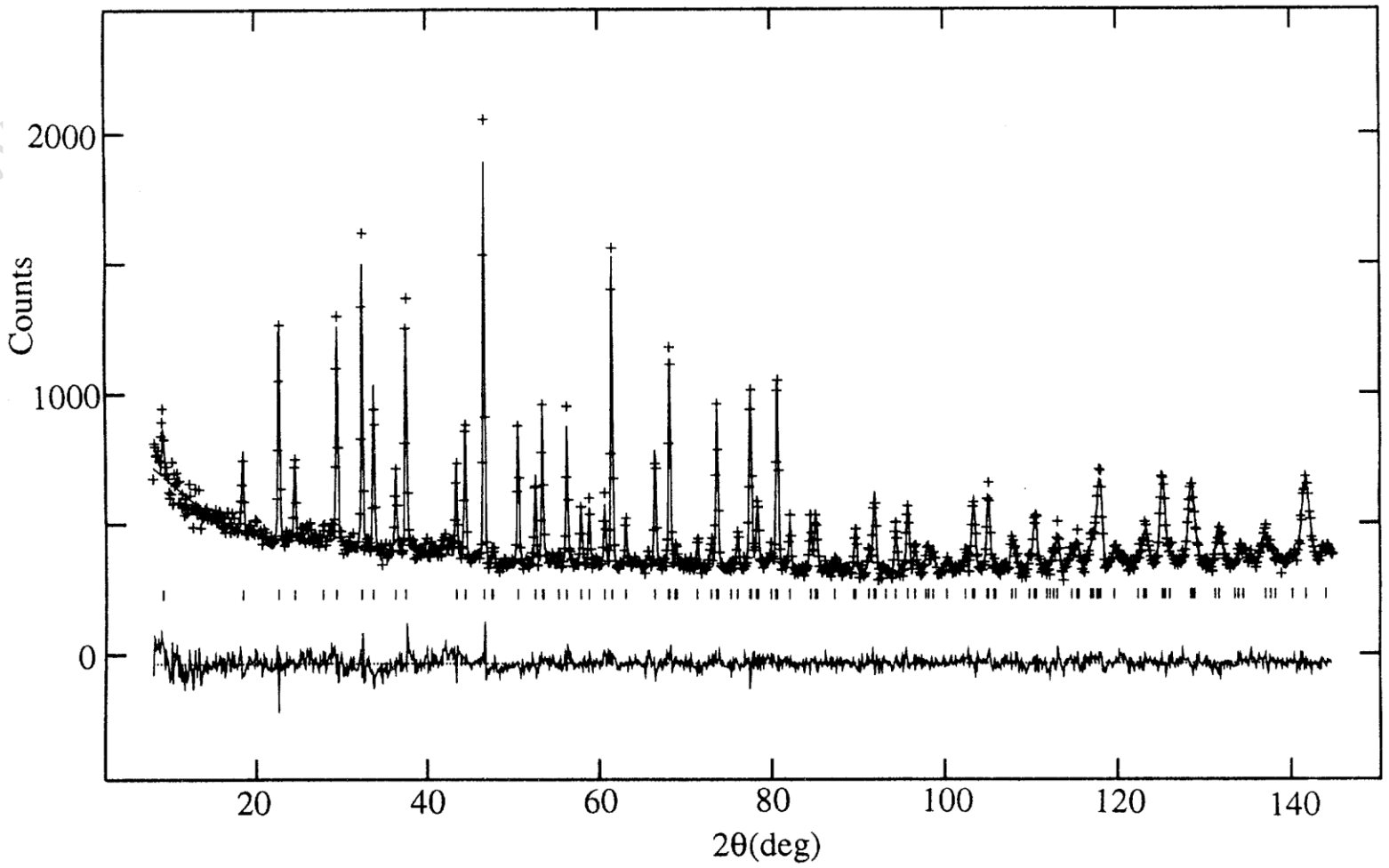


**Rietveld refinement profile of the neutron powder diffraction data obtained on the as-prepared sample of $HgBa_2CuO_{4+\delta}$ at 296 K. The observed data are represented by the points (+ ), and the refinement by the solid curve. The positions of the Bragg peaks are also indicated. The difference between the observations and the calculated profile is shown at the bottom of the figure.**

# Oxygen dependence of the crystal structure of $HgBa_2CuO_{4+\delta}$ and its relation to superconductivity

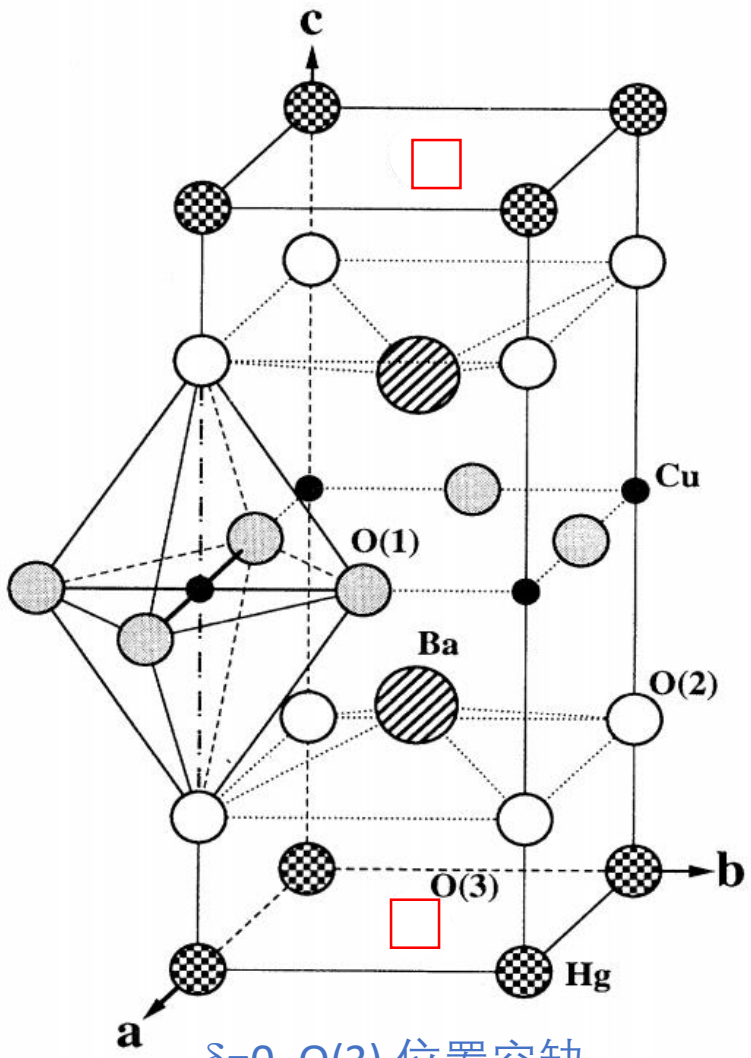


δ=0, O(3) 位置空缺
化合物不超导

TABLE IV. (Top) Occupancy parameters of Hg (at room temperature). (Bottom) Anisotropic temperature factors of Ba ($B_{22}=B_{11}$) and Ba splitting into $[\frac{1}{2},\frac{1}{2},z(1)]$ and $[\frac{1}{2},\frac{1}{2},z(2)]$; constraints: $n_{Ba(2)}=n_{O(3)}=1-n_{Ba(1)}$, $B_{Ba(1)}=B_{Ba(2)}$ (at room temperature).

| Sample label ($\delta$)/[$T_c$ (K)] | *S*1-AP (0.18)/(95) | *S*1-AV (0.08)/(53) | *S*1-RAO (0.18)/(94) | *S*1-RAV (0.04)/(0) | *S*2-PHP (0.21)/(80) | *S*1-RAOHP (0.23)/(30) |
|---|---|---|---|---|---|---|
| *n* | 0.99(1) | 0.97(1) | 0.92(1) | 0.95(1) | 0.90(1) | 0.91(1) |
| *B* (Å$^2$) | 1.37(5) | 1.15(7) | 1.13(6) | 1.07(6) | 0.84(8) | 1.12(6) |

| Sample label ($\delta$)/[$T_c$ (K)] | *S*1-RAV (0.04)/(0) | *S*1-AV (0.08)/(53) | *S*1-AP (0.18)/(95) | *S*2-PHP (0.21)/(80) | *S*1-RAOHP (0.23)/(30) |
|---|---|---|---|---|---|
| Anisotropic temperature factor | | | | | |
| $B_{11}$ (Å$^2$) | 0.84(7) | 0.50(8) | 0.51(7) | 0.5(1) | 0.72(6) |
| $B_{33}$ (Å$^2$) | 0.8(1) | 0.9(1) | 1.2(1) | 1.0(1) | 1.3(2) |
| $B_{33}/B_{11}$ | 0.95 | 1.8 | 2.4 | 2.0 | 1.8 |
| Ba splitting | | | | | |
| Ba(1) $z(1)$ | | 0.3045(5) | 0.3025(7) | 0.3001(10) | 0.3006(7) |
| *n* | | 0.92(1) | 0.83(1) | 0.79(1) | 0.77(1) |
| Ba(2) $z(2)$ | | 0.276(7) | 0.275(3) | 0.284(4) | 0.281(2) |
| *n* | | 0.08(1) | 0.17(1) | 0.21(1) | 0.23(1) |
| *B* (Å$^2$) | | 0.61(8) | 0.59(6) | 0.64(9) | 0.57(6) |

Q. HUANG, J. W. LYNN, Q. XIONG, AND C. W. CHU, Oxygen dependence of the crystal structure of HgBazCuO4+z and its relation to superconductivity. PRB, VOL. 52, NUMBER 1 1, JULY 1995-I

# Oxygen dependence of the crystal structure of $HgBa_2CuO_{4+\delta}$ and its relation to superconductivity

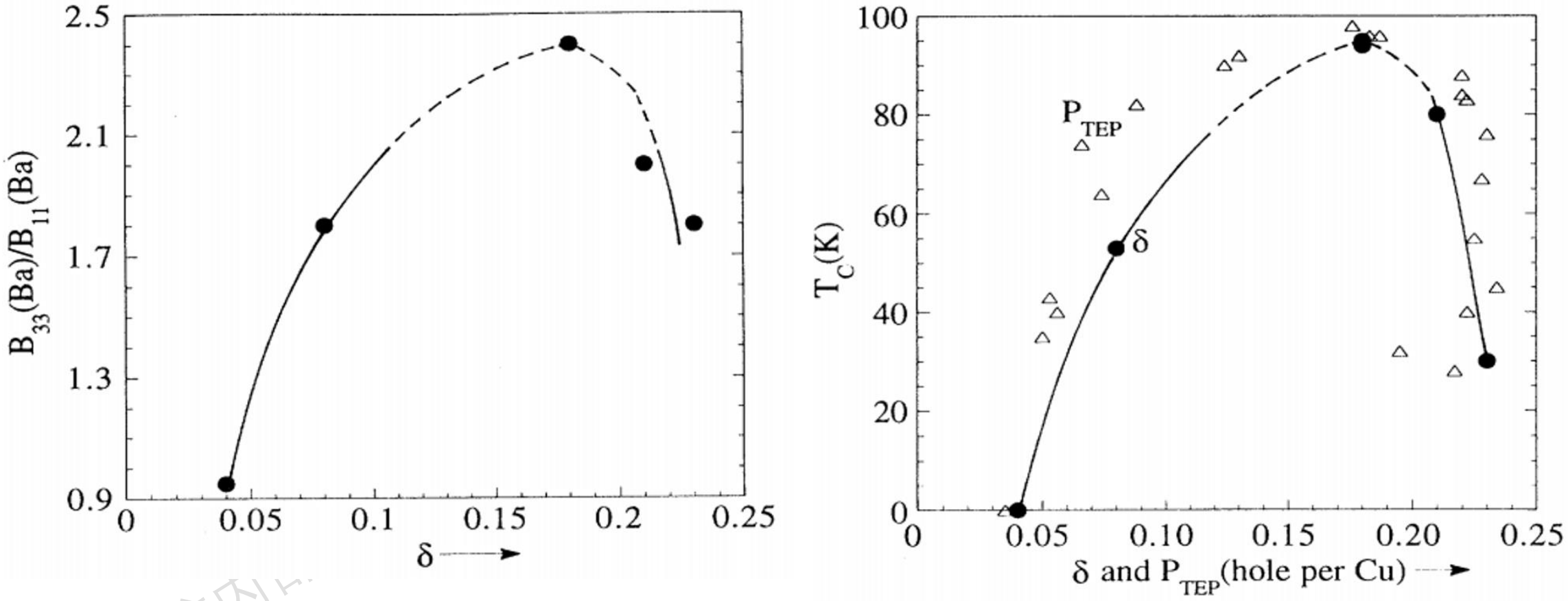


FIG. 8. (a) The ratio $B_{33}(Ba)/B_{11}(Ba)$ plotted versus oxygen content $\delta$. (b) The behavior of $T_c$ vs $\delta$ and $T_c$ vs hole concentration. The solid points are from this study, while the triangles are taken from Ref. 15. The solid curves are simply a guide to the eye for the neutron data; parabolic fits to the $T_c$ vs hole concentration are given in Ref. 15.

# Oxygen dependence of the crystal structure of $HgBa_2CuO_{4+\delta}$ and its relation to superconductivity

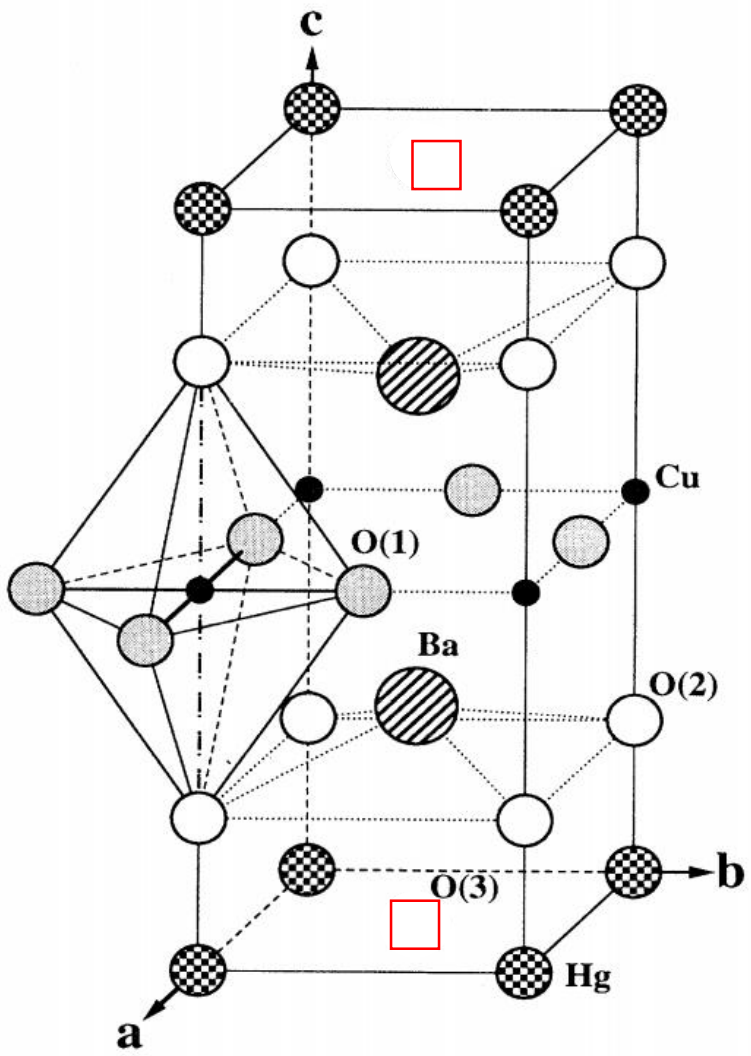


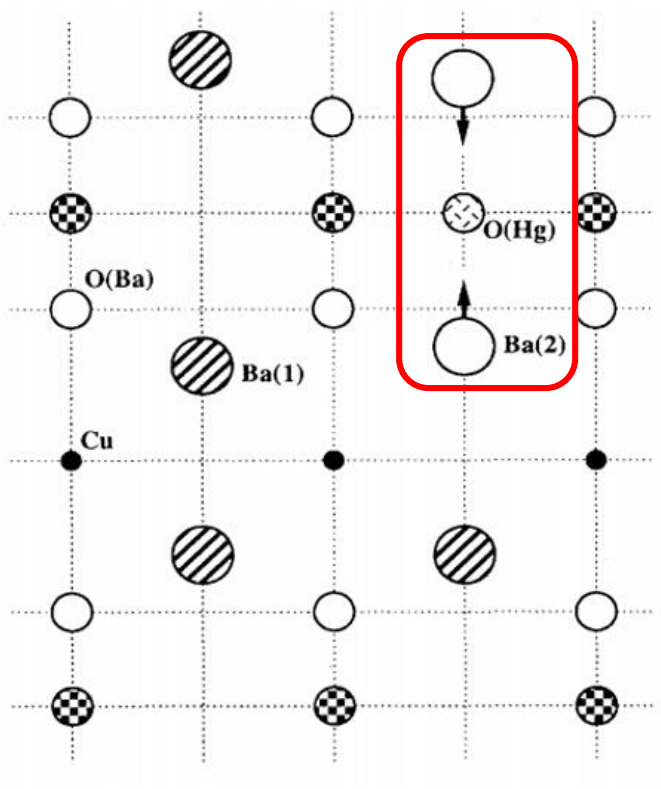


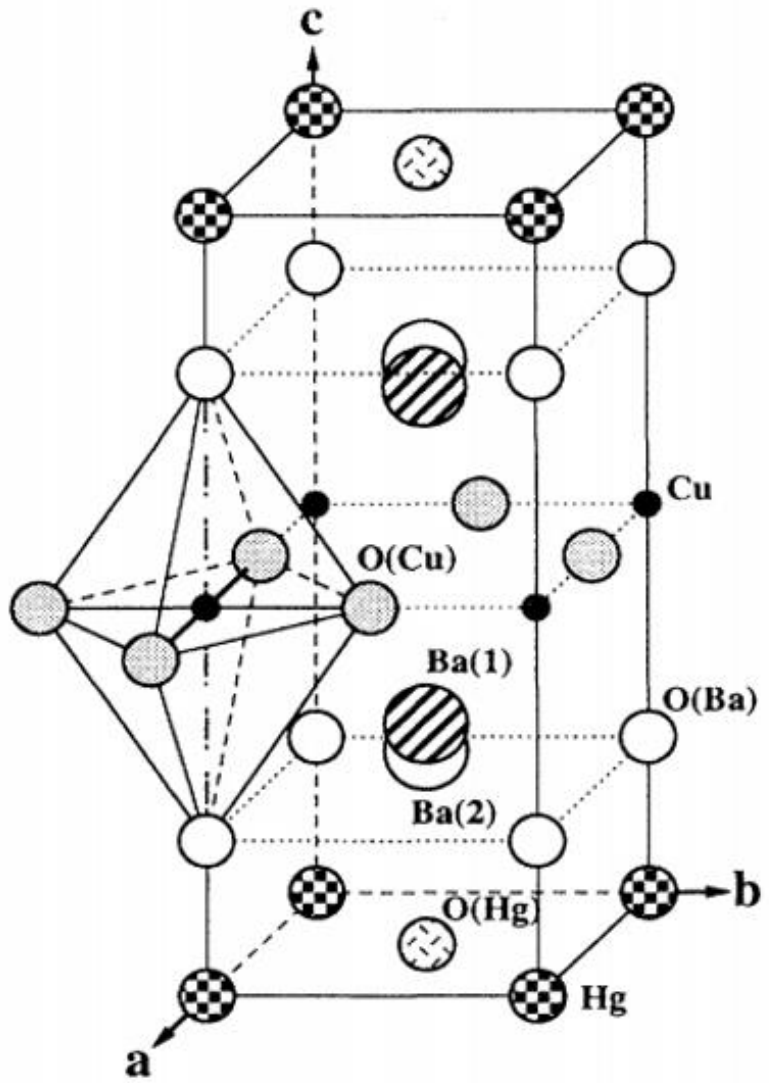

# Oxygen dependence of the crystal structure of $HgBa_2CuO_{4+\delta}$ and its relation to superconductivity

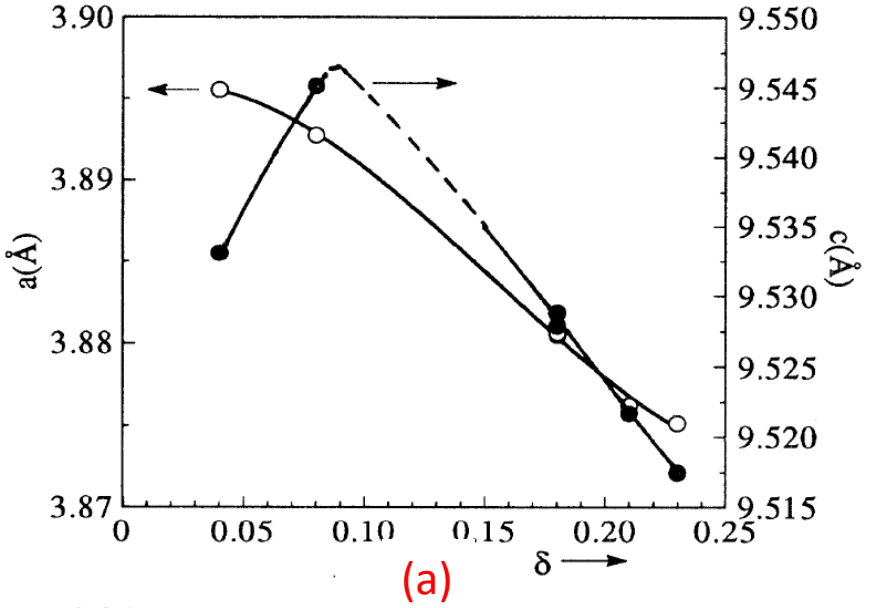


(a)

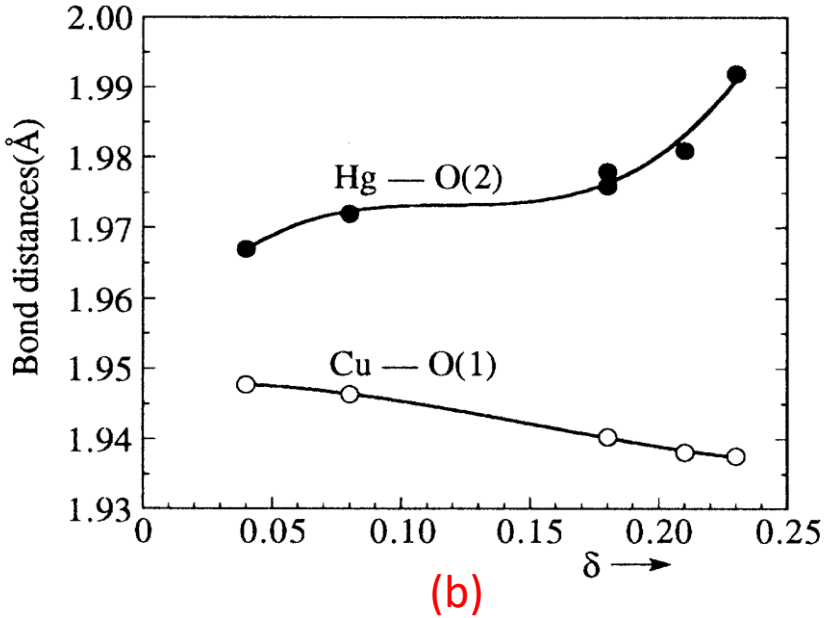


(b)

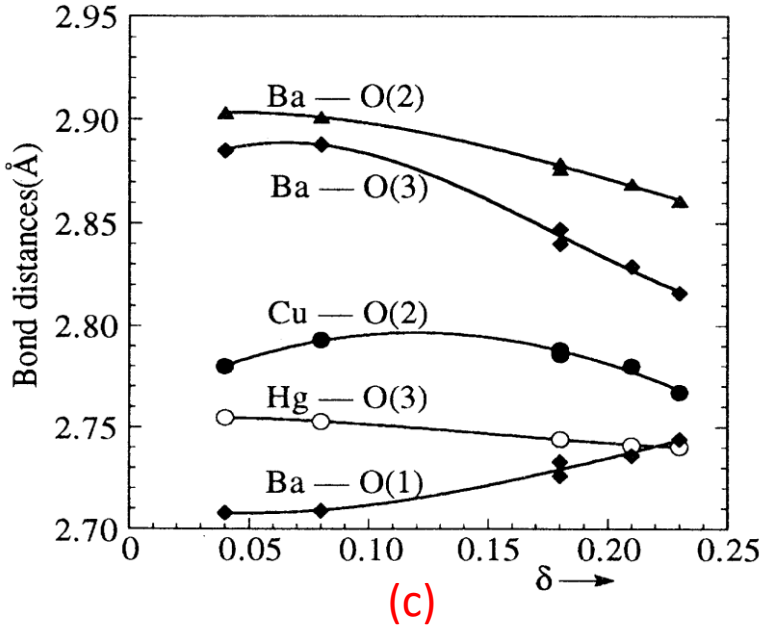


(c)

(a) Lattice parameters.
(b), (c) selected bond distances, versus the oxygen content 5.
(d) Structure of which shows that the Ba atoms shift toward the O(3) as δ increases.

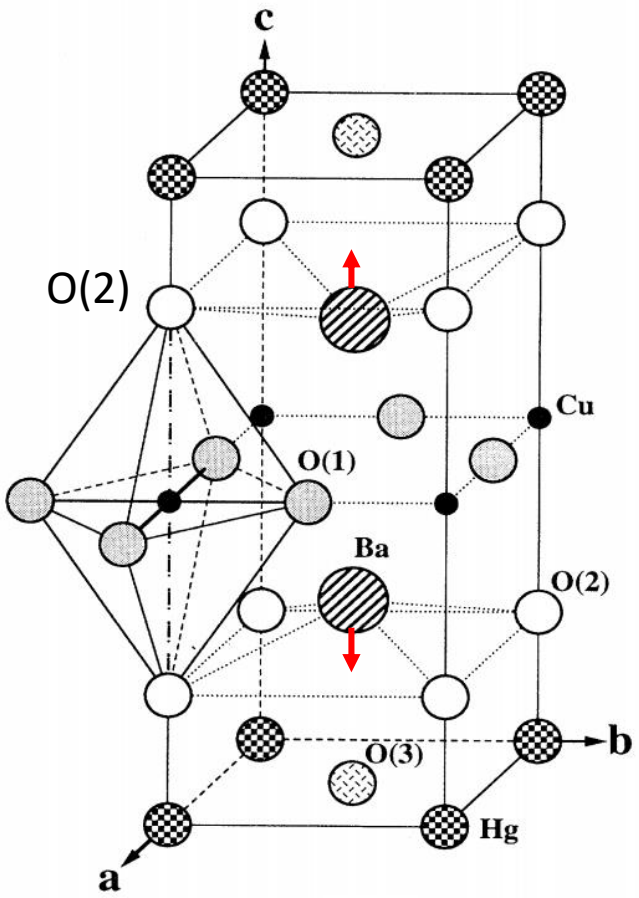


(d)

# Oxygen dependence of the crystal structure of $HgBa_2CuO_{4+\delta}$ and its relation to superconductivity

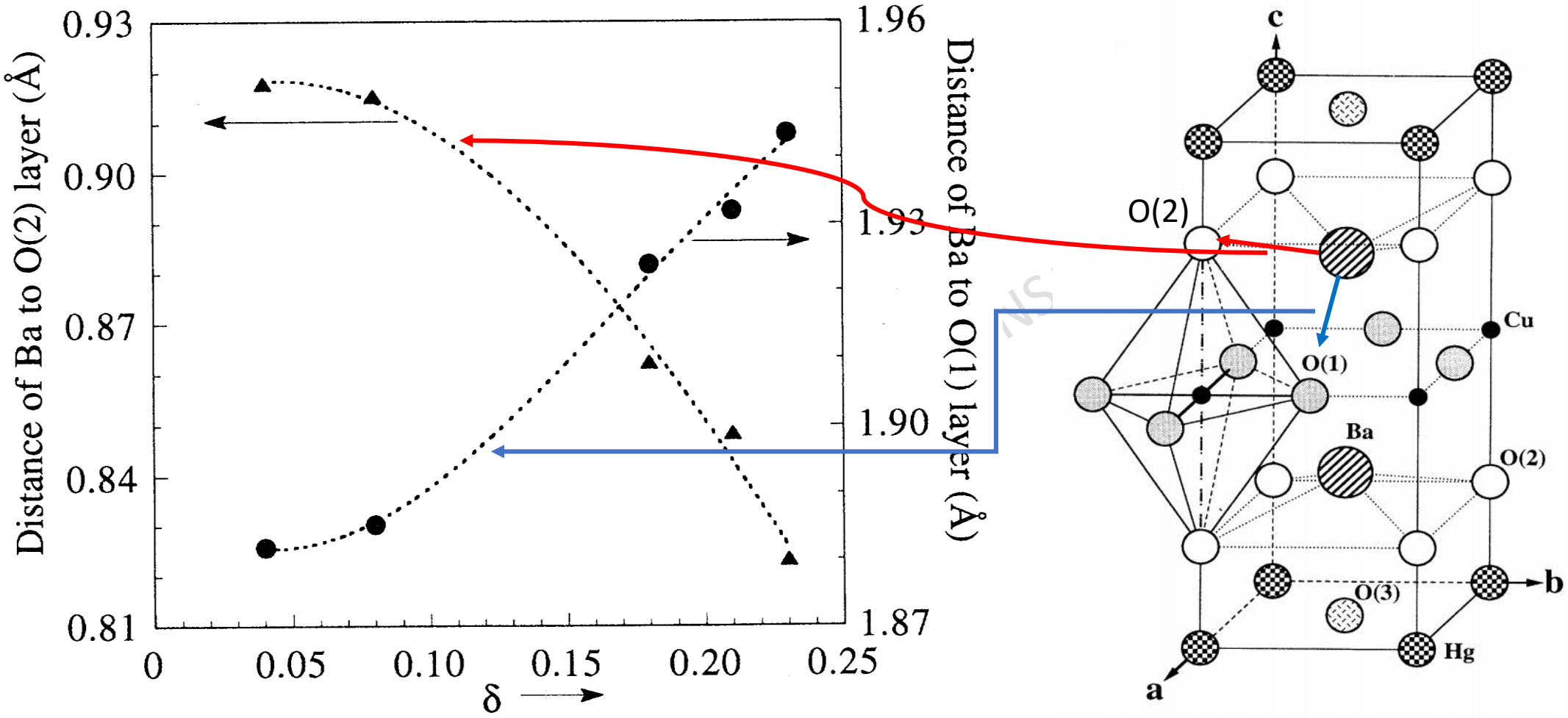


Distance of the Ba ion (z coordinate) from the O(1) and O(2) planes of oxygen ions, showing that the Ba ion moves towards the Q(3) site with increasing 5.

# Oxygen dependence of the crystal structure of $HgBa_2CuO_{4+\delta}$ and its relation to superconductivity

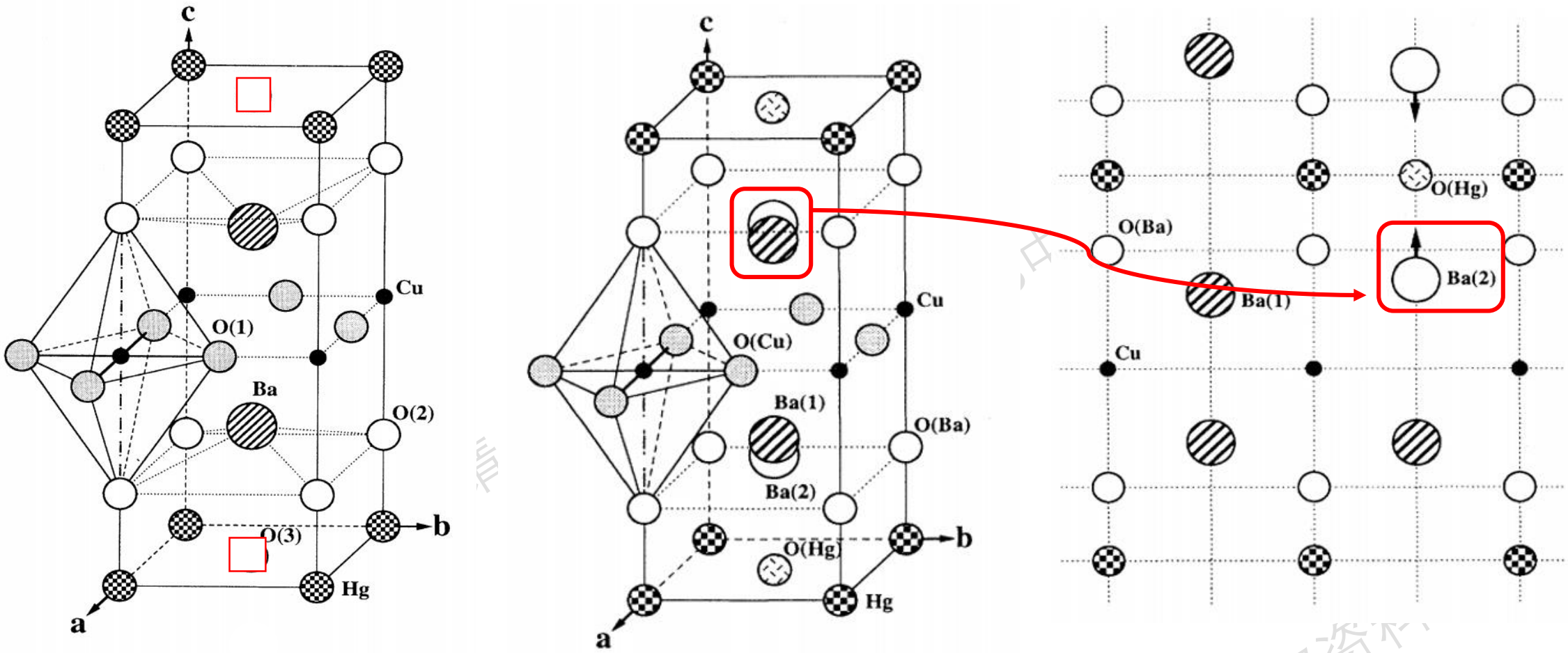


(a) The parent compound structure $HgBa_2CuO_4$ where no oxygen on the Hg layer. (b) Two-site model [Ba(1) and Ba(2)] for the Ba ions in $HgBa_2CuO_{4+\delta,}$ (c) the section of a=1/2 (or 6 =1/2). When the O(3) site is occupied, the Ba moves away from the Cu layer and towards the Hg layer.

# Oxygen dependence of the crystal structure of $HgBa_2CuO_{4+\delta}$ and its relation to superconductivity

TABLE V. Valences (u.v.—unit valence) calculated from cation-oxygen bonds.

| Sample label ($\delta$)/[$T_c$ (K)] | *S*1-RAV (0.04)/(0) | *S*1-AV (0.08)/(53) | *S*1-AP (0.18)/(95) | *S*2-PHP (0.21)/(80) | *S*1-RAOHP (0.23)/(30) |
|---|---|---|---|---|---|
| $\Sigma V_{Hg}$ (u.v.) | 1.827 | 1.824 | 1.836 | 1.836 | 1.795 |
| $\Sigma V_{Ba}$ (u.v.) | 2.064 | 2.072 | 2.075 | 2.085 | 2.083 |
| $\Sigma V_{Cu}$ (u.v.) | 2.036 | 2.040 | 2.075 | 2.088 | 2.094 |
| $\Sigma V_{O(1)}$ (u.v.) | −2.259 | −2.259 | −2.195 | −2.193 | −2.166 |
| $\Sigma V_{O(2)}$ (u.v.) | −1.719 | −1.710 | −1.749 | −1.758 | −1.755 |
| $\Sigma V_{O(3)}$ (u.v.) | −0.831 | −0.830 | −0.896 | −0.913 | −0.931 |

$V_i = \sum_j v_{ij}$, $v_{ij} = \exp[(R_{ij} - d_{ij})/b]$, e=2.71828, b=0.37, $d_{ij}$ is bond distance

*International Tables for Crystallography* (2019). Vol. H, Chapter 6.1, pp. 698–715.

6.1. Survey of computer programs for powder diffraction

C. J. Gilmore, J. A. Kaduk and H. Schenk

**Table 6.1.1**
Software for powder diffraction

| Program | Description | Function(s) | Reference(s) | URL or other source | Availability |
|---|---|---|---|---|---|
| ACerS–NIST Phase Equilibria Diagrams Database | Phase-equilibria diagrams | Database | ACerS–NIST Phase Equilibria Diagrams Database (2013) | | Commercial |
| *ADM* | Software suite including device control, pattern evaluation, qualitative and quantitative phase analysis, indexing, lattice-parameter refinement, crystal-size evaluation, microstress analysis, profile analysis and pattern simulation | Phase analysis, indexing, lattice-parameter refinement, crystal size, stress, profile analysis, pattern simulation | | http://www.RMSKempten.de/ | Commercial |
| American Mineralogist Crystal Structure Database (AMCSD) | Online database that includes every structure published in *The American Mineralogist*, *The Canadian Mineralogist*, *European Journal of Mineralogy* and *Physics and Chemistry of Minerals*, as well as selected data sets from other journals | Minerals, database | Downs & Hall-Wallace (2003) | http://rruff.geo.arizona.edu/AMSamcsd.php | Free to use |
| *ANAELU* | Computer-based tools for inferring single-crystal structures and fibre textures from two-dimensional diffraction diagrams | Modelling, glasses | Fuentes-Montero *et al.* (2011) | http://www.esrf.eu/computing/scientific/ANAELU/Anelu_Page.htm | Free |
| *ARITVE* | Modelling of glass structures using the Rietveld method | Modelling, glasses | Le Bail (1995, 2000) | http://sdpd.univ-lemans.fr/aritve.html | Free |
| *ATOMS* | Structure visualization. Part of the *SHAPE* software package | Structure visualization | Shape Software, 521 Hidden Valley Road, Kingsport, TN 37663, USA | http://www.shapesoftware.com/ | Commercial |
| *AUTOFP* | GUI for highly automated Rietveld refinement using an expert system algorithm based on *FULLPROF* | Rietveld refinement | Cui *et al.* (2015) | http://pmedia.shu.edu.cn/autofp | Free |
| *AUTOX* | Autoindexing multiphase samples; included with *VMRIA* | Indexing | Zlokazov (1995); Bergmann *et al.* (2004) | http://www.ccp14.ac.uk/ccp/web-mirrors/vmria | Free |
| *AXES* | Program for X-ray powder diffraction data evaluation, specially designed for peak-shape analysis and data preparation for Rietveld refinement in connection with *FULLPROF* | Data conversion, peak-shape analysis | Mändar *et al.* (1996) | http://www.ccp14.ac.uk/ccp/web-mirrors/axes/~hugo/axes/ | Free for academic use |

Table 6.1.1 Software for powder diffraction. Continue

| Program | Description | Function(s) | Reference(s) | URL or other source | Availability |
|---|---|---|---|---|---|
| *AXES-20B* | Estimation of crystal size and shape. Links to a wide range of programs and includes a range of data-processing and display functions | Phase identification, data conversion, structure visualization, peak location, peak profiling, indexing | Mändar & Vajakas (1998); Mändar *et al.* (1999) | http://www.ccp14.ac.uk/ccp/web-mirrors/axes/ | Free |
| *Balls&Sticks* | Structure visualization and animation | Structure visualization | Ozawa & Kang (2004) | http://www.toycrate.org/ | Free |
| *BALSAC* | Construction, visualization and interactive analysis of crystal lattices | Structure visualization | K. Hermann, Fritz-Haber-Institut der MPG, Berlin, Germany | http://www.fhi-berlin.mpg.de/~hermann/Balsac/ | Free |
| *BEARTEX* | Texture analysis in polycrystalline materials | Texture analysis | Wenk *et al.* (1998) | http://eps.berkeley.edu/~wenk/TexturePage/beartex.htm | Free |
| *BGMN* | Fundamental parameters, Rietveld refinement and quantitative-analysis software | Fundamental parameters, Rietveld refinement, quantitative analysis | Bergmann *et al.* (1998) | http://www.bgmn.de/methods.html | Free |
| Bilbao Crystallographic Server | Variety of symmetry tools including space-group retrieval tools, Wyckoff positions of space groups and group–subgroup relations | Symmetry | Aroyo *et al.* (2011) | http://www.cryst.ehu.es/ | Free |
| B-IncStrDB | Database of incommensurate structures | Database | Kroumova *et al.* (2005) | http://www.cryst.ehu.es/icsdb/ | Free |
| *Bond Valence Wizard* | Predicts interatomic distances in crystals by the bond-valence method | Bond-length prediction | Orlov *et al.* (1998); Brown (1977) | http://orlov.ch/bondval/ | Free |
| *BRASS 2* | Rietveld refinement, Fourier-map calculation and visualization software | Rietveld refinement, visualization | Birkenstock *et al.* (2003) | http://www.brass.uni-bremen.de/ | Free |
| *BREADTH* | Analysis of diffraction line broadening | Line broadening | Balzar (1995) | http://www.du.edu/~balzar/breadth.htm | Free |
| Cambridge Structural Database | Database (including structures derived from powder data) with associated software and software suites; organics and organometallics | Database | Groom *et al.* (2016) | http://www.ccdc.cam.ac.uk/ | Commercial |
| *CaRine* | Visualization of lattices, surfaces, interfaces and diffraction patterns | Visualization | C. Boudias & D. Monceau, 1989–2004, CaRIne Crystallography | http://carine.crystallography.pagesperso-orange.fr/ | Commercial |

Table 6.1.1 Software for powder diffraction. Continue

| Program | Description | Function(s) | Reference(s) | URL or other source | Availability |
|---|---|---|---|---|---|
| *CASTEP* | Calculates the properties of materials from first principles | Physical properties | Segall *et al.* (2002) | http://www.castep.org/ | Free for European academics |
| CCP14 | Web page with links to powder diffraction software | Software database | Stephenson *et al.* (2006) | http://www.ccp14.ac.uk/ | Free |
| *cctbx* | A set of basic programming tools for X-ray crystallography | Programming | Grosse-Kunstleve *et al.* (2002) | https://github.com/cctbx/cctbx_project | Free |
| *CDASH* | Runs *DASH* over a network of computers | Structure solution | Spillman *et al.* (2015) | https://www.ccdc.cam.ac.uk/Solutions/PowderDiffraction/Pages/DASH.aspx | Commercial |
| *Celref* | Program for refining the unit cell | Unit-cell refinement | Laugier & Bochu (2004) | http://www.ccp14.ac.uk/ccp/web-mirrors/lmgp-laugier-bochu/ | Free |
| *CHECKCELL* | Indexing and space-group determination, links into *Crysfire* | Indexing, space-group determination | | http://www.ccp14.ac.uk/tutorial/lmgp/chekcellb.htm | Free |
| *checkCIF* | Cif checking service | CIF | | http://journals.iucr.org/services/cif/checking/checkfull.html | Free |
| Chemical Database Service (CDS) | EPSRC-funded access to a large number of scientific databases, including all the main crystallographic databases, to UK-based academics and students | Database | Fletcher *et al.* (1996) | http://cds.dl.ac.uk/ | Free within UK |
| *CIFTOOLS* | Includes two programs: *pdCIFplot* to plot Rietveld results from pdCIF files, and *CIFEDIT* to create, browse through and edit CIF files | CIF | | ftp://ftp.ncnr.nist.gov/pub/cryst/cif/ | Free |
| *Cinema:Debye-Scherrer* | Interactive visualization of multi-data-set Rietveld analyses | Data visualization | Vogel *et al.* (2018) | https://github.com/cinemascience/cinema_debye_scherrer | Free |

Table 6.1.1 Software for powder diffraction. Continue

| Program | Description | Function(s) | Reference(s) | URL or other source | Availability |
|---|---|---|---|---|---|
| *Crystal Maker X* | Visualization, structure design, simulation and 3D printing package | Visualization, simulation | CrystalMaker Software Ltd, 5 Begbroke Science Park, Sandy Lane, Yarnton, OX5 1PF, UK | http://www.crystalmaker.com/ | Commercial |
| *Crystal Studio* | Visualization including surfaces, interfaces, defects and simulation of diffraction data | Visualization, defects, data simulation | Crystalsoftcorp, PO Box 7006, Wattle Park, VIC 3128, Australia | http://www.crystalsoftcorp.com, http://www.crystal0studio.com/ | Commercial |
| *Crystallographica* | A software toolkit for crystallography | Visualization, pattern simulation | Oxford Cryosystems (1997) | http://www.oxcryo.com/cg/ | Free |
| Crystallography Open Database (COD) | Open-access database including predicted structures, covering organics, inorganics, metal–organics and minerals | Database | Grazulis *et al.* (2009) | http://www.crystallography.net/ | Free |
| CRYSTMET | Database of metals, alloys and intermetallics | Database | White *et al.* (2002); Toth Information Systems, Inc., 2045 Quincy Avenue, Ottawa, Ontario, K1J 6B2, Canada | https://cds.dl.ac.uk/cds/datasets/crys/mdf/llmdf.html | Free to UK academic users |
| *DAJUST* | Intensity extraction and space-group determination. Part of the *XLENS* package | Space-group determination, cell-parameter refinement, profile fitting, Le Bail method | Vallcorba *et al.* (2012) | https://departments.icmab.es/crystallography/news/42-pdsoftware | Free to non-commercial users |
| *DANSE* | General software for neutron scattering | Neutron scattering | Cummings *et al.* (2002) | http://wiki.cacr.caltech.edu/danse/index.php/Main_Page | Free |
| *DASH* | Software for solving crystal structures from X-ray powder diffraction patterns | Structure solution | David *et al.* (2006) | http://www.ccdc.cam.ac.uk/products/powder_diffraction/dash/ | Commercial |
| Database of Zeolite Structures | Provides structural information on all of the zeolite framework types that have been approved by the Structure Commission of the International Zeolite Association (IZA-SC) | Database | Baerlocher *et al.* (2003) | http://www.iza-structure.org/databases/ | Free |
| *DataScan* | Diffractometer automation hardware and software | Instrumentation, diffractometer control | Materials Data, Inc., 2551 Second Street, Livermore, CA 94550, USA | http://www.materialsdata.com/ds.htm | Commercial |

Table 6.1.1 Software for powder diffraction. Continue

| Program | Description | Function(s) | Reference(s) | URL or other source | Availability |
|---|---|---|---|---|---|
| *CMPR* | Displays diffraction data, manual and auto-indexing, and peak fitting | Data visualization, indexing, peak fitting | Toby (2005) | http://www.ncnr.nist.gov/xtal/software/cmpr/ | Free |
| *CMWP-fit* | Determination of microstructural parameters from diffraction profiles | Profile fitting | Ribárik *et al.* (2001) | http://csendes.elte.hu/cmwp/ | Free |
| *CONEX* | Angular calibration and averaging of two-dimensional powder diffraction patterns | Two-dimensional data | Gommes & Goderis (2010) | Available from the authors | Free |
| *Conograph* | Integrated system with a graphical user interface for indexing | Indexing | Esmaeili *et al.* (2017) | https://osdn.net/projects/conograph/releases/ | Free |
| *ConQuest* | Software for searching the Cambridge Structural Database | Database searching | Bruno *et al.* (2002) | http://www.ccdc.cam.ac.uk/ | Commercial |
| *ConvX* | Data-conversion program that can convert multiple files at once. Also possible to select a particular angular range to convert | Data conversion | Bowden (2000) | http://www.ccp14.ac.uk/ccp/web-mirrors/convx/ | Free |
| *Corina* | Structure generator for drug-like molecules | Structure prediction | Molecular Networks GmbH, Nuremberg, Germany; Sadowski *et al.* (1994); Schwab (2010) | https://www.mn-am.com/products/corina | Commercial |
| *CRISP* | Uses crystallographic image processing to extract information from electron micrographs | Electron diffraction | Hovmöller (1992) | http://www.calidris-em.com/crisp.php | Commercial |
| *CRYSCA* | Crystal-structure calculations for flexible molecules | Structure prediction | Schmidt & Kalkhof (1997) | Available from the authors | |
| *Cryscon* | Allows conversion between several popular crystallographic file formats | Data conversion | Eric Dowry, Shape Software, 521 Hidden Valley Road, Kingsport, TN 37663, USA | http://www.shapesoftware.com/ | Shareware |
| *Crysfire* | Automatic powder-pattern indexing | Indexing | Shirley (2002) | http://www.ccp14.ac.uk/tutorial/crys/, http://www.ccp14.ac.uk/ccp/web-mirrors/crys-r-shirley/ | Free |
| *CrystalDiffract* | Data processing and visualization | Peak fitting | CrystalMaker Software Ltd, 5 Begbroke Science Park, Sandy Lane, Yarnton, OX5 1PF, UK | http://crystalmaker.com/crystaldiffract/index.html | Commercial |

Table 6.1.1 Software for powder diffraction. Continue

| Program | Description | Function(s) | Reference(s) | URL or other source | Availability |
|---|---|---|---|---|---|
| *Datasqueeze* | Graphical interface for analysing data from two-dimensional X-ray diffraction detectors | Two-dimensional data analysis | Heiney (2002) | http://www.physics.upenn.edu/~heiney/datasqueeze/index.html | Free |
| *DDM* | Refinement using the Rietveld method or derivative difference minimization | Rietveld refinement, derivative difference refinement | Solovyov (2004) | https://sites.google.com/site/ddmsuite/ | Free |
| *Debussy 2.0* | Analysis of powder diffraction data from nanocrystalline, defective and/or nonperiodic materials | Nanocrystalline and non-periodic materials, defects | Cervellino *et al.* (2015) | http://debussy.sourceforge.net/debussy/debussy.html | Free |
| *DEBVIN* | Rietveld refinement with the use of generalized coordinates | Rietveld refinement, polymers | Brückner & Immirzi (1997) | https://vdocuments.site/debvin-a-program-for-Rietveld-refinement-with-generalized-coordinates.html | Free |
| *decryst* | Software suite for structure determination from powder diffraction using the direct-space method | Structure solution | Liu (2018) | https://gitlab.com/CasperVector/decryst/ | Free |
| *Diamond* | Crystal and molecular structure visualization and exploration | Structure visualization | Crystal Impact – K. Brandenburg and H. Putz GbR, Postfach 1251, D-53002 Bonn, Germany | http://www.crystalimpact.com/ | Commercial |
| *DICVOL* | Automatic indexing | Indexing | Boultif & Louër (2004) | http://www.ccp14.ac.uk/ccp/web-mirrors/dicvol/ | Free |
| *DIFFaX* | Simulation of powder diffraction patterns for faulted materials | Stacking faults, simulation | Treacy *et al.* (1991) | http://www.public.asu.edu/~mtreacy/DIFFaX.html | Free |
| *DIFFaX+* | A modified version of *DIFFaX* for the refinement of disordered stack materials | Refinement, disordered stack materials | Leoni *et al.* (2004) | Available from the author (matteo.leoni@unitn.it) on request | Free |
| *Diffpy-CMI* | Python software for diffraction analysis and the study of the atomic structure of materials | Modelling | See https://www.diffpy.org/publications.html | http://diffpy.org | Free |
| *DIFFRAC.EVA* | Data processing, phase identification and quantitative analysis. Cluster analysis allows high-throughput screening | Profile fitting, cluster analysis, quantitative phase analysis | Bruker AXS GmbH, Oestliche Rheinbrueckenstr. 49, D-76187 Karlsruhe, Germany | https://www.bruker.com/products/x-ray-diffraction-and-elemental-analysis/x-ray-diffraction/xrd-software/eva/overview.html | Commercial |
| *DIFFRAC.TOPAS* | Profile and structure analysis (see *TOPAS*) | Profile analysis, Rietveld refinement | Bruker AXS GmbH, Oestliche Rheinbrueckenstr. 49, D-76187 Karlsruhe, Germany | https://www.bruker.com/products/x-ray-diffraction-and-elemental-analysis/x-ray-diffraction/xrd-software/topas.html | Commercial |

Table 6.1.1 Software for powder diffraction. Continue

| Program | Description | Function(s) | Reference(s) | URL or other source | Availability |
|---|---|---|---|---|---|
| *DISCUS* | Simulates defect structures and diffuse scattering, plus the simulation of perfect structures of non-crystalline materials | Defect structures, simulation | Proffen & Neder (1997, 1999) | https://www.xray.cz/ecm-cd/soft/xray/general/discus/discus/disfeat.html | Free |
| *DLS-76* | Structure refinement with distance constraints; part of *FOCUS* | Rietveld refinement | Baerlocher *et al.* (1976, 1977) | https://github.com/stefsmeets/focus_package, http://www.crystal.mat.ethz.ch/Software/index.html | Free |
| *DRAWxtl* | Open-source program for producing crystal-structure drawings | Visualization | Finger *et al.* (2007) | http://www.lwfinger.net/drawxtl/ | Free |
| *DRXWin* | Diffraction data manipulation and qualitative analysis | Visualization, qualitative phase analysis, peak search | Vicent Primo Martín, El Instituto de Ciencia de los Materiales, Universitat de Valencia, Avda. Blasco Ibáñez, 13, 46010 Valencia, Spain | http://www.ccp14.ac.uk/ccp/web-mirrors/drxwin/drxwin/ | Free |
| *Dysnomia* | Calculates electron and nuclear densities from observed structure factors by the maximum-entropy method | Electron and nuclear density calculations | Momma *et al.* (2013) | http://jp-minerals.org/dysnomia/en/ | Free |
| *Eager* | Genetic algorithm for crystal structure solution from powder diffraction data | Structure solution | Harris *et al.* (2004) | Contact K. D. M. Harris | |
| *EFLECH/INDEX* | Whole-pattern indexing | Indexing | Bergmann (2007) | http://www.bgmn.de/indexpgm.html | Free |
| *ELD* | Quantitative information from electron-diffraction patterns | Electron diffraction | Calidris, Sweden | http://www.calidris-em.com/eld.php | Commercial |
| *enCIFer* | Viewing and editing CIF files | CIF editing | Allen *et al.* (2004) | https://www.ccdc.cam.ac.uk/Community/csd-community/encifer/ | Free |
| *Endeavour* | Direct-space method for *ab initio* solution of structures from powder diffraction data by combined global optimization of pattern difference and potential energy | Structure solution | Putz *et al.* (1999) | http://www.crystalimpact.com/endeavour/ | Commercial |
| *EPCryst* | Structure solution from powder diffraction data using models generated by an equivalent-position combination algorithm based on unit-cell content and space-group information | Structure solution | Deng & Dong (2011) | http://www.epcryst.com | Free |
| *ESPOIR* | Structure solution by Monte Carlo analysis of powder diffraction data | Structure solution | Le Bail (2001) | http://www.cristal.org/sdpd/espoir/ | Free |

Table 6.1.1 Software for powder diffraction. Continue

| Program | Description | Function(s) | Reference(s) | URL or other source | Availability |
|---|---|---|---|---|---|
| *EXPGUI* | Graphical interface for *GSAS* | Rietveld refinement, visualization | Toby (2001) | http://www.ncnr.nist.gov/programs/crystallography/software/expgui/ | Free |
| *EXPO2014* | Structure-solution toolkit for phasing crystal structures from powder data | Structure solution | Altomare *et al.* (2013) | http://www.ba.ic.cnr.it/softwareic/expo/expo2014-installation/ | Free for non-profit users |
| *ExtSym* | Space-group assignment. Bundled with *DASH* but can be obtained separately from Anders Markvardsen | Space-group determination | Markvardsen *et al.* (2001) | http://www.markvardsen.net/projects/ExtSym/main.html | Free |
| *FABLE* | Reads many X-ray detector image formats | Data processing | Schmidt *et al.* (2009) | http://sourceforge.net/projects/fable/ | Free |
| *FAULTS* | Refinement of structures with extended defects, based on *DIFFaX* | Defect structures, simulation | Casas-Cabanas *et al.* (2016) | | Free |
| *FIT* | Decomposition of powder diffraction patterns and profile analysis of pair correlation functions | Profile analysis, PDF analysis | Petkov & Bakaltchev (1990) | http://web.pa.msu.edu/people/petkov/software.html | Free for academic use |
| *FIT2D* | Calibration and correction of detector distortions, integration of two-dimensional data to a variety of one-dimensional scans, and one- and two-dimensional model fitting | Data analysis, visualization | Hammersley (1998, 2016); Hammersley *et al.* (1996) | http://www.esrf.fr/computing/scientific/FIT2D/ | Free |
| *FitAllb* | Fitting centre-of-mass grain positions, orientation and elastic strain tensors | Strain | Oddershede *et al.* (2010) | https://sourceforge.net/p/fable/wiki/FitAllB/ | Free |
| *FitGISAXS* | Modelling and analysis of grazing-incidence small-angle X-ray scattering data | GISAXS | Babonneau (2010) | https://www.pprime.fr/?q=en/node/1013; contact D. Babonneau, david.babonneau@univ-poitiers.fr | Free |
| *FlexCryst* | Program suite including crystal-structure prediction, structure determination and clustering | Structure prediction, structure determination | Hofmann & Apostolakis (2003) | http://www.flexcryst.com/html/home.pdf | Commercial |
| *FOCUS* | Automated structure determination of zeolites. Can use electron-diffraction data | Structure determination, zeolites | Grosse-Kunstleve *et al.* (1997) | https://github.com/stefsmeets/focus_package | Free |
| *FOX* | *Ab initio* structure determination using global-optimization algorithms, suitable for any type of crystal structure (organic, inorganic including automatic correction of special positions); can combine several data sets | Structure solution | Favre-Nicolin & Cerný (2002) | http://objcryst.sourceforge.net/Fox/ | Free |

Table 6.1.1 Software for powder diffraction. Continue

| Program | Description | Function(s) | Reference(s) | URL or other source | Availability |
|---|---|---|---|---|---|
| *FOXGrid* | Structure solution using *FOX* with distributed computing | Structure solution | Rohlíček *et al.* (2007) | https://fox.vincefn.net/Manual/Fox.Grid | Free |
| *FULLPAT* | Full-pattern quantitative phase analysis merging the advantages of existing full-pattern fitting methods with the traditional reference intensity ratio method. Coded into Excel | Quantitative phase analysis | Chipera & Bish (2002) | http://www.ccp14.ac.uk/ccp/web-mirrors/fullpat/ | Free |
| *FULLPROF* | Rietveld refinement and pattern matching | Rietveld refinement, pattern matching | Rodriguez-Carvajal (1990) | https://www.ill.eu/sites/fullprof/ | Free |
| *GDASH* | Structure solution using grid computing | Structure solution | Griffin *et al.* (2009) | Contact Tom Griffin, tom.griffin@stfc.ac.uk | |
| *GEST* | Structure solution using a genetic algorithm | Structure solution | Feng & Dong (2007) | Contact Zhen Jie Feng, fengzhenjie@gmail.com | Free |
| *GETSPEC* | Calculates the symmetry operators and special positions for any setting of any space group based on the Hall space-group symbol | Symmetry | Altermatt & Brown (1987) | http://www.ccp14.ac.uk/ccp/web-mirrors/i_d_brown/getspec/ | Free |
| *Gnu Xtal System* | Set of portable crystallographic routines | Software development | | http://xtal.sourceforge.net/ | Free |
| *GrainSpotter* | Indexing grains in monophase crystalline materials | Indexing | Schmidt (2014) | https://sourceforge.net/p/fable/wiki/grainspotter/ | Free |
| *Gretep* | Displacement-ellipsoid plot structure viewing and analysis. Part of the *LMGP* suite | Visualization | Laugier & Bochu (2004) | http://www.ccp14.ac.uk/tutorial/lmgp/#gretep, http://www.ccp14.ac.uk/ccp/web-mirrors/lmgp-laugier-bochu/ | Free |
| *GRINSP* | Inorganic structure prediction | Structure prediction | Le Bail (2005) | http://www.cristal.org/grinsp/ | Free |
| *GSAS* | Comprehensive system for the refinement of structural models to both X-ray and neutron diffraction data. Superseded by *GSAS-II* | Pattern fitting, structure solution, Rietveld refinement, visualization | Larson & Von Dreele (2004) | http://subversion.xray.aps.anl.gov/trac/EXPGUI | Free |
| *GSAS-II* | Open-source Python project that addresses all types of crystallographic studies, from simple materials through macromolecules, using both powder and single-crystal diffraction and with both X-ray and neutron probes | Pattern fitting, structure solution, Rietveld refinement, visualization | Toby & Von Dreele (2013) | https://subversion.xray.aps.anl.gov/trac/pyGSAS | Free |
| gsaslanguage | A language that provides input to and processes output from the *GSAS* package | Scripting | Vogel (2011) | http://code.google.com/p/gsaslanguage/ | Free |

Table 6.1.1 Software for powder diffraction. Continue

| Program | Description | Function(s) | Reference(s) | URL or other source | Availability |
|---|---|---|---|---|---|
| *GSASIIscriptable* | Scripting interface for *GSAS-II* | Scripting | O'Donnell *et al.* (2018) | https://gsas-ii.readthedocs.io/en/latest/GSASIIscriptable.html | Free |
| *GudrunN* and *GudrunX* | Programs for correcting raw neutron and X-ray total-scattering data to differential cross sections | Data processing, neutron diffraction, total scattering | Soper & Barney (2011) | In-house software at ISIS | |
| *HELIX* | Simulation of helical diffraction | Powder-pattern calculation | Knupp & Squire (2004) | https://www.diamond.ac.uk/Instruments/Soft-Condensed-Matter/small-angle/SAXS-Software/CCP13.html | Free |
| Hypertext book of crystallographic space-group diagrams and tables | Space-group diagrams | Space-group information | Cockcroft (1999) | http://img.chem.ucl.ac.uk/sgp/ | Commercial |
| ICDD Powder Diffraction File | Comprehensive powder database: PDF-4+, PDF-4 organics and PDF-2, plus derivatives | Database, phase identification | International Centre for Diffraction Data, 12 Campus Boulevard, Newtown Square, PA, 19073–3273, USA | http://www.icdd.com/ | Commercial |
| *IGOR Pro* | Scientific data-analysis software | Data analysis | Kline (2006) | https://www.wavemetrics.com/products/igorpro | Commercial |
| *ImageD11* | Python codes for processing diffraction data from 2D detectors at the ID11 beamline at the ESRF | Data processing, neutron diffraction | Wright (2011) | http://sourceforge.net/projects/fable/files/ImageD11 | Free |
| Inorganic Crystal Structure Database (ICSD) | Database of inorganic structures | Database | Belsky *et al.* (2002) | http://www2.fiz-karlsruhe.de/icsd_home.html | Commercial |

Table 6.1.1 Software for powder diffraction. Continue

| Program | Description | Function(s) | Reference(s) | URL or other source | Availability |
|---|---|---|---|---|---|
| *input4MAUD* | Input of two-dimensional data into *MAUD* | Data conversion | Raue (2014) | http://kristall.uni-mki.gwdg.de/Docs/raue/input4MAUD/main.html | Free |
| *International Tables Online* | Online editions of all volumes of *International Tables for Crystallography*, including Volume A (*Space-Group Symmetry*), and an extensive symmetry database | Space-group information, database | *International Tables Online* (2019) | https://it.iucr.org | Commercial |
| *iotbx.cif* | Input, output and validation of CIFs | CIF | Gildea *et al.* (2011) | https://cci.lbl.gov/cctbx_docs/iotbx/iotbx.cif.html | Free |
| *ISAACS* | Interactive structure analysis of amorphous and crystalline systems | Structure analysis, amorphous materials | Le Roux & Petkov (2010) | http://isaacs.sourceforge.net | Free |
| *IsoDEC* | Calculation of diffraction elastic constants | Strain | Gnäupel-Herold (2012) | https://www.ncnr.nist.gov/xtal/software/isodec | Free |
| *IsoStar* | Information on intermolecular interactions derived from small-molecule crystal structures in the Cambridge Structural Database and from protein–ligand interactions observed in the Protein Data Bank (PDB) | Database | Bruno *et al.* (1997) | https://www.ccdc.cam.ac.uk/solutions/csd-system/components/isostar/ | Commercial |
| *ISOTROPY* | Applies group-theoretical methods to the analysis of phase transitions in crystalline solids | Space-group determination | Stokes & Hatch (2002) | http://stokes.byu.edu/isotropy.html | Free web service |
| *ITO* | Powder-pattern indexing. Incorporated into many other packages, both free and commercial | Indexing | Visser (1969) | http://sdpd.univ-lemans.fr/ftp/ito13.zip | Free/commercial |
| *JADE* | Comprehensive powder diffraction data-processing suite. *JADE Standard* is available as perpetual license and *JADE Pro* as an annual subscription | Cluster analysis, data conversion, indexing, Le Bail fitting, Pawley fitting, peak location, peak profiling, phase identification, powder-pattern viewing, quantitative phase anaysis, Rietveld refinement, size–strain analysis | Materials Data, Inc. (2016) | http://www.materialsdata.com/products.htm; http://www.icdd.com/ | Commercial |

Table 6.1.1 Software for powder diffraction. Continue

| Program | Description | Function(s) | Reference(s) | URL or other source | Availability |
|---|---|---|---|---|---|
| *Jana2006* | Analysis of incommensurate, modulated and composite structures, as well as standard Rietveld refinement | Le Bail fitting, Rietveld refinement, Fourier-map calculation and visualization, structure solution | Petříček *et al.* (2000); Dusek *et al.* (2001) | http://jana.fzu.cz/ | Free |
| *JEMS* | Simulation of high-resolution TEM (HRTEM), CBED, PED and SAED patterns, and simulation of powder diffraction rings | Electron diffraction, simulation | Stadelmann (2003) | http://www.jems-saas.ch/Home/jemsWebSite/jems.html | Free for students |
| *J-ICE* | Visualization of crystallographic and electronic properties using *Jmol* | Visualization, data conversion | Canepa *et al.* (2011) | http://j-ice.sourceforge.net | Free |
| *Jpowder* | JAVA data viewer | Data visualization | Markvardsen *et al.* (2010) | https://sourceforge.net/projects/jpowder/ | Free |
| *KoalaRiet* | Powder-pattern viewing, peak profiling and Rietveld refinement, fundamental parameters approach | Pattern visualization, peak fitting, Rietveld refinement | Cheary & Coelho (1996) | http://www.ccp14.ac.uk/ | Free |
| *LABOTEX* | Crystallographic texture analysis of rocks, semiconductors and superconductors, ceramics and composites, polymers, metals and alloys | Texture analysis | Pawlik & Ozga (1999) | http://www.labosoft.com.pl/ | Commercial |
| *LAPOD* | Refinement of lattice parameters using optimal regression | Unit-cell refinement | Dong & Langford (2000) | http://www.ccp14.ac.uk/ccp/web-mirrors/powderx/lapod/ | Free |
| *LauePt* | GUI for Laue-pattern simulation and analysis | Data analysis, simulation | Huang (2010) | http://www.ccp14.ac.uk/ccp/web-mirrors/xianrong-huang/ | Free |
| *MacDiff* | Analysis and display of powder data on Macintosh platforms | Database, phase identification, data conversion | Petschick (2001) | http://www.geol-pal.uni-frankfurt.de/Staff/Homepages/Petschick/MacDiff/MacDiffInfoE.html | Free |
| *MATCH!* | Compares the diffraction pattern of the unknown to a database containing reference patterns; additional knowledge such as known phases, elements or density can also be used | Phase identification, quantitative phase analysis | Crystal Impact – K. Brandenburg and H. Putz GbR, Postfach 1251, D-53002 Bonn, Germany | http://www.crystalimpact.com/match/ | Commercial |
| *Materials Studio* | Multipurpose suite | Indexing, model building, structure solution, visualization | | http://accelrys.com/products/collaborative-science/biovia-materials-studio/ | Commercial |

Table 6.1.1 Software for powder diffraction. Continue

| Program | Description | Function(s) | Reference(s) | URL or other source | Availability |
|---|---|---|---|---|---|
| *MAUD* | Rietveld-based program for combined analysis. Can be used to fit diffraction, fluorescence and reflectivity data collected using X-rays, neutrons or electrons | Data integration, indexing, space-group assignment, texture analysis, size–strain analysis, Rietveld refinement, quantitative phase analysis | Lutterotti *et al.* (1999) | http://maud.radiographema.eu/ | Free |
| *MCE-Marching Cubes* | Interactive visualization of electron and other density maps, optimized for small molecules | Fourier-map calculation and visualization | Husák & Kratochvíl (2003) | https://sourceforge.net/projects/mce-marching-cube-eld/ | Free |
| *McMaille* | Indexing using Monte Carlo methods | Indexing | Le Bail (2004) | http://www.cristal.org/McMaille | Free |
| *Mercury* | Statistical analysis of data from the Cambridge Structural Database, structure visualization and simulation of powder patterns | Structure visualization | Sykes *et al.* (2011) | http://www.ccdc.cam.ac.uk/products/mercury/ | Free; commercial version has more functions |
| MINCRYST | Contains crystal-structure data for minerals | Database | Chichagov *et al.* (2001) | http://database.iem.ac.ru/mincryst/ | Free |
| The Mineralogy Database | Includes information on the crystal structures, powder diffraction patterns, chemical composition, and physical and optical properties of minerals | Database | | http://webmineral.com | Free |
| *Mogul* | Validation of bond lengths, angles and torsions against the Cambridge Structural Database | Structure validation | Bruno *et al.* (2004) | http://www.ccdc.cam.ac.uk/products/csd_system/mogul/ | Commercial |
| *MOPAC2016* | Semi-empirical quantum chemistry calculations. *Mercury* has an interface to *MOPAC* | Structure validation, structure building | Stewart (2012) | http://openmopac.net | Free for academic use |
| *Mstruct* | Microstructure analysis using powder diffraction | Microstructure analysis | Matěj *et al.* (2014) | http://www.xray.cz/mstruct/ | Free |

Table 6.1.1 Software for powder diffraction. Continue

| Program | Description | Function(s) | Reference(s) | URL or other source | Availability |
|---|---|---|---|---|---|
| *Multifit/Polydefit* | Open-source IDL software package for data analysis of synchrotron-based plasticity, rheology or other time-dependent experiments | Texture analysis | Merkel & Hilairet (2015) | http://merkel.texture.rocks/Multifit-Polydefix/ | Free |
| *MultiRef* | *MATLAB* framework for *GSAS*; Rietveld refinement of multiple powder diffractograms from *in situ*, scanning or diffraction tomography experiments | Rietveld refinement | Frølich & Birkedal (2015) | http://chem.au.dk/en/research/research-areas/inorganicchemistrymaterialschemistry/biological-and-bioinspired-materials/multiref/downloads/ | Free |
| *NanoPDF64* | Software package for analysis of pair-distribution functions of nanocrystals, also capable of calculating theoretical powder diffraction patterns and pair-distribution functions for atomistic models of nanocrystals | PDF analysis | Skrobas *et al.* (2017) | http://www.unipress.waw.pl/nanopdf | Free |
| *NEWMOD II* | Modelling of interstratified layer structures | Powder-pattern calculation | Yuan & Bish (2010) | https://newmod-for-clays.com | Commercial |
| Nickel–Nichols Mineral Database | Mineral database | Phase identification | The Nickel–Nichols Mineral Database, Materials Data, Inc., 1224 Concannon Blvd, Livermore, CA 94550, USA; Nickel & Nichols (1991) | http://www.materialsdata.com/MINERALS.htm | Free |
| *Nika* | Open-source *Igor Pro*-based program for reduction of two-dimensional scattering data from area-detector small- and wide-angle scattering instruments. Can be used in transmission and grazing-incidence geometries | SAXS, WAXS | Ilavsky (2012) | https://usaxs.xray.anl.gov/software/nika | Free |
| *NXS* | Library for neutron cross-section calculations | Neutron diffraction | Boin (2012) | https://www.helmholtz-berlin.de/people/boin/nxs_en.html | Free |
| *OpenBabel* | Open-source chemistry toolbox, allowing users to search, convert, analyse or store data from molecular modelling, chemistry, solid-state materials, biochemistry or related areas | File conversion | O'Boyle *et al.* (2011) | http://openbabel.sourceforge.net/ | Free |

Table 6.1.1 Software for powder diffraction. Continue

| Program | Description | Function(s) | Reference(s) | URL or other source | Availability |
|---|---|---|---|---|---|
| *OpenGenie* | Neutron-data analysis | Powder-pattern visualization | Akeroyd *et al.* (1999) | http://www.opengenie.org/Main_Page | Free |
| *PASCal* | Online tool for determining principal coefficients of thermal expansion and compressibilities using variable-pressure and variable-temperature lattice-parameter data | Strain | Cliffe & Goodwin (2012) | http://pascal.chem.ox.ac.uk | Free web access |
| *PATE* | *GSAS* powder-pattern extractor | Data conversion | | http://www.ccp14.ac.uk/ccp/web-mirrors/scott-belmonte-software/pate/ | Free |
| *PCED3* | Simulation of polycrystalline electron diffraction and phase identification | Electron diffraction, phase identification | | http://www.unl.edu/ncmn-cfem/xzli/download | Free |
| PCOD | Open database of structures of inorganic compounds predicted or enumerated mainly using *ZEFSA II* or *GRINSP* | Phase identification, database | | http://www.crystallography.net/pcod/ | Free |
| *PDXL 2* | Provides various analysis tools such as automatic phase identification, quantitative analysis, crystallite-size analysis, lattice-constants refinement, Rietveld analysis, *ab initio* structure determination and data clustering. Peak shapes can be modelled using a fundamental-parameters approach | Rietveld refinement, quantitative analysis, phase identification, structure determination | Rigaku (2014) | https://www.rigaku.com/en/service/software/pdxl | Commercial |
| *PeckCryst* | Molecular crystal structure determination from powder diffraction data using a particle swarm optimization algorithm | Structure solution | Feng *et al.* (2009) | Contact J. C. Zhang, jczhang@shu.edu.cn | Free |
| *PLATON* | Implements a large variety of standard geometrical calculations and tests (*e.g.* for missing symmetry, voids in the lattice *etc.*), and includes utilities for cell transformation and graphics. Used in *checkCIF* | Data conversion, space-group assignment, structure refinement, H-atom placement, structure validation, powder-pattern calculation, structure visualization | Spek (1998, 2003) | http://www.cryst.chem.uu.nl/platon/ | Free |
| *PM2K* | Full-pattern fitting allowing microstructural investigation of nanocrystalline materials. Includes analysis of size broadening due to an analytical or to a generic (unconstrained) distribution of crystallites, the presence of dislocations, stacking faults and antiphase boundaries | Whole-powder-pattern modelling | Leoni *et al.* (2006) | Contact M. Leoni, matteo.leoni@unitn.it | Free for academic use |

Table 6.1.1 Software for powder diffraction. Continue

| Program | Description | Function(s) | Reference(s) | URL or other source | Availability |
|---|---|---|---|---|---|
| *PolySNAP3* | Clustering powder diffraction, XRF and spectroscopic data. Semi-quantitative analysis | Cluster analysis, phase analysis | Barr *et al.* (2009) | http://www.bruker.com/ | Commercial |
| *popLA* | Pole-figure evaluation using the harmonic and WIMV methods | Texture analysis | Kocks *et al.* (1998) | http://lansce.lanl.gov/facilities/lujan/instruments/hippo/popLA.php | Free |
| *Powder Cell* | Represents the crystal structure and the corresponding powder pattern simultaneously. Translations and rotations of a preselected part of the asymmetric unit allow manipulation of the structure | Data conversion, powder-pattern calculation, powder-pattern viewing, Le Bail fitting, size–strain analysis, Rietveld refinement, quantitative phase analysis, structure visualization | Kraus & Nolze (1996) | http://powdercell-for-windows.software.informer.com/2.4/ | Free |
| *Powder3D* | Multiple-pattern data reduction and graphical presentation. Part of *Materials Studio* | Data integration, data conversion, powder-pattern viewing, peak location | Hinrichsen *et al.* (2008) | https://www.fkf.mpg.de/4708688/Powder-3D-Software | Free |
| *PowderX* | Uses include plotting X-ray patterns, data smoothing, background subtraction, $\alpha_2$-peak elimination, peak search, indexing, zero-angle error correction and data-format conversions | Data conversion, powder-pattern viewing, peak location, indexing | Dong (1999) | http://www.ccp14.ac.uk/ccp/web-mirrors/powderx/Powder/ | Free |
| *PowDLL* | .NET dynamic link library used for interconversion between variable formats of X-ray powder diffraction files | Data conversion | Kourkoumelis (2005) | http://users.uoi.gr/nkourkou/powdll.htm | Free |
| *PRODD* | Refinement of crystal and magnetic structures from powder diffraction data, can be used with time-of-flight and constant-wavelength neutron data as well as synchrotron X-ray data | Pawley fitting, Rietveld refinement, proteins | Wright (2004); Wright & Forsyth (2000); Wright *et al.* (2007) | http://www.ccp14.ac.uk/ccp/web-mirrors/prodd/~jpw22/ | Free |
| *PROFEX* | A platform-independent open-source graphical user interface for the Rietveld refinement program *BGMN*. Reads and converts a variety of proprietary raw data formats | Rietveld refinement, data conversion | Doebelin & Kleeberg (2015) | http://profex.doebelin.org/ | Free |

Table 6.1.1 Software for powder diffraction. Continue

| Program | Description | Function(s) | Reference(s) | URL or other source | Availability |
|---|---|---|---|---|---|
| *Profil* | Rietveld refinement and utilities. Can be used for organics and organometallics requiring restrained refinement | Unit-cell refinement, Rietveld refinement, Fourier-map calculation, visualization, data conversion | Cockcroft (1994) | http://img.chem.ucl.ac.uk/www/cockcroft/profil.htm | Free for academic use |
| *publCIF* | Editing, validating and formatting CIF files | CIF editing | Westrip (2010) | http://journals.iucr.org/services/cif/publcif/ | Free |
| *PyCifRW* | Support for reading and writing of CIF files using Python, with optional validation against DDL dictionaries | CIF editing | Hester (2006) | https://pypi.org/project/PyCifRW/4.3/ | Free |
| *PyMOL* | A comprehensive software package for rendering and animating 3D structures | Structure visualization | | https://pymol.org/2/ | Commercial |
| *Quanto* | Allows automatic estimation of the weight fraction of each crystalline phase in a mixture. The amorphous content can be estimated using the internal-standard method, and corrections for preferred orientation and microabsorption effects are available | Quantitative phase analysis | Altomare *et al.* (2001) | http://www.ic.cnr.it/ | Free |
| *RIETAN-FP* | A package of programs for analysing crystal structures from X-ray and neutron powder diffraction data and visualizing the results in three dimensions, along with electronic-state calculations | Rietveld refinement, data conversion | Izumi & Momma (2007) | http://fujioizumi.verse.jp/download/download_Eng.html | Free |
| *Rietica* | Aids the creation and updating of Rietveld input files for and provides point-and-click control of the Rietveld program *LHPM* | Le Bail fitting, Rietveld refinement, visualization | Hunter (1998) | http://www.rietica.org/ | Free |
| *RMC++* | Reverse Monte Carlo modelling of the structure of disordered materials, mainly using diffraction data, but additional information such as EXAFS data and different constraints can also be used | PDF analysis | Evrard & Pusztai (2005) | http://www.szfki.hu/~nphys/rmc++/opening.html | Free |
| *RMCAW95* | Uses the reverse Monte Carlo method for modelling both lattice and magnetic disorder in powder crystalline materials by direct calculation of the structure factor | PDF analysis | Mellergård & McGreevy (1999) | http://www.cristal.org/glasses/rmca/rmcaw95.html | Free |

Table 6.1.1 Software for powder diffraction. Continue

| Program | Description | Function(s) | Reference(s) | URL or other source | Availability |
|---|---|---|---|---|---|
| *RMCprofile* | Built from the original *RMCA* code of McGreevy & Pusztai to determine the local structure of crystalline materials while still being capable of analysing disordered systems. Can be used to fit many data types (including total scattering, EXAFS, diffuse scattering) simultaneously | PDF analysis | Tucker *et al.* (2007) | http://www.rmcprofile.org | Free |
| *ROCKJOCK* | Quantitative analysis of mineralogical samples with or without using an internal standard by automatically fitting the sum of stored X-ray diffraction patterns of pure standard minerals to the measured pattern | Quantitative phase analysis, minerals | Eberl (2003) | http://pubs.er.usgs.gov/publication/ofr200378 | Free |
| *Siroquant* | Comes with a comprehensive database of over 1800 phases. Phases from public sources such as the ICSD and AMCSD can also be added | Phase identification | Sietronics (2012) | http://www.siroquant.com | Commercial |
| *SPEC* | Software for the control of data acquisition. Includes *C-PLOT* for data display and analysis | Instrumentation | SPEC, Certified Scientific Software, PO Box 390640, Cambridge, MA, 02139-0007, USA | http://www.certif.com/ | Commercial |
| *STEREOPOLE* | Analysis of X-ray diffraction pole figures, allowing experimental data to be compared graphically with simulated results, and epitaxic relationships between up to five different crystal layers to be evaluated | Texture analysis | Salzmann & Resel (2004) | http://www.if.tugraz.at/amd/stereopole/ | Free |
| *Struvir* | Converts *STRUPLO* data files into Virtual Reality Modeling Language (VRML) for 3D visualization | Visualization | Le Bail (1996); Fischer (1985) | http://www.cristal.org/vrml/struvir.html | Free |
| *SUPERFLIP* | Structure solution from diffraction data using charge flipping. Can solve periodic structures, incommensurately modulated structures and the structures of quasicrystals from X-ray and neutron diffraction data | Structure solution | Palatinus & Chapuis (2007) | http://superflip.fzu.cz | Free |

Table 6.1.1 Software for powder diffraction. Continue

| Program | Description | Function(s) | Reference(s) | URL or other source | Availability |
|---|---|---|---|---|---|
| *TOPAS* and *TOPAS-Academic* | Nonlinear least-squares optimization programs written in C++, allowing users to easily modify program functionality to suit the problem at hand | Peak fitting, Le Bail fitting, Pawley fitting, Rietveld refinement, PDF analysis, indexing, structure solution, charge flipping, magnetic structures, stacking-fault analysis | Coelho (2018) | https://www.bruker.com/products/x-ray-diffraction-and-elemental-analysis/x-ray-diffraction/xrd-software/topas.html, http://www.topas-academic.net | Free |
| *VALENCE* | Calculates bond valences from bond lengths and *vice versa*. Can also calculate bond-valence sums and average bond lengths, and can determine bond-valence parameters from the bonding environments of various cations | Structure validation | Brown (1996) | http://netlib.ccp14.ac.uk/ccp/web-mirrors/valence | Free |
| *VMRIA* | Full-profile analysis of neutron-diffraction time-of-flight data for multiphase samples. Includes *Autox* | Rietveld refinement, indexing | Zlokazov & Chernyshev (1992); Zlokazov (2003) | http://www.ccp14.ac.uk/ccp/web-mirrors/vmria/ | Free |
| *WinPLOTR* | A graphical user interface for displaying powder patterns; part of *FULLPROF* | Powder-pattern viewing | | http://www.cdifx.univ-rennes1.fr/winplotr/readme.htm | Free |
| *WinPSSP* | Uses direct-space methods to solve the crystal structures of small-molecule organic materials from X-ray powder diffraction data | Structure solution | Pagola *et al.* (2017) | http://users.uoi.gr/nkourkou/winpssp/ | Free |
| *WinXPow* | Comprehensive package for data collection, profile fitting, indexing, and size–strain and crystallinity analysis | Phase identification, profile fitting, indexing, size–strain analysis, crystallinity | STOE & Cie GmbH, Hilpertstr. 10, D-64295 Darmstadt, Germany | https://www.stoe.com/product/software-powder-xrd/ | Commercial |
| *XDrawChem* | Two-dimensional molecule drawing program for Unix operating systems | Model building | Herger (2002) | http://xdrawchem.sourceforge.net/ | Free |
| *xINTERPDF* | Analysis of intermolecular pair-distribution functions of organic compounds from X-ray total-scattering data | PDF analysis | Shi (2018) | https://github.com/curieshicy/xINTERPDF | Free |
| *XLENS* | Uses Patterson-function direct methods instead of the modulus function. Well suited for handling powder diffraction data for organic compounds | Structure solution | Rius (2011, 2013) | https://departments.icmab.es/crystallography/software | Free for academic use |

Table 6.1.1 Software for powder diffraction. Continue

| Program | Description | Function(s) | Reference(s) | URL or other source | Availability |
|---|---|---|---|---|---|
| *xPDFsuite* | Suite of algorithms and software for pair-distribution-function analysis | PDF analysis | Juhás *et al.* (2013) | https://www.diffpy.org/products/xPDFsuite.html | Free for academic use |
| *X'Pert HighScore Plus* | Integrated powder-processing suite including profile fitting, structure solution, Rietveld refinement, quantitative analysis and cluster analysis | Cluster analysis, data conversion, indexing, Le Bail fitting, Pawley fitting, peak location, peak profiling, phase identification, powder-pattern viewing, quantitative phase analysis, Rietveld refinement, size–strain analysis | Malvern Panalytical BV, De Schakel 18, Kamer 50, Eindhoven, 5651 GH, Netherlands | https://www.malvernpanalytical.com/products/category/software/x-ray-diffraction-software/highscore-with-plus-option | Commercial |
| *Xpowder* | Identification, quantification and characterization of the crystalline components of solids, including natural minerals, artificial compounds and biological crystals | Phase identification | Quetzal Com S. L., La Carrera 5, 18110 HIJAR– Las Gabias, Granada, Spain | http://www.xpowder.com/ | Commercial |
| *XRD2DScan* | Display and analysis of two-dimensional X-ray diffraction patterns collected with an area detector | 2D data | Rodriguez-Navarro (2006) | http://www.ugr.es/~anava/xrd2dscan.htm | Free |
| *XRDUA* | Reconstruction of crystalline phase distribution maps from two-dimensional diffraction patterns collected by scanning and tomographic X-ray powder diffraction | Data processing, phase distributions | de Nolf (2014) | http://xrdua.ua.ac.be | Free |
| *ZEFSA II* | Zeolite structure solution using a biased Monte Carlo scheme | Structure solution, zeolites | Falcioni & Deem (1999) | http://www.mwdeem.rice.edu/zefsaII/ | Free |